Mobilization and Mobility of Colloidal Phosphorus in Sandy Soils

vorgelegt von
Diplom Agrarbiologin
Katrin Ilg

von der Fakultät VI – Planen Bauen Umwelt
der Technischen Universität Berlin
zur Erlangung des akademischen Grades

Doktor der Naturwissenschaften
-Dr. rer. nat.-

genehmigte Dissertation

Promotionsausschuss:
Vorsitzender: Prof. Dr. Gerd Wessolek
Berichter: Prof. Dr. Martin Kaupenjohann
Berichter: Prof. Dr. Ruben Kretzschmar
Tag der wissenschaftlichen Aussprache: 4. Juni 2007

Berlin 2007
D 83

Dedicated to my father
Hans Ilg

Table of Contents

List of Figures

List of Tables

Abstract

Subsurface losses of phosphorus (P) contribute to the translocation of P from terrestrial to aquatic ecosystems and may cause or enhance the eutrophication of surface waters. In addition to the dissolved fraction, P in seepage water may be mobile as colloidal P (P_{coll}). Since the sorption of P to dispersible solids such as iron (Fe) and aluminum (Al) oxides and hydroxides changes their surface charge, P itself may contribute to the mobilization and mobility of colloids.

In this study I tested the hypotheses that 1) the sorption of P to goethite and to sandy soils disperses goethite and soil particles, 2) inositol hexaphosphate (IHP) is a more efficient dispersing agent than ortho-phosphate (ortho-P), 3) an increasing P saturation of sandy soils increases the release of P_{coll} under batch conditions and 4) an accumulation of P in soils increases the leaching of P_{coll} under field conditions.

To test hypothesis 1 and 2 I conducted two batch experiments, in which I added increasing concentrations of IHP and ortho-P to model systems consisting of quartz sand synthetically coated with goethite and to natural subsoils. In another batch experiment I investigated the colloid mobilization of a set of soil samples with a wide range of P saturation, but without any addition of P (hypothesis 3). Further, I tested hypothesis 4 with a column experiment using undisturbed soils of different P saturations. In all experiments I measured dissolved P (P_{diss}) and P_{coll} concentrations as well as colloid-characterizing parameters such as zeta potential and optical density. To evaluate the best-suited colloid sampling system for the column experiment of hypothesis 4, I compared different sampling systems in a column experiment using colloidal ^{59}Fe-goethite.

The addition of P caused the mobilization of colloids in the first two batch experiments. Larger equilibrium concentrations of P_{diss} were necessary to induce colloid dispersion in the batch experiment with natural subsoils (0.07-2.22 mg P_{diss} l^{-1}) than in the experiment with coated quartz sand (0.01-0.03 mg P_{diss} l^{-1}). In both experiments the critical P saturation, above which colloids were mobilized, corresponded to a zeta potential of colloids of about -20 mV. The sorption of IHP reduced the zeta potential of colloids more effectively and caused the release of larger colloid concentrations than ortho-P. In the batch experiment without any addition of P, P_{coll} concentrations in supernatants increased with increasing P saturation because additional colloids were released and because the P content of the colloids increased.

The test of different lysimeter systems showed that after an application of 10 mg colloids per liter to different lysimeter systems, zero-tension and 10 µm membrane lysimeters collected the largest amount of applied ^{59}Fe (9.1% and 6.8%) and wick lysimeters

the smallest amount of applied ^{59}Fe in the outflow (0.7%), which was related to a trapping of colloids in the wick. In contrast to the results of batch experiments, the leaching of P_{coll} in the column experiment was not significantly affected by the P saturation of soils. Colloidal P concentrations ranged from 0.01 to 0.31 mg P l^{-1} and contributed between 1 and 37% to the leaching of total P < 1.2 µm.

The lack of an enhancing effect of P accumulation on P_{coll} mobility in the column experiment I ascribe to i) a missing application of P in the column experiment compared to the first two batch experiments. Furthermore ii) physical disturbance, which probably enhanced colloid mobilization in all batch experiments, was lacking in the column experiment and iii) factors such as water content or pH additionally affected colloid transport and deposition thereby superimposing the colloid mobilizing effect of P accumulation in soils. An increasing complexity and similarity of experimental approaches to reality generally tended to obliterate the originally strong effect of P sorption on the mobilization of colloids in simple systems. In addition to soil physical or hydraulical constraints, pH and soil organic matter affect the surface charge and aggregation of oxides and hydroxides thereby masking P effects. Furthermore the increasing diversity of P sorbents from model systems to real soils blurs colloid mobilization by P sorption.

My results of batch experiments with model systems and various soils point to a colloid-mobilizing effect of P accumulation in sandy soils. Organically-bound P, contained in manure, likely has a stronger dispersing effect than inorganic P. However, due to the superimposing effects of other factors controlling the mobility of colloids, a P-induced mobilization of colloids does not necessarily result in an increased leaching of P_{coll}.

Based on the improved process understanding and the presented findings concerning colloid sampling systems, future research should clarify and quantify the environmental relevance of P-induced colloid mobilization on the field scale using the best-suited colloid sampling system.

Zusammenfassung

Die Auswaschung von Phosphor (P) trägt zur Verlagerung von P aus terrestrischen in aquatische Ökosysteme bei und kann die Eutrophierung von Oberflächengewässern verursachen oder verstärken. Neben der gelösten Form kann P im Sickerwasser auch an Kolloide gebunden auftreten. Die Sorption von P an potentiell dispergierbare Bestandteile der Bodenmatrix, z.B. Eisen- und Aluminiumoxide und -hydroxide, beeinflusst deren Oberflächenladung und kann dadurch zur Mobilisierung und Mobilität von Kolloiden beitragen.

In meiner Studie testete ich folgende Hypothesen: 1) Die Sorption von P an Goethit und an sandige Böden dispergiert kolloidalen Goethit, bzw. Bodenkolloide, 2) Inositol Hexaphosphat (IHP) wirkt stärker dispergierend als ortho-Phosphat (ortho-P), 3) eine steigende P-Sättigung von sandigen Böden führt zur Dispergierung von kolloidalem P im Schüttelversuch und 4) zur Auswaschung von kolloidalem P unter Feldbedingungen.

Um die Hypothesen 1 und 2 zu testen, führte ich zwei Schüttelversuche mit synthetischen Systemen (Quarzsand beschichtet mit Goethit) und Unterböden durch, denen ich jeweils steigende IHP-, bzw. ortho-P-Konzentrationen zusetzte. In einem weiteren Schüttelversuch untersuchte ich die Mobilisierung von Kolloiden an einem Probenkollektiv mit einer breiten Spanne an P-Sättigungen ohne eine weitere Zugabe von P (Hypothese 3). Zur Überprüfung von Hypothese 4 bestimmte ich die Auswaschung von kolloidalem P aus Säulen mit ungestörten Böden unterschiedlicher P-Sättigung. In allen Versuchen ermittelte ich gelöste und kolloidale P-Konzentrationen sowie zur näheren Charakterisierung der Kolloide das Zeta Potential und die optische Dichte. In einem, dem Säulenexperiment vorangestellten Versuch, testete ich fünf verschiedene Lysimetertypen, um das am besten geeignete System zur Beprobung von Kolloiden im Feld zu ermitteln. Dazu bestimmte ich in einem ungesättigten Säulenexperiment die Kolloidwiederfindung nach Applikation von kolloidalem ^{59}Fe-Goethit.

Die Zugabe von P in Schüttelversuchen führte zur Mobilisierung von Kolloiden. In dem Versuch mit Unterböden wurden Kolloide erst bei einer höheren Gleichgewichtskonzentration an gelöstem P dispergiert (0.07-2.22 mg gelöster P l^{-1}) als in dem Versuch mit Quarzsand (0.01-0.03 mg gelöster P l^{-1}). In beiden Versuchen ging die kritische P-Sättigung, bei der Kolloide mobilisiert wurden, mit einem Zeta Potential der Kolloide von -20 mV einher. Die Sorption von IHP verringerte das Zeta Potential der Kolloide stärker und mobilisierte höhere Kolloidkonzentrationen als ortho-P. Im Schüttelversuch ohne zusätzliche P-Zugabe nahmen die kolloidalen P-Konzentrationen mit steigender

P-Sättigung der Böden zu. Dies ließ sich zum einen auf eine zunehmende Mobilisierung von Kolloiden, aber auch auf eine steigende P-Konzentration der Kolloide zurückführen.

Der Test der verschiedenen Lysimetertypen ergab, dass nach Applikation von 10 mg Kolloiden pro Liter frei drainende Lysimeter sowie Unterdrucklysimeter mit einer 10 µm-Membran die größte Menge (9.1% und 6.8%) und Dochtlysimeter die geringste Menge (0.7%) des applizierten ^{59}Fe sammelten. Letzteres lässt sich auf das Zurückhalten von Kolloiden im Docht zurückführen.

Die Konzentrationen an kolloidalem P im Säulenausfluss reichten von 0.01 bis 0.31 mg P l^{-1} und machten zwischen 1 und 37% des ausgewaschenen Phosphors der Fraktion < 1.2 µm aus. Im Gegensatz zu den Schüttelversuchen konnte ich im Säulenexperiment keinen Einfluss der P-Sättigung auf die Auswaschung von kolloidalem P feststellen. Dies führe ich auf i) die fehlende P-Applikation im Säulenversuch im Vergleich zu den ersten beiden Schüttelversuchen zurück. Außerdem unterstützt ii) der Schüttelprozess die Mobilisierung von Kolloiden, was im Säulenversuch nicht der Fall ist. Mit steigender Komplexität der untersuchten Systeme steigt iii) der Einfluss anderer Faktoren die die Mobilisierung und Mobilität von Kolloiden beeinflussen und die P-induzierten Kolloidmobilisierung unter Umständen überdecken. Neben der P-Sorption beeinflussen beispielsweise der pH Wert oder der Gehalt an organischer Substanz die Oberflächenladung von Oxiden und Hydroxiden. Außerdem kommen in den natürlicheren Systemen vielfältigere Sorbenten vor, z.B. Tonminerale oder Eisen- und Aluminiumoxide und -hydroxide mit verschiedenen Sorptionskapazitäten, die alle unterschiedlich auf den dispergierenden Einfluss von P reagieren.

Meine Ergebnisse aus den Schüttelversuchen mit den Modellsystemen und den verschiedenen Böden belegen eine P-induzierte Mobilisierung von Kolloiden. Dabei wirkt organisch gebundener P stärker dispergierend als ortho-P. Aufgrund des überlagernden Einflusses anderer Faktoren führt die P-induzierte Mobilisierung von Kolloiden jedoch nicht zwangsläufig zu einer erhöhten Auswaschung von kolloidalem P.

Aufbauend auf dem verbesserten Prozessverständnis und den Ergebnissen zu den Probenahmesystemen, die diese Arbeit lieferte, sollte in zukünftigen Untersuchungen die Umweltrelevanz der P-induzierten Kolloidmobilisierung mit Hilfe von geeigneten Probenahmesystemen auf der Feldskala ermittelt und möglichst quantifiziert werden.

1 General introduction

1.1 Phosphorus in soils

Phosphorus (P) as an essential nutrient element for all organisms takes part in numerous biochemical processes. Especially in aquatic ecosystems very often P is the growth-limiting factor. Therefore these ecosystems may be subjected to eutrophication as a consequence of increased inputs of P (Schindler, 1971; Lee, 1973). In the USA, for example, eutrophication due to P input was identified to be the main problem for lake waters next to N input (US EPA, 2000).

In Germany and many other industrialized countries P immissions into surface waters have been reduced by more than 50% within the last 20 years. The inputs of P from point sources like sewage treatment plants have decreased, whereas diffuse sources have gained in importance. Today, the major diffuse source is agriculture, accounting for 20-50% of total P input to surface water (Kronvang et al., 2005; Umweltbundesamt Germany, 2006). This can be attributed to excessive fertilization of farmlands over several decades, especially in regions with high livestock densities (Sharpley et al., 1994; Leinweber et al., 1997; Haygarth and Jarvis, 1999).

Due to the strong sorption of P to soils, surface runoff and erosion were regarded as the most important vectors of P from agricultural land to surface waters (Sharpley et al. 1994, Daniel et al., 1998; Auerswald et al., 2002). However, subsurface losses of P to groundwater and drains received increasing attention, because several recent studies have proven the leaching of ecologically relevant P concentrations to drain- and ground water (e.g. James, 1996; Siemens et al., 2004; Nelson et al., 2005). Rubæk et al. (2002) and Stamm (1997) found an increase in P leaching after manure application and rainfall events. In dye and lysimeter experiments Sinaj et al. (2002) and Toor et al. (2005) showed that P is discharged to a large extent via preferential flow paths.

Heckrath et al. (1995) and Maguire and Sims (2002) observed a sharp increase in molybdate reactive P (< 0.45 µm), if soil-sorbed P exceeded a certain critical value, which was termed “change point”. This “change point” can be related to the nonlinear sorption of ortho-phosphate (ortho-P) to soil, which drastically decreases at large P saturations of P sorbents (Ryden and Syers, 1977; Barrow,

1983, Koopmans et al., 2002). Van der Zee and van Riemsdijk (1988) introduced the ratio of oxalate extractable P and iron (Fe) + aluminum (Al) as an indicator for the degree of P saturation (DPS). In sandy soils dissolved P (P_{diss}) concentrations > 100 µg l^{-1} have to be expected for a DPS > 0.25 (Breeuwsma and Silva, 1992, van der Zee and de Haan, 1994; Siemens et al., 2004).
In addition to P_{diss}, colloidal P (P_{coll}) contributes to losses from soils (e.g. Jensen et al., 2000; Hens and Merckx, 2001; Heathwaite et al., 2005). In the following I review the state-of-the-art concerning P sorption to colloids, subsurface transport of P_{coll}, and its relevance for P losses from soils.

1.2 Formation and composition of P-containing colloids

Colloids are defined as particles sufficiently small to remain in suspension because Brownian motion forces are stronger than gravitation (Brady and Weil, 2002) and large enough to scatter passing light (Brezesinski and Mögel, 1993). In this review I define the colloid size fraction from 1 nm to 1 µm diameter following Kretzschmar et al. (1999). Thus, P_{coll} in soils is defined as i) inorganic or organic P sorbed to colloids and ii) P-containing organic macromolecules larger than 1 nm.
The dissolved fraction of P is often defined as the fraction < 0.45 µm, which is problematic because it may contain part of the truly colloidal fraction (Haygarth et al., 1997; Shand et al., 2000, Koopmans et al., 2005). In addition to P_{coll}, the parameter particulate P is widely used in literature. Particulate P comprises total P except for the dissolved fraction, but lacking an upper size limit. Therefore it may exceed the colloidal size fraction. In the following I differentiate between particulate P and P_{coll}.
In non-calcareous soils P is mainly sorbed to Fe and Al oxides* and to a lesser extent to clay minerals. In neutral to basic calcareous soils the application of P results in the precipitation of phosphate-containing solid phases like Ca phosphates and sorption of P to Ca minerals like calcite (Parfitt, 1978; Frossard et al., 1995). The sorption capacity for P per unit mass is about 5000 times larger for colloids than for the immobile soil matrix, because of the large surface to mass ratio of colloids (McGechan and Lewis, 2002).

* For the sake of simplicity the expression „oxides“ comprises oxides, hydroxides and oxide hydroxides throughout the manuscript.

Both inorganic and organic P can be sorbed to soil colloids. Organically-bound P represents 4 to 90% of total P in soils (as reviewed by Dalal, 1977). Especially inositol hexaphosphate (IHP) was the focus of many previous studies, because it is one of the most stable organic P forms in soils. It can comprise more than 50% of total P in manure (Barnett, 1994) and can account for more than 50% of organic P in soils (Dalal, 1977). Celi et al. (1999) compared the sorption characteristics of IHP and inorganic phosphate on goethite, illite, and kaolinite: IHP had a stronger affinity to these minerals than inorganic P and its desorption was considerably smaller. In accordance with these results Leytem et al. (2002) found a larger sorption maximum of IHP to soils compared to inorganic P. Less persistent organic P compounds such as nucleotides are quickly mineralized and are probably less relevant for sorption to colloids (Leytem et al., 2002).

Colloidal P may be indirectly associated with organic matter via metal-bridges (Kreller et al., 2003). In aqueous extracts about 90% of P_{diss} were removed from solution by precipitating the humic fraction of DOM with $CaCl_2$ or HCl. At the same time Al and Fe were completely removed from solution, which implies that Fe and Al were associated with organic matter and strongly influenced the speciation and mobility of P in solution (Dolfing et al., 1999). Gerke (1992) found a significant decrease of P, Fe, and Al concentrations in soil solution after removing organic carbon (C) by ultrafiltration. This decrease was more pronounced for soil solutions with larger concentrations of organic C. These results suggest the existence of humic- Fe (Al-) phosphate complexes. Hens and Merckx (2001) fractionated P_{coll} via gel filtration chromatography and confirmed the model of complexes consisting of organic matter, metals, and P in colloidal form.

To summarize, P_{coll} in soils occurs associated with colloidal Fe and Al oxides (Fe_{coll} and Al_{coll}), organic matter, and to a lesser extent to clay minerals. Due to the strong interactions between organic matter, oxides, and clay minerals, associations of P_{coll} with these sorbents can hardly be separated from each other in soils.

1.3 Influence of P on colloid mobilization and stabilization

Most soils mainly consist of negatively charged minerals like clay minerals. Therefore positively charged soil constituents are sorbed to the soil matrix and only negatively charged particles may become mobile as colloids. Sorption of P may modify the surface charge of its sorbents (Stumm and Sigg, 1979; Lima et al., 2000). Iron oxides for example have their point of zero charge (PZC) at pH 7-9. At pH < PZC they are positively and at pH > PZC they are negatively charged. In pure systems oxides were dispersed if they were negatively or positively charged and flocculated only around the PZC (Liang and Morgan, 1990; Puls and Powell, 1992). In titration experiments the PZC of Fe oxides decreased upon P sorption (Stumm and Sigg, 1979; Puls and Powell, 1992). Saturated with P, Fe oxide colloids were negatively charged at a pH > 4 (Puls et al., 1993). Celi et al. (1999) observed a decrease in surface charge and the dispersion of goethite, illite, and kaolinite after P sorption at pH > 3. In that study the decreasing surface charge was accompanied by a decrease in goethite particle size from 1.4 µm to 0.8 µm.

Decreasing the surface charge of sorbents by P sorption enhances mobilization of colloids from the negatively charged soil matrix and stabilizes colloid suspensions. Siemens et al. (2004) found a significant mobilization of soil colloids in batch experiments and soil columns after application of P. Furthermore, the authors reported indications for an existing threshold of P saturation above which particle-bound P is dispersed. They hypothesized that existing threshold values of soil P mobilization (e.g. the DPS value of van der Zee and de Haan, 1994) may be explained in part by the dispersion of P_{coll}.

Results contradicting the dispersing character of P were presented by Anderson et al. (1985) and He et al. (1996), who showed that phosphate uptake by Fe oxides caused an aggregation of particles. The authors attributed their observations to phosphate bidentate bridging between Fe oxide particles of the type Fe-O-P-O-Fe. However, He et al. (1996) added phosphate to a Fe(III) nitrate stock solution. Then Fe oxide colloids were precipitated by adding NaOH. Therefore P was directly incorporated into the Fe oxide crystal structure and the experiment cannot be compared with P sorption experiments using Fe-minerals.

It is reported that divalent cations in soil solution coagulate colloids and lower colloid mobilization and transport (as reviewed by DeNovio et al., 2004). At first view being contradictory to this finding, Turner et al. (2004) found a positive correlation between water-dispersible P_{coll} and $CaCO_3$ for calcareous soils. They attributed their finding not to an effect of divalent cations in soil solution but to Ca- and Mg-phosphate minerals in the colloidal phase.

In addition to inorganic P, organic P is supposed to play an important role in colloid mobilization and stabilization. Because of its smaller acid dissociation constants and the resulting larger negative charge IHP decreases the surface charge of sorbents more than inorganic P. Goethite saturated with IHP is dispersed at pH values of 2-10 while goethite saturated with inorganic P is dispersed only at pH larger than 5 (Celi et al., 2001). Investigating the sorption of IHP and inorganic P to calcite, small concentrations of P cause an aggregation of calcite particles. With increasing P concentration the negative charge of the calcite particles increases and they are re-dispersed. As for goethite the sorption of IHP decreases the surface charge of calcite more than the sorption of inorganic P (Celi et al., 2000).

Sorption of P to colloidal soil constituents as well as its effect on their mobilization is frequently superimposed by other factors, which complicates the interpretation of experimental findings. Similar to phosphate, organic matter sorbs to oxides and clay minerals and increases the negative charge of its sorbents. Thus, the mobilization and stabilization of colloids as a consequence of C sorption is enhanced (Kretzschmar et al., 1993; Kaplan et al. 1993; Heil and Sposito, 1993, Karathanasis, 1999). Low and high molecular weight organic substances compete with P for sorption sites (Yan, 1980; Kaiser and Zech, 1996; Chen et al., 2000; Kreller et al., 2003). McDowell and Sharpley (2001a) found that dairy manure rich in organic matter saturated P sorption sites in soils. Therefore sorption of P added as super phosphate was larger than sorption of P originating from dairy manure. In an experiment conducted by Lima et al. (2000) an increasing addition of P decreased the surface charge of clay particles in the B horizon, but not in the A horizon. According to the authors explanation, P sorption in the A horizon mainly occurred by replacing organic compounds and therefore did not change surface charge.

In calcareous soils organic acids, e.g. tannic, fulvic, humic, and citric acid, may reduce the precipitation rate of Ca phosphates by sorption to crystal seeds and blocking crystal growth. Therefore the resulting Ca phosphate particles are small and a potential source of mobile colloids (Inskeep and Silvertooth, 1988; Grossl and Inskeep, 1991).

Moreover, the mobilization and stability of P_{coll} is influenced by conditions which generally influence colloid mobilization, such as pH, ionic strength, and the ratio of divalent to monovalent cations. However, specific studies evaluating the effect of these parameters on mobilization and transport of P_{coll} are scarce. Hens and Merckx (2001) found significantly smaller concentrations of P_{coll} in forest soils compared to agricultural soils, which they attributed to the small pH of 3.2 in forest soils, for which inorganic colloids are either dissolved or immobile.

Overall, the majority of experimental findings suggest a colloid-mobilizing effect of P sorption in soils. Organic P, namely IHP, has a stronger positive effect on colloid mobility and stability than ortho-P, which may indicate a special risk of organic fertilizers. The complex interplay of P sorption with organic matter, pH, ionic strength, types of cations, and other factors regarding the mobilization and stabilization of colloids has hardly been investigated yet.

1.4 Mobility and transport of colloidal P

Because of their positive charge, pure Fe oxides are extremely immobile in soils except under very alkaline conditions. In columns packed with aquifer solids, no breakthrough of Fe_{coll} occurred at pH < PZC indicating electrostatic interactions with the negatively charged matrix (Puls and Powell, 1992). However, in the presence of NaH_2PO_4 99% of applied Fe oxide colloids passed through the columns because of the increased repulsion between colloids and aquifer matrix. Similar results were presented by Zhang et al. (2003): In columns packed with sandy soil, Fe_{coll} transport was caused by P application. Thus, P sorption is not only able to enhance the mobilization of originally positively charged colloids by charge reversal but also their mobility in soils. Both charge reversal and decrease in particle size induced by P sorption, as observed by Celi et al. (1999), may enhance the mobility of colloids in soils (Karathanasis, 1999).

It was not investigated yet if the strong dispersing effect of organic P has consequences for the transport of P_{coll} in soils. However, there are some hints on the impact of organic P on P_{coll} transport in soils. Chardon et al. (1997) found that P leaching increased after pig slurry application compared to an application of mineral P-fertilizer. Maximum concentrations of P were observed in winter and spring, when NO_3^-- und Cl^-- concentrations were small, indicating a small ionic strength of drainage water. Therefore the authors assumed that DOM and colloids mediated P transport. Comparing manured and unmanured soils in a column experiment, Makris et al. (2006) found that applied water-dispersible soil colloids enhanced the leaching of particulate organic and inorganic P from soils columns. Preedy et al. (2001) compared effects of slurry and mineral fertilizer application on P export from a grassland soil. They detected larger organic and particulate P concentrations in lysimeter discharge of the slurry variant, which they attributed to the high mobility of dissolved organic P forms in soils. Furthermore the authors concluded that slurry particles themselves acted as carriers for P transfer. McGechan and Lewis (2002) also mentioned the input of large quantities of colloid-sized particles and P by slurry application, which in combination provide an additional important source of P_{coll}. Karathanasis and Johnson (2006) showed that colloids originating from poultry manure are mobile in undisturbed soil columns. However, the large salt concentration of fertilizer may counteract the mobility of these colloids as was reported for sewage sludge by Han and Thompson (1999).

Factors such as the soil water regime, which generally influence the transport of colloids, do also influence the transport of P_{coll}: In a column experiment Motoshita et al. (2003) found a larger accumulated mass of P_{coll} at a smaller irrigation rate and explained their observation with a diminished contact between the mobile and immobile phase at larger irrigation rates. The results seem to contradict e.g. a study of de Jonge et al. (2004a), in which they found a positive correlation between macropore flow water velocity and the accumulated mass of particulate P. Also Stamm et al. (1998) and Laubel et al. (1999) showed that particulate P is mainly transported via preferential flow paths and rapid macropore flow. It seems as if the transport, but not the mobilization of colloidal/particulate P is enhanced by large flow water velocities. However, it has to be taken into

account that large water flow velocities in soils (e.g. during heavy rainfall events) often correlate with small ionic strengths, which enhance colloid mobilization (Kaplan et al., 1993). During rain simulation experiments de Jonge et al. (2004a) and Laubel et al. (1999) observed a first flush effect of particulate and P_{coll} leaching, which is in accordance with other studies generally dealing with colloids (as reviewed by DeNovio et al., 2004). Another important process that mobilizes colloids and increases the transport of P_{coll} is plowing (Ulen, 2004; Schelde et al., 2006), which is in accordance with a study of Watts et al. (1996), who observed the same influence of plowing on the mobilization of dispersible clay.

Despite the fact that a promoting effect of P sorption on the transport of P_{coll} has been documented in laboratory experiments, such an effect has not been demonstrated unambiguously under field conditions. In fertilization experiments differentiation between P_{coll} released from soils and P_{coll} already contained in manure is difficult. Moreover, leaching of P_{coll} under field conditions seems to be triggered by several factors including P fertilization, rapid flow, and/or plowing. Further, concentrations of P_{coll} may change depending on soil depth.

1.5 Environmental significance of colloidal P in soils

Most studies addressing P_{coll} analyzed surface waters and groundwater. Comparable to soils, Fe_{coll} seems to be the most important sorbent of organic and inorganic P in surface waters and groundwater (Buffle et al., 1989; Mayer and Jarrell, 1995; Lienemann et al., 1999). Humic substances may be associated with Fe-P colloids (Shaw et al., 2000). Colloidal P appears in anoxic as well as in oxic zones of groundwater and lakes (Gschwend and Reynolds, 1987; Buffle et al., 1989; Lienemann et al., 1999) and comprises up to 50% of total P in surface waters (Mayer and Jarrell, 1995; Haygarth et al., 1997). It has been shown that P associated with colloids such as Fe oxides is available to algae (Dorich et al., 1985).

Indirect hints on P_{coll} in soils were found in studies that documented an accumulation of P with decreasing soil particle size, i.e. P was accumulated in the clay fraction. Soil components occurring in the clay fraction are a potential source for soil colloids and therefore it is very likely to find P associated with soil colloids

(Choudhury, 1988; Guzel and Ibrici, 1994; Agbenin and Tiessen, 1995; Ogaard, 1996). In column experiments conducted by Hesketh et al. (2001), outflow P concentrations were correlated with the concentration of suspended material. Thus, the authors concluded that the transport of P was facilitated by particulate soil material.

Colloidal P concentrations measured in soil extracts are also an indirect indication of P_{coll} in soils. Heathwaite et al. (2005) developed a soil test for P_{coll}, which is based on an extraction of fresh soil samples with H_2O and 0.01 M $CaCl_2$ and a filtration < 2 µm. The difference of total P concentrations extracted with H_2O and $CaCl_2$ is supposed to represent the P_{coll} fraction. However, like other extraction techniques, the soil test rather quantifies the concentration of P_{coll} that is potentially mobile than the amount of P_{coll} that will actually be leached under field conditions. Up to now, the test has not been validated against field measurement of P_{coll} losses.

Further hints on the quantity of P_{coll} export were found in studies in which particulate P was detected in column outflow and in seepage or drainage water (e.g. Heckrath et al., 1995; Stevens et al., 1999; Jensen et al., 2000; de Jonge et al., 2004a). Particulate P contributed between 10 and 70% to total P leaching (five exemplary studies are cited in Table 1.1). Particulate P concentrations showed a seasonal variability with a maximum in springtime (Turner and Haygarth, 2000). On the one hand, in springtime the ionic strength of soil leachate is low, which enhances colloid release. On the other hand, the authors ascribed the increase of particulate P_{coll} in spring to an increased release of P from soil microbial biomass. Yet, these studies do not take the whole range of particle-bound and P_{coll} into account, because mostly particle sizes > 0.45 µm were measured.

Up to now only few studies dealt with the explicit detection of P_{coll} in undisturbed soil, mainly because undisturbed sampling of colloids in soils is much more difficult than in surface water or groundwater (Kretzschmar et al., 1999). The results of the available studies show that often P_{coll} concentrations exceed 100 µg P l^{-1}, which is supposed to be critical, because beyond eutrophication of surface waters is enhanced (Breeuwsma et al., 1995). The proportion of P_{coll} ranges from 1 to approximately 80% of P in drainage water depending on soil

Table 1.1: *Particulate P in soil drainage and soil solution*

authors	experiment	P form, size range	chemical analysis of P	proportion of particulate P on total P %	concentration of particulate P mg P l^{-1}	total P, plant available P	pH	soil texture	comments
Heckrath et al. (1995)	drain water (65 cm depth)	particulate P > 0.45 µm	TP†	23-68	0.01-1	7-90 mg Olsen P kg^{-1}	7.6-8.2	silty loam-silty clay loam	critical threshold of Olsen P above which TP increases; authors hypothesize that small P loads cause higher particulate P fraction because of high surface affinity
Stamm et al. (1998)	drain water samples (50 and 100 cm depth)	colloidal P > 0.05 µm and < 0.45 µm particulate P > 0.45 µm	TP	12 (50 cm) 22 (50 cm), 44 (100 cm)	0-0.02		5.5-7.3	loamy	P transported mainly via preferential flow paths
Turner and Haygarth (2000)	monolith lysimeters (135 cm depth)	particulate P > 0.45 µm	TP RP UP*	 11 33	 0.01-0.03 0.01-0.13	879-1048 mg TP kg^{-1} 15-75 mg Olsen P kg^{-1}	5.7-7.3	silty clay-sand	soil P status without influence on particulate P
de Jonge et al. (2004a)	undisturbed soil columns (topsoil)	particulate P after centrifugation (5420 g, 10 min)	PIP§ POP¶	63 18	0.06-0.55	734 mg TP kg^{-1} 44 mg Olsen P kg^{-1}	7.3	sandy loam	colloidal P positively correlated with clay content , mass of particles, continuous macropores and macropore flow velocity; negatively correlated with electrical conductivity
Schelde et al. (2006)	drain water (1.1 m depth) from field plot experiments	particulate P > 0.24 µm	TP MRP	23-87	0.19-3.6	11-51 mg Olsen P kg^{-1}	6.3-7.1	sandy loam	macropore flow; decrease in particulate P fraction after slurry application; plowing mobilizes particulate P

†TP total phosphorus after persulfate digestion
‡(M)RP (molybdate) reactive P after Murphy and Riley (1962)
§PIP particulate inorganic P (TP-dissolved reactive P)
¶POP particulate organic P (TP- total dissolved P) – PIP
*(M)UP (molybdate) unreactive P (TP-RP)

characteristics, but also on the method used to determine colloids (Table 1.2). Hens and Merckx (2001, 2002) reported that soil solutions of sandy soils from pasture and arable land in Belgium contained colloidal particles comprising 45-60% of total P in the fraction < 0.45 µm. In forest soils they detected less than 30% of total P passing a filter < 0.45 µm in the colloidal fraction, which they ascribed to the small solution pH of 3.2. Unfortunately techniques for sampling and detecting P_{coll} in soil solution are not uniform yet. Thus, different studies can not directly be compared with each other and general trends can hardly be detected, such as an influence of soil depth or of the soil P saturation status on P_{coll} concentrations in drainage water.

Overall, I may state that P_{coll} forms an important, but not the dominating fraction of total P in soil solution or in drainage water of undisturbed soils.

1.6 Conclusions derived from the state-of-the-art

Colloids play a significant role as carriers for P through soils to drains and groundwater. The sorption of P to oxides and clay minerals enhances the stabilization of colloidal suspensions in laboratory experiments. These findings give reason for concern that an accumulation of P in soils as a consequence of excessive fertilization, especially with manure, might trigger the mobilization of P_{coll}. Further experiments under laboratory and field conditions have to be conducted to clarify the influence of P accumulation, for example via fertilization, on the mobilization and transport of P_{coll}.

Especially transient pertubations of the equilibrium between P in soil solution, P sorbed to potentially mobile colloids, and P sorbed to the stationary solid phase cause leaching of P_{coll}. Typical perturbations are storm flow events or mechanical disturbances like plowing. Data regarding the contribution of P_{coll} to total P concentrations in soil solution or drainage vary widely from 1 to 80% because of the multitude of factors controlling the leaching of P_{coll}, but also because of the diversity of methods that are used to determine P_{coll} concentrations. Therefore harmonization of sampling protocols and methods, e.g in the framework of the International P workshops, seems vital to gain additional information from in-situ studies.

Table 1.2: *Colloidal P in soil drainage and soil solution*

authors	experiment	P form, size range	chemical analysis of P	proportion of colloidal P on total P	concentration of colloidal P	total P, plant available P	degree of P saturation	pH	soil texture	comments
				%	mg P l^{-1}					
Haygarth et al. (1997)	seepage water (free drained, 135 cm depth)	< 0.45µm[§] > 1000 MW[¶]	MRP[†]	6	0.005	0.08 mg P l^{-1} (TP)		7.2		
Shand et al. (2000)	soil solution from organic topsoil gained by centrifuging (1000 g, 60 min)	< 1.2µm[§] > 0.22 µm[§] (1st experiment) < 0.45 µm[§] > 10 KD[¶] (2nd experiment)	TP[‡]	1st experiment 35 2nd experiment 83	1.2 0.54	65 mg P kg^{-1} (acetic acid extractable)		5		
Hens and Merckx (2001, 2002)	soil solution (topsoil) gained by centrifuging (1000g)	< 0.45µm[§] > 0.025 µm[¶]	TP MRP (malachite green and Murphy & Riley method)	45-65 (arable, pasture) 1-30 (forest)	0.62 (arable) 2.2 (pasture) 0.03-0.22 (forest)	574 mg P kg^{-1} (oxalate extractable) (arable) 521 (pasture) 12 (forest)	0.09-0.44	6.1 (arable, pasture) 3.2 (forest)	sandy loam	authors emphasize importance of excessive fertilization, pH and ionic strength for colloid mobilization; indications for associations between humic substances, Fe and/or Al and P
Motoshita et al. (2003)	repacked topsoil columns (20 cm depth)	< 1 µm[§$]	TP	14-19	0-1, max. 2	0.17% total P 93 mg Olsen P kg^{-1} soil		8.2	loam	higher colloidal P concentration at lower irrigation (10 vs 30 mm h^{-1})
Ulen (2004)	drain water samples (1 m depth)	< 1.2µm[$] > 0.2 µm[§]	TP	35	0.01-0.3				clay	destroying grass sod by plowing mobilizes colloidal P

[§] membrane filtration
[¶] ultrafiltration
[$] (ultra)centrifugation
[†] (M)RP (molybdate) reactive P after Murphy and Riley (1962)
[‡] TP total phosphorus after persulfate digestion

1.7 Objectives

This thesis was written following the publication “Adsorption controls mobilization of colloids and leaching of dissolved phosphorus” by Siemens et al. (2004). In this publication the authors found out that large concentrations of dispersible P were released from soil with large DPS and that an addition of P induced further dispersion of soil particles. My intention was to elucidate the mechanism of P-induced colloid mobilization. In a series of batch and column experiments of increasing complexity I came step by step from a pure model system to quasi field conditions and investigated, in detail, the following five hypotheses:

a) The sorption of P to Fe oxides, which are sorbed or precipitated to a quartz sand matrix, causes the dispersion of Fe oxides from the matrix. There is a critical threshold of P accumulation for the release of Fe oxide colloids. (Chapter 2)

To test this hypothesis I conducted batch experiments with two model systems consisting of goethite adsorbed and precipitated to a quartz sand matrix and added increasing amounts of P.

b) The threshold of P accumulation estimated in pure systems consisting of P, goethite and quartz is also valid for the P-induced release of colloids from sandy soils. Dominant colloidal sorbents for P in soils are Fe and Al oxides. (Chapter 2)

In a similar experimental design as in chapter 2 I investigated P-induced dispersion of colloids from two sandy subsoils.

c) Organically-bound P, an important fraction of total P in organic manure and soils, enhances the dispersion of Fe oxides and soil colloids more effectively than inorganic P. (Chapter 2)

Both experiments presented in chapter 2 were performed with ortho-P and IHP to compare the dispersing power of inorganic and organic P.

d) The accumulation of P in sandy soils enhances the release of P_{coll} from soils and there is a critical P saturation above which concentrations of P_{coll} increase sharply. (Chapter 3)

In a batch experiment a soil sample collective from several fertilization experiments with different DPS was extracted without an addition of P to determine colloid mobilization depending on long-term accumulation of P in fertilized soils.

e) An increasing P saturation of soil increases the leaching of P_{coll} under field conditions. (Chapter 5)

In chapter 5 columns with undisturbed sandy soils were irrigated with artificial rain solution to investigate the mobility and transport of colloids and P_{coll} depending on the soil P saturation status.

Chapter 4 is not dealing with the P-induced dispersion of colloids, but is a preliminary test for the column study of chapter 5. In a column experiment I investigated the colloid-sampling efficiency of five different lysimeter systems (with a 1.2 µm membrane, a 10 µm membrane, a porous plate, a wick and zero-tension) to select an optimal sampling system for the following column experiment. The experiment was conducted under unsaturated conditions using ^{59}Fe labeled goethite as model colloid.

2 Phosphorus-induced mobilization of colloids - model systems and soils

2.1 Abstract

An increasing P saturation of sandy soils may intensify losses of P_{diss} to groundwater. I hypothesized that an increasing sorption of P also mobilizes soil colloids such as Fe oxides, because the adsorption of P shifts the surface charge to more negative values and enhances the colloidal stability of these oxides. Single goethite particles adsorbed to fine quartz sand and precipitated goethite coatings on coarse quartz sand were used as model systems. Also, samples from a cambisol Bw-horizon and a gleysol Bg-horizon were investigated. I conducted batch experiments with increasing concentrations of ortho-P and IHP. The adsorption of P and the dispersion of colloids were determined by measuring P, Fe, Al and C concentrations in supernatants before and after ultracentrifugation. Dispersed colloids were characterised by optical density, zeta potential and particle size. The addition of P caused the mobilization of goethite and soil colloids if a critical P saturation corresponding to a zeta potential of about -20 mV was exceeded. To induce colloid mobilization, 1-2 orders of magnitude larger equilibrium concentrations of P_{diss} were necessary for soil samples than for model systems. The adsorption of IHP reduced the zeta potential of colloids more effectively per mol P than the adsorption of ortho-P. Environmentally relevant concentrations of P_{coll} (> 0.1 mg P l^{-1}) were released from soil samples at equilibrium concentrations of P_{diss} < 0.1 mg P l^{-1}. I concluded that sorption and accumulation of P in sandy subsoils as a consequence of excessive fertilization might induce the mobilization of colloids and P_{coll}.

2.2 Introduction

Besides erosion and surface runoff, subsurface leaching contributes to P losses from farmland (James, 1996; Turner and Haygarth, 2000, Siemens et al., 2004). Roughly 30% of diffuse P emissions in Germany originate from drainage and groundwater (Umweltbundesamt, 2006). Eutrophication of surface waters can occur at concentrations larger than 0.65 µmol total P l^{-1} (0.02 mg P l^{-1}, Sharpley and Rekolainen, 1997). Therefore already a small increase of P concentrations in drainage water may have environmental implications. In sandy soils P_{diss} concentrations in drainage water increase sharply, if the soil P saturation (DPS) exceeds a certain critical value (McDowell and Sharpley, 2001b). The DPS is defined as the ratio of oxalate-extractable P and Fe+Al (van der Zee and van Riemsdijk, 1988; Breeuwsma and Silva, 1995), which are the most important sorbents for P in sandy soils (Beek, 1978). From long-term sorption and desorption experiments, conducted with sandy soils in the Netherlands, it can be concluded that concentrations of P_{diss} larger than 100 µg l^{-1} in drainage occur at DPS larger than 25% (van der Zee et al., 1988; Schoumans and Groenendijk, 2000).

Recently, P_{coll} in drainage and soil solution as an additional mobile form of P has attracted increasing attention. Colloidal P may account for up to 80% of total P in soil water samples (Haygarth et al., 1997; Shand et al., 2000; Hens and Merckx, 2001). Several factors, such as ionic strength, pH and the composition of soil solution, affect the mobilization and transport of colloids. Colloid release rates increase with decreasing ionic strength and increasing pH (e.g. Grolimund et al., 1996; de Jonge et al., 2004b). Besides, sorbed substances may influence the mobilization and transport of colloids. The adsorption of P decreases the surface charge of its sorbents (Stumm and Sigg, 1979). Thus, the originally positive surface charge of Fe and Al oxides changes to negative (Puls and Powell, 1992, Celi et al., 1999). Whilst the effect of P adsorption on the surface charge and colloidal stability of suspensions has been thoroughly studied, it is still unclear to which extend the sorption of P causes the displacement of colloidal particles that are attached to surfaces such as quartz sand or that are part of micro aggregates.

Zhang et al. (2003) found that an application of P to sandy soil columns induced the mobilization of Fe_{coll} and P_{coll}. Similarly, Siemens et al. (2004) showed in batch experiments that the adsorption of P caused the release of P_{coll} from sandy soils and supposed the existence of a certain DPS marking a change point for the release of P_{coll} from soils. In another former study I analysed long-term fertilization trials with varying DPS in batch experiments (Ilg et al., 2005). However, I did not detect a distinct point of P saturation above which the release of P_{coll} sharply increased, but found a positive linear correlation between DPS and the release of P_{coll}. The lack of a distinct trigger DPS may be due to the effect of other factors such as pH, solute concentrations and/or interactions with organic matter that mask or modify the pure effect of P sorption on Fe and Al oxide surface charge. Furthermore I assume that the variability of soil oxides, varying associations between oxides and other soil components as well as different P_{diss} species lead to a range of critical DPS for the mobilization of P_{coll} (Ilg et al., 2005).

The type and characteristics of oxides in soils are the result of different physico-chemical conditions during pedogenetic processes. Iron oxides in the subsoil of gleysols build thick cross-linked, multilayers around mineral surfaces due to a long-lasting precipitation of Fe(II) (Cornell and Schwertmann, Plate 16/I number D and pp. 267, 2003). In subsoils of cambisols Fe oxides originating from weathered silicates accumulate at mineral surfaces. Assuming given concentrations of dithionite-soluble Fe oxides and clay, these oxide layers are probably less thick and discontinuous in cambisols than in gleysols.

In addition to the variability of pedogenetic oxides, different species of P_{diss} influence the dispersion of colloids to different extent. Dissolved P can generally be divided into a fraction of organic P (e.g. IHP) and inorganic P (mainly ortho-P). The sorption of IHP, one of the most stable and therefore most abundant organic P forms in soils (Anderson, 1980), decreases the surface charge of Fe oxides more than the sorption of ortho-P (Celi et al., 2001). Therefore a stronger dispersing effect can be expected for IHP than for ortho-P.

The objective of my research was to study the effect of P addition on colloid mobilization from solid matrices. I hypothesize that (i) an increasing addition of P mobilizes colloids from quartz sand and from soils above a distinct level of P

accumulation, because sorbed P shifts the surface charge of its sorbents to more negative values and may induce their repulsion from the solid matrix; (ii) the nature of Fe oxides in model and soil systems influences the amount of sorbed P necessary for the dispersion of colloids; (iii) the mobilizing effect of IHP is stronger than that of ortho-P, because of its stronger effect on the surface charge of P sorbents. To test these hypotheses I conducted batch experiments with two model systems (goethite adsorbed and precipitated on a quartz sand matrix) and two soil samples (a Bw-horizon from a cambisol and a Bg-horizon from a gleysol).

2.3 Materials and methods

2.3.1 Model systems

Fine and coarse quartz sand with a particle size distribution of 0.06-0.3 mm (GEBA, Sand-Schulz, Germany) and 0.6-1.2 mm respectively (DORSILIT®, Sand-Schulz, Germany) was calcined at 1000°C for two hours to remove organic residues. Afterwards I removed impurities of the quartz sand like oxides, clay minerals or feldspars by digestion in HCl (30%) at 90°C for 10 days. Finally, the sand was washed several times with deionised water and dried at 110°C. The equilibrium pH in a water extract (1:2.5) was 5.5. At this pH the surface potential of quartz measured as zeta potential should be around -65 mV in 1 mmol NaCl l^{-1} (Elimelech et al., 2000) or -50 mV in 1 mmol KCl l^{-1} (Johnson, 1999). X-ray diffraction (XRD) measurements of my treated quartz sand using an XRD-apparatus (STOE Stadi P) with a G111 monochromator, Bragg-Brentano-geometry and Cu-K_α-radiation showed pure quartz.

To prepare a system of single goethite particles sorbed to quartz sand, I used commercial Bayferrox 920 goethite (Lanxess, Germany). The oxide was purified as described by Scheidegger et al. (1993) with diluted HNO_3 (pH 2) and NaOH (pH 10) to remove 0.5% water-soluble residues (Lanxess, Germany) and other potential impurities. Afterwards I washed the goethite with deionised water and brought it to neutral pH with diluted HNO_3. The X-ray diffraction of the purified mineral using an XRD-apparatus with Debye-Scherrer-geometry and Mo-K_α-radiation showed pure goethite.

One hundred and fifty gram of the purified Bayferrox 920 goethite were suspended in 1 l of 5 mmol l^{-1} $NaNO_3$ and shaken end-over-end at 10 rpm for 24 h with 1 kg of the fine sand (modified after Scheidegger et al., 1993). Afterwards the sand was washed free from surplus goethite until the washing water remained visibly clear. The coated sand was dried at 30°C. An extraction with dithionite as described by Schlichting et al. (1995) resulted in a Fe oxide concentration of 16 µmol FeOOH g^{-1} sand.

The multilayer of goethite precipitated on coarse sand was produced by oxidizing Fe(II) to Fe(III) with a subsequent precipitation of goethite. Coarse quartz sand was percolated in a gas-tight column with an anoxic solution under unsaturated conditions. The infiltration solution consisted of 2 mmol l^{-1} $FeCl_2$ and was adjusted to pH 5.6 by 2.6 mmol l^{-1} HCO_3^- and gassing with N_2:CO_2. 64:36. During infiltration, a mixture of air:CO_2 64:36 passed the column bottom-up. In combination with HCO_3^- the latter controlled the pH and, thus, also the oxidation rate of Fe(II) in such a way that solely goethite crystallized on the quartz surface. Contrary to the other model system coarse sand had to be used, because only with coarse sand a uniform gassing of the unsaturated column and, thus, a uniform goethite precipitation could be ensured. Electron diffraction and TEM images showed a pure goethite. The Fe concentration was 21.4 µmol Fe g^{-1} sand.

The specific surface area of the minerals was determined with a Quantachrome Autosorb-1 automated gas sorption system (Quantachrome, Syosset, NY) using N_2 (original Bayferrox goethite) or krypton (coated sand). Approximately 100 mg of goethite and 10 g of coated sand respectively were degassed until the rate of pressure increase by vapour evolution was below 1.3 Pa min^{-1} within a 1-min interval. Helium was used as a backfill gas. I used adsorption at 77 K using an 11-point BET (p/p_0=0.05-0.3) (Brunauer et al., 1938).

2.3.2 Soils

I used two subsoils from a site called “Langes Luch” (52°22´ northern latitude and 13°39´ western longitude) located in the southeast of Berlin in Germany (Table 1):

1. a Bw-Horizon of a cambisol
2. Fe oxide mottles of a Bg-Horizon of a gleysol (FAO, 2006).

Both soils originate from the same catena under pine forest described by Alaily and Brande (2002). The climate at the site is temperate and oceanic-continental. Mean annual precipitation is 600 mm and the average annual temperature 8.9°C. Soil samples were air-dried and sieved to a particle size of < 2 mm. I chose the site because cambisol and gleysol originate from the same parent material and because of small P concentrations in subsoils compared to agricultural soils.

Table 2.1: *General characteristics of soil samples*

		Bw	Bg
soil type		cambisol	gleysol
soil texture		fine sand	fine sand
pH		4.6	4.4
electrical conductivity	/µS cm^{-1}	33	76
C		1.17	1.04
N	/g kg^{-1}	0.04	0.05
Al_d		1.87	2.25
Al_o		1.36	1.85
Fe_d	/g kg^{-1}	1.36	3.0
Fe_o		0.442	2.31
P_o		0.073	0.184
DPS*	/%	6	13

Al_d, Fe_d, dithionite extractable Al and Fe
Al_o, Fe_o, P_o, oxalate extractable Al and Fe
DPS, degree of Phosphorus saturation

I measured organic C and nitrogen (N) (vario EL III, Elementar, Hanau, Germany) as well as pH and electrical conductivity in the supernatant of aqueous soil extracts (10 g soil, 25 ml H_2O, inoLab pH/Cond, WTW, Weilheim, Germany). Furthermore dithionite-extractable Fe and Al according to Schlichting et al. (1995) and oxalate-extractable Fe, Al and P according to Schwertmann (1964) were determined. I measured Al concentrations by atomic absorption

spectrometry (Model 1100B, PerkinElmer, USA) with a detection limit of 37 µmol Al l^{-1}. Iron concentrations were measured photometrically using the method of Dominik and Kaupenjohann (2000): Fe(III) was reduced to Fe(II) with ascorbic acid, sequestered as ferrozine complex and measured at a wavelength of 562 nm. The detection limit was 0.3 µmol Fe l^{-1}. Concentrations of P were determined photometrically according to the method of Murphy and Riley (1962) at a continuous flow analyser (Skalar, Erkelenz, Netherlands) with a detection limit of 0.3 µmol P l^{-1}. In the continuous flow analyzer P compounds are transferred from the sample flow line to an analyte flow line in a dialysis chamber. Therefore the method minimizes the hydrolyses of organic P compounds during the molybdenum-blue colour reaction (Baldwin, 1998) and measures mainly concentrations of ortho-P. Throughout the experiment all vessels were rinsed with 0.1 M HNO_3 prior to P analyses. The DPS was calculated according to Breeuwsma and Silva (1992) and van der Zee and de Haan (1994):

$$DPS = \frac{[P_o]}{0.5([Fe_o]+[Al_o])} * 100\% \qquad (1)$$

where $[P_o]$, $[Fe_o]$ and $[Al_o]$ are the concentrations of oxalate-extractable elements in mmol kg^{-1}.

2.3.3 Batch experiments with ortho-phosphate and inositol hexaphosphate

In batch experiments 7 g of goethite-coated sands and soils were shaken with 50 ml of 0.05 M $NaNO_3$ and increasing concentrations of either NaH_2PO_4 or IHP as Na salt in 100 ml PE bottles for 24 h end-over-end at 10 rpm. The levels of P-addition were derived from sorption isotherms of goethite reported by Strauss et al. (1997) for ortho-P and by Celi et al. (1999) for IHP (Table 2). Graduations between minimum and maximum were evenly distributed on a logarithmic scale. Before starting the experiment all solutions were adjusted to pH 5.7 for the model systems and to pH 4.5 for the soils with NaOH and HNO_3. A pH of 5.7 was chosen for the model systems to mimic a typical pH of sandy agricultural soils. We decided to keep the pH of the soil samples close to their original pH to avoid strong disturbances of their inherent pH buffering system. For the same

reason, we allowed a variation of pH as a consequence of P adsorption. All experiments were run in triplicate.

Table 2.2: *Range of amounts of ortho-phosphate and inositol hexaphosphate (IHP) added to model systems and subsoil samples and resulting changes of average pH in supernatants*

			adsorbed goethite system	precipitated goethite system	Bw	Bg
ortho-P	/ µmol P g^{-1}		0-2.33	0-1.03	0-147	0-64.2
IHP			0-0.63	0-0.65	0-61.7	0-71
	blank		5.4	5.4	4.4	4.2
ortho-P	start of colloid mobilization	pH	5.7	5.9	4.9	4.6
	maximum P addition		5.8	6.1	5.3	4.9
	blank		5.2	5	4.3	4.2
IHP	start of colloid mobilization	pH	5.8	5.6	4.9	4.7
	maximum P addition		6.7	6.2	5.9	5.7

After shaking, the suspended solids of the model systems were allowed to sediment for one hour before the supernatant was decanted to analyse only colloidal particles. According to Stokes' law, particles > 1 µm settled during that time. Afterwards the supernatants were ultracentrifuged with 300.000 g for one hour (Beckman Optima TL, Unterschleissheim, Germany). The supernatants of soil samples were filtered with paper filters (No 512 ½, Whatman Schleicher and Schuell, Dassel, Germany) and 1.2 µm cellulose acetate filters (Sartorius, Göttingen, Germany). Filtration was performed to ensure that only particles of the colloidal fraction < 1.2 µm were analysed. Since no clogging of filters was observed, the actual size cutoff should have been similar to the pore size of the filters. Soil filtrates were ultracentrifuged with 150.000 g for two hours (Optima L-90k ultracentrifuge, Beckmann Coulter, Krefeld, Germany). Assuming a density larger than 2 g cm^{-3} and a spherical shape of colloids, both ultracentratifugation treatments should have sedimented particles larger than 10 nm. Ultracentrifugation allowed us to determine P_{coll}, Fe_{coll}, Al_{coll} and colloidal C (C_{coll}) concentrations as the difference between concentrations in filtrated extracts

(total concentration) and ultracentrifuged (dissolved fraction) solutions. In the following element concentrations in ultracentrifuged solutions are denoted as “dissolved”.

Electrical conductivity and pH were measured in the supernatants (inoLab pH/Cond, WTW, Weilheim, Germany). To characterise the released colloids I determined the average particle size (High Performance Particle Sizer, HPP 5001, Malvern Instruments, United Kingdom) and electrophoretic mobility (zeta sizer DTS 5200, Malvern Instruments, United Kingdom). The electrophoretic mobility was converted with the Smoluchowsky equation to zeta potential (2).The zeta potential refers to the electrostatic potential generated by the accumulation of ions at the surface of a colloidal particle and is a central parameter determining the stability and mobility of colloid suspension.

$$\zeta = \mu \frac{\eta}{\varepsilon_0 \cdot \varepsilon_r} \quad (2)$$

where ζ denotes the zeta potential, μ the electrophoretic mobility, η the dynamic viscosity of water, ε_0 the general dielectric constant, ε_r the dielectric constant of water.

The optical density of supernatants, an indirect and dimensionless measure of the colloid concentration, was measured using a photometer at a wavelength of 525 nm according to Kretzschmar et al. (1997) with a detection limit of an absorption of 0.008 (specord photometer, Jena, Germany). Ultracentrifugation and the measurement of colloid characterising parameters were finished within one day after the batch experiment to avoid coagulation.

In the model system samples Fe oxides were destroyed before Fe analyses by digestion with 0.022 M oxalic acid and 0.011 M ascorbic acid in a 95°C water bath for one hour. Total P concentrations in filtrated and ultracentrifuged samples were determined after adding 1.4 ml of a solution of 150 mmol $K_2O_8S_2$ l^{-1} and 180 mmol H_2SO_4 l^{-1} to 7 ml of samples and autoclaving at 121°C for one hour (modified after Rowland and Haygarth, 1997). Following this oxidation step, 1 ml of 188 mmol ascorbic acid l^{-1} was added and samples were digested at 100°C for one hour to remove excess oxidizing agent and to reduce residual Fe oxides. Ortho-P concentrations were measured with the method of Murphy

and Riley (1962). I determined IHP concentrations in model system samples by inductively coupled plasma mass spectrometry (ICP-MS, Varian, Australia). The detection limit was 0.2 µmol l^{-1} P. Iron concentrations were quantified photometrically using the method of Dominik and Kaupenjohann (2000). Aluminium concentrations were measured using an ICP-OES (Vista Pro, Varian, Australia) with a detection limit of 3.7 µmol Al l^{-1}. Organic C concentrations were determined using a TOC analyser (TOC-Analyser 5050A, Shimadzu Europa GmbH, Germany) with a detection limit of 83 µmol C l^{-1}.

2.3.4 Microscopic analyses of model systems

I prepared scanning electron microscopic (SEM, Hitachi S-4000, Japan) images for the system with adsorbed goethite. Transmission electron microscopic (TEM, JEOL JSEM 200B, Japan) images were taken of the original Bayferrox goethite and of dispersed goethite crystals after batch experiments. Furthermore, TEM images of the precipitated goethite system were taken (Phillips EM 400). The surface areas of dispersed goethite colloids could not be measured with gas adsorption because of small sample volumes. Therefore I measured the diameter and length of single goethite crystals on SEM and TEM images and calculated the surface and mass of individual colloids assuming a cylindrical shape and a density of 4.1 g cm^{-3}. The specific surface area was then calculated as:

$$\text{specific surface area} = \sum_{i=1}^{n} surface\ area \Big/ \sum_{i=1}^{n} mass \qquad (2)$$

n= number of colloids (152-459)

The polydispersity of specific surfaces was calculated as

$$s^2 = \frac{1}{N-1} \sum_{i=1}^{n} (d_i - d)^2 \qquad (3)$$

and

$$d^* = \frac{s * 100}{d} \qquad (4)$$

where s^2 denotes the variance, N the number of colloids, d the average surface area, d_i the surface area of sample i and d* the polydispersity as relative, percental standard deviation.

Because the goethite crystals in the system with precipitated goethite were less crystalline than in the system with adsorbed goethite, single crystal contours were difficult to detect and had no uniform shape. Thus, the procedure outlined above to calculate specific surface areas could be applied only to the system with adsorbed goethite. The specific surface area of original Bayferrox goethite and of goethite sorbed to sand was determined with the geometric method and gas adsorption measurements to check the comparability of both methods.

2.3.5 Calculations and statistical evaluations

To characterise the C content of soil colloids I calculated the quotient of C_{coll} concentrations and optical density (mg C l^{-1} absorbance^{-1}). Furthermore, I estimated the quantitative contribution of Fe and Al oxides and organic matter as sorbents for P_{coll} in soil samples. To this end I combined Fe_{coll} and Al_{coll} concentrations with the following assumptions to estimate the maximum sorption capacity of Fe_{coll} and Al_{coll} for P according to equation (5): An average specific surface area of 60 m^2 g^{-1} for goethite (Schwertmann, 1988) and 280 m^2 g^{-1} for ferrihydrite (McLaughlin, 1981) as the two most common Fe oxides in soils of the temperate climate; a specific surface area of 250 m^2 g^{-1} for an amorphous Al hydroxides (Lookman et al., 1994); a maximum P sorption capacity of 2.5 µmol ortho-P m^{-2} (Strauss et al., 1997), 3.84 µmol IHP-P m^{-2} (Celi et al., 1999) for Fe oxides and of 6.2 µmol P m^{-2} for Al oxides (Lookman et al., 1994).

$$P_{coll\text{-}pot} = a * n * M * conc*10^{-6} \qquad (5)$$

$P_{coll\text{-}pot.}$ - concentration of P_{coll} potentially bound to goethite, ferrihydrite or Al oxide colloids [µmol l^{-1}]

a - average specific surface area of oxides [m^2 g^{-1}]

n - maximum P sorption capacity [µmol m^{-2}]

M - molar mass of oxides [g mol^{-1}]

conc - concentrations of colloidal Fe and Al oxides [µmol l^{-1}]

It has to be noted that the results of these calculations are rough estimates, which should be interpreted rather as a kind of orientation than as exact numbers. To estimate the quantitative contribution of colloidal organic matter for P sorption, I calculated the C/P ratios from C_{coll} and P concentrations.

Arithmetic means and standard deviations were calculated for all data. Negative calculated colloid concentrations were set to zero. Statistical calculations were done using STATISTICA 6.0 software (StatSoft, Tulas, USA). I used only non-parametric tests, because the number of replicates was too small to test the data for normality. I checked the significance of differences between mean values with the Mann-Whitney-U-Test and the Kruskal-Wallis H-test and correlations between parameters with Spearmans rank R. Using non-parametric partial correlation the influence of P sorption on zeta potential was quantified independently from pH (Hartung and Elpelt, 1992). Because non-parametric correlation analysis does not rely on metric differences between sample values, non-linear relationships, which I expect for relations between P adsorption and e.g. surface potential or dispersion of particles, can be analysed as good as linear relationships. To determine the variability of the specific surface area of the sand with adsorbed goethite 250.000 bootstrap samples were generated with the statistic software R (R Development Core Team, 2005). Bootstrapping is used to estimate distribution parameters by a resampling procedure with replacement (Shao and Tu, 1995). I used a level of significance of $p < 0.05$ for all tests.

2.4 Results

2.4.1 Microscopic analyses of coated sand and surface area measurements

The SEM image of the system with adsorbed goethite showed single goethite crystals randomly distributed over the quartz surface, which was only partially covered (Figure 1). In some cases goethite crystals lay one upon another or intersected, but did not form a continuous layer. The quartz surface was uneven and in holes and cavities goethite particles accumulated. After adding a P quantity exceeding a critical level, nearly all goethite crystals were removed from the even, exposed parts of the sand surface, whereas in holes and cavities no visual differences to the original system were detectable (Figure 2). The surface area of Bayferrox goethite and of coated sand determined with gas adsorption was comparable to the surface areas determined with the geometric method (Table 3). The surface areas of goethite colloids dispersed by an addition of ortho-P or IHP were significantly larger than that of the original goethite and goethite adsorbed to quartz sand. On the TEM image of the system with precipitated goethite longish crystals on the quartz surface with an inner lengthwise structure could be identified (Figure 3). These structures of the outer crystals had a thickness of 15-20 nm. Some of the crystals were arranged parallel, but in most cases perpendicular to the quartz surface. Iron oxides close to the quartz surface were grown so compact that no single crystals could be identified (Dominik et al., 2007). I could not measure, whether the surface area of dispersed particles released from precipitated goethite was different from that of sorbed goethite. Gas adsorption was not applicable, because the mass of dispersed goethite was too small. Further, based on TEM images dispersed goethite particles were too irregular to apply geometric methods for surface determination.

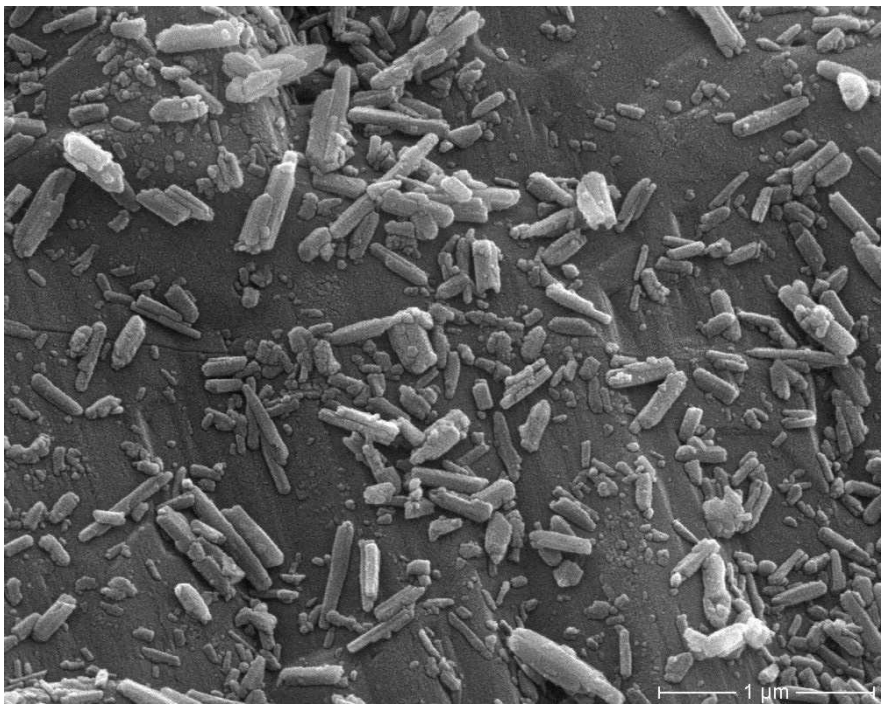

Figure 2.1: *Scanning electron microscopic image of the fine quartz sand coated with adsorbed goethite before the batch experiment with an addition of P*

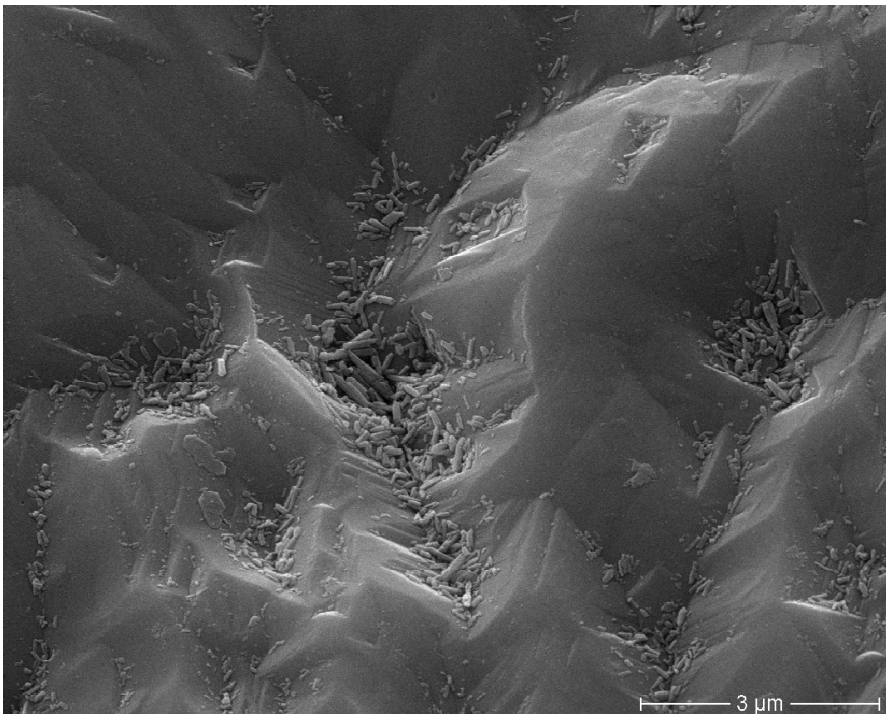

Figure 2.2: *Scanning electron microscopic image of the fine quartz sand coated with adsorbed goethite after the batch experiment with an addition of P*

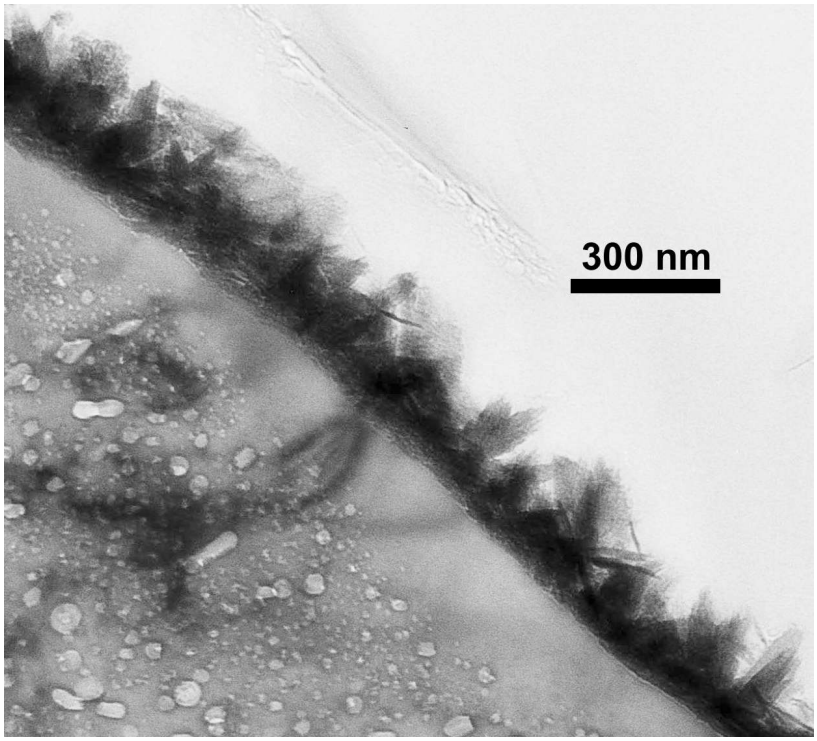

Figure 2.3: *Transmission electron microscopic image of the coarse quartz sand with precipitated goethite before the experiment with an addition of P*

Table 2.3: *Specific surface areas of goethite crystals and coated sand; standard deviations in parenthesis*

			adsorbed goethite				precipitated goethite
			original Bayferrox goethite	goethite on quartz sand	dispersed with ortho-P	dispersed with IHP	goethite on quartz sand
surface area	nitrogen/krypton adsorption	/m^2 g^{-1}	14.5	10.6			29
	SEM images			12.7 (0.42)			na
	TEM images		15.8 (0.67)		20.2 (0.51)	20 (0.82)	na
	number of colloids counted		152	181	423	459	
	polydispersity of surface area (equation 3 & 4)	/%	37	40	41	41	
	lower size cut-off of particles	/nm length/width	57/22	65/24	36/15	36/15	

na, no data available

2.4.2 Batch experiments

In all experiments pH increased with an increasing addition of P (Table 2). The increase was more distinct for the addition of IHP than for ortho-P. In experiments with model systems electrical conductivity ranged between 567 and 594 µS cm^{-1} and increased only slightly with increasing P addition. In the supernatants of soil samples electrical conductivity increased from 600 µS cm^{-1} to > 1000 µS cm^{-1} with increasing addition of P in all variants except for the Bg samples exposed to ortho-P. This increase in electrical conductivity was positively correlated with the concentrations of P_{diss} and colloids in the supernatant.

The addition of inorganic and organic P dispersed colloids from all investigated systems (Figure 4). The increase in optical density with increasing equilibrium concentrations of P_{diss} in supernatants was more pronounced for IHP than for ortho-P. This difference was significant for all systems except for the Bg horizon. The dispersion of adsorbed goethite from quartz sand started at an equilibrium concentration of P_{diss} of about 0.9 µmol ortho-P l^{-1} and of 0.5 µmol IHP-P l^{-1} and reached a maximum at P_{diss} concentrations only slightly larger than these critical concentrations. In contrast, the dispersion of goethite precipitated onto quartz sand increased more gradually above a P_{diss} concentration of about 0.5 µmol ortho-P l^{-1} and 0.2 µmol IHP-P l^{-1}. Compared to the adsorbed goethite, one order of magnitude less Fe oxides was dispersed from coatings of goethite that precipitated on quartz sand. The total amount of sorbed P referred to the specific surface area of goethite ranged from 7 to 12 µmol P m^{-2} (ortho-P, pH range 5.5-5.8) and 6 to 12 µmol P m^{-2} (IHP, pH range 5.9-6.7) for the system with adsorbed goethite. For the system with precipitated goethite it ranged from 3 to 6 µmol P m^{-2} (ortho-P, pH range 6.0-6.1) and 3 to 5 µmol P m^{-2} (IHP, pH range 5.6-6.2).

For the Bw samples colloid release started above an equilibrium concentration of P_{diss} of about 38 µmol ortho-P l^{-1} and 2.4 µmol IHP-P l^{-1}. For the Bg samples colloid mobilization started above a P_{diss} concentration of 71.5 µmol ortho-P l^{-1} and 10.4 µmol IHP-P l^{-1}. Assuming that the majority of P is adsorbed to oxalate-extractable Fe- and Al oxides, I calculated a critical DPS for the release of colloids using concentrations of sorbed P, oxalate-extractable P, Fe and Al concentrations of table 1 and equation (1). This critical DPS was 15% (ortho-P) and

13% (IHP) for the Bw horizon and 16% (ortho-P) and 21% (IHP) for the Bg horizon.

Optical density measured in the supernatants of soil samples reached a maximum for the Bw samples, but not for the Bg samples. Maximum measured optical densities were larger for the Bg samples than for the Bw samples.

For all systems except for the Bg horizon I found a strong increase in concentrations of dispersed colloids below a zeta potential of less than -20 mV (Figure 5). The zeta potentials of dispersed colloids were significantly smaller in experiments with IHP than in experiments with ortho-P. Following the addition of ortho-P to goethite adsorbed to sand, colloids were released only in some, but not in all samples showing a zeta potential around -20 mV. For goethite precipitated to sand the increase of dispersed Fe with decreasing zeta potential was gradual and not as abrupt as for goethite adsorbed to sand, especially after the addition of ortho-P.

As for the precipitated goethite system the increase in optical density with decreasing zeta potential was more gradual in the supernatants of the Bw horizon. For the Bg samples the correlation between optical density and zeta potential was significant, but not as clear as for the Bw samples. Samples with small and large optical densities overlapped at the same zeta potential and therefore a critical zeta potential, below which dispersion occurred, could not be identified.

The zeta potential of colloids was influenced not only by P adsorption, but also by pH. However, pH in turn, was influenced by P sorption itself, because P sorption on goethite released OH^- ions. Therefore I used partial correlation to check whether P sorption influenced the zeta potential independently of pH (Table 4). Correlation coefficients between P sorption and zeta potential were still significant except for the system with adsorbed goethite exposed to IHP and for the Bw samples exposed to IHP.

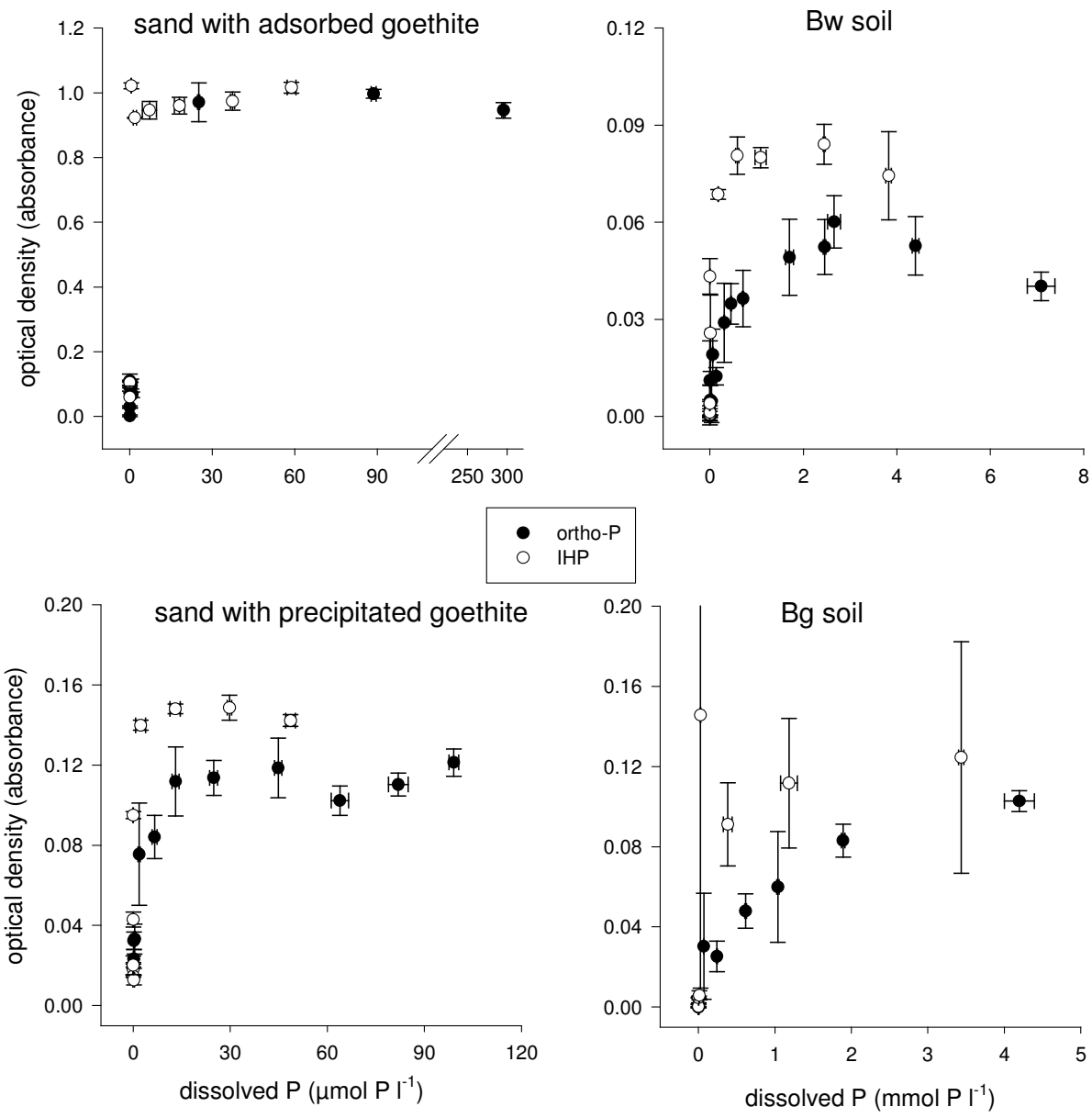

Figure 2.4: *Optical density as related to the dissolved equilibrium P concentrations in supernatants of model systems and soils after the batch experiment; error bars denote standard deviations*

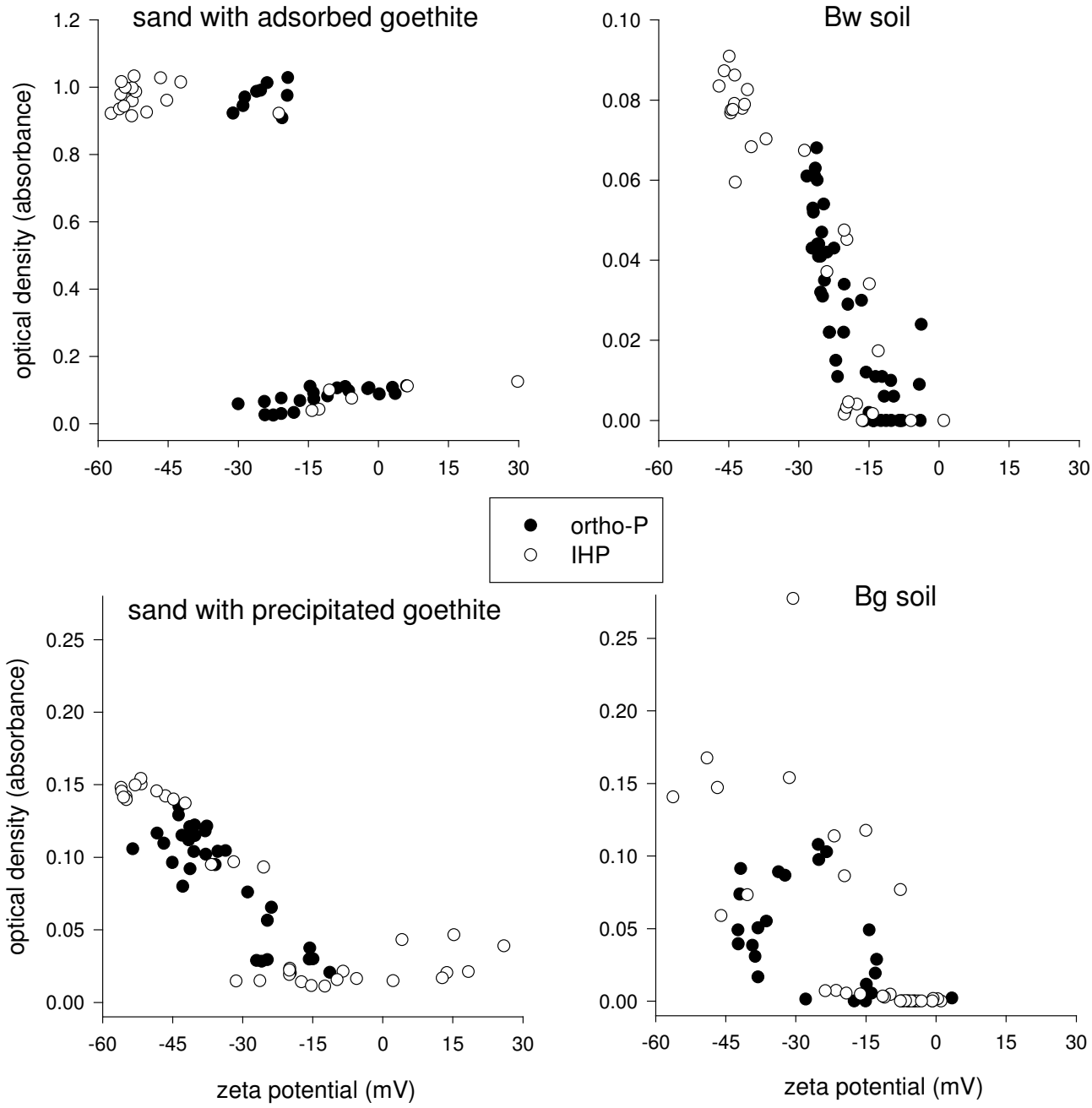

Figure 2.5: *Optical density as related to the zeta potential of dispersed particles in supernatants after the batch experiment*

Table 2.4: *Non-parametric correlation coefficients for relations between sorption of P, pH at the end of the experiment, and zeta potential of released colloids*

		P sorption - pH	P sorption - zeta potential	pH - zeta potential	P sorption - zeta potential†
adsorbed goethite system	ortho-P	0.49	-0.86	-0.60	-0.81
	IHP	0.89	-0.73	-0.81	-0.03
precipitated goethite system	ortho-P	0.59	-0.68	-0.58	-0.51
	IHP	0.96	-0.92	-0.92	-0.34
Bw	ortho-P	0.85	-0.90	-0.90	-0.59
	IHP	0.84	-0.74	-0.86	-0.06
Bg	ortho-P	0.63	-0.64	-0.46	-0.51
	IHP	0.92	-0.90	-0.83	-0.62

† *after elimination of the factor pH using partial correlation*

Particle size measurements with laser scattering provided reliable data only for turbid supernatants, because samples with small optical densities did not contain enough colloids. The average particle size of released colloids decreased significantly with increasing P_{diss} concentrations in all experiments except for the system with adsorbed goethite exposed to ortho-P and for Bg samples exposed to IHP. The average particle size of colloids released from the system with adsorbed goethite exposed to ortho-P was significantly larger (670 ± 160 nm) than that of colloids released by IHP (330 ± 140 nm). For the precipitated goethite system I measured an average particle size of 490 ± 120 nm (ortho-P) and 370 ± 100 nm (IHP). Colloids released from the Bw samples had an average particle size of 400±150 nm after an addition of ortho-P and of 410±190 nm following an addition of IHP. Whereas colloids dispersed from Bg samples after addition of IHP were of similar size (420± 240 nm), those released after an addition of ortho-P were much larger (1710±800 nm).

2.4.3 Composition of soil colloids released upon P sorption

The C content of colloids released from Bw samples (80 µmol C_{coll} l^{-1} absorbance^{-1} ± 48) was larger than that of colloids from Bg samples (52 µmol C_{coll} l^{-1} absorbance^{-1} ± 54). Excellent correlations between Fe_{coll} concentrations, Al_{coll}

concentrations, and optical density indicated that Fe- and Al oxides made up a significant fraction of colloids released from soil samples (Table 5). Correlation coefficients for relations between P_{coll} concentrations, C_{coll} concentrations, and optical densities were smaller. Positive correlations between P_{coll} concentrations on the one hand and Fe_{coll}, Al_{coll}, and C_{coll} concentrations on the other hand attest that especially Fe- and Al oxides and to a lesser extent colloidal organic matter probably act as carrier of P_{coll}. Assuming all Fe_{coll} to be composed of goethite with a surface area of 60 m^2 g^{-1}, a maximum of 5% of P_{coll} could be sorbed to goethite. In the case of ferrihydrite, a maximum of 27% could be sorbed (Table 6). Between 10 and 100% of P_{coll} could be sorbed to colloidal Al oxides assuming a surface area of 250 m^2 g^{-1}. The ratios of C_{coll}/P_{coll} ranged between 0.03 and 4.4.

Table 2.5: *Coefficients of non-parametric correlations for relations of variables characterising concentration and composition of colloids*

		Bw		Bg	
		ortho-P	IHP	ortho-P	IHP
optical density	P_{coll}	0.40	0.42	na	0.67
	Fe_{coll}	0.91	0.95	0.97	0.96
	Al_{coll}	0.94	0.80	nd	nd
	C_{coll}	0.61	0.79	0.86	0.59
P_{coll}	Fe_{coll}	0.48	0.41	na	0.69
	Al_{coll}	0.45	0.3	na	na
	C_{coll}	0.28	0.47	na	0.3

na, no data available

Table 2.6: *Fraction of colloidal P potentially sorbed to colloidal Fe oxides (assumed to be goethite with a surface area of 60 m^2 g^{-1} or ferrihydrite with a surface area of 280 m^2 g^{-1}) and colloidal Al oxide (assumed to be an amorphous Al oxide with a surface area of 250 m^2 g^{-1}) and C/P ratios; standard deviations in parenthesis*

		$(P_{coll\text{-}pot} / P_{coll}) \times 100$			C_{coll}/P_{coll}
		goethite	ferrihydrite	Al oxide	
		/%			
Bw	ortho-P	1.77 (1.9)†	8.95 (9.6)	46.7 (33.7)	1.26 (1.37)
	IHP	1.33 (0.8)	6.7 (3.9)	58.5 (27.9)	1.56 (0.7)
Bg	ortho-P	na	na	na	na
	IHP	3.29 (1.13)	16.59 (5.7)	62.2 (21.2)	0.61 (0.98)

na, no data available

2.4.4 Maximum P_{coll} concentrations

For soil samples exposed to increasing IHP concentrations, the maximum P_{coll} concentrations of 0.28 mmol P l^{-1} (Bg) and 0.31 mmol P l^{-1} (Bw) were reached at equilibrium P_{diss} concentrations in supernatants of 1.16 mmol P l^{-1} and 0.02 mmol P l^{-1}. In the latter experiment I found P_{coll} concentrations of 0.04 mmol P l^{-1} at a P_{diss} concentration of 0.002 mmol P l^{-1}. The addition of ortho-P to the Bw sample produced maximum concentrations of P_{coll} of 0.16 mmol P l^{-1} at equilibrium P_{diss} concentrations in supernatants of 1.68 mmol P l^{-1}.

2.5 Discussion

2.5.1 Microscopic analyses of coated sand and surface area measurements

The image of the system with adsorbed goethite (Figure 1) is similar to the SEM images of goethite coated sand taken by Scheidegger et al. (1993). The authors also observed an accumulation of goethite in holes and cavities of the sand matrix. I ascribe this observation to the protection of goethite particles in holes and cavities against shear forces caused by shaking. Hence, shear forces, which are absent under natural conditions might also have supported the preferential desorption of goethite particles from outer, exposed surfaces following P addition (Figure 2). The specific surface area of Bayferrox goethite determined with

the geometric method was only slightly larger than the surface area measured with gas adsorption. Hence, I assume that in my experiment surface area determination with SEM and TEM images yields data comparable to those of gas adsorption. The specific surface area of dispersed goethite significantly exceeded the one of goethite adsorbed to sand. It seems that smaller crystals with a larger specific surface area were preferentially released from the sand surface.

The goethite crystals produced by oxidation of Fe(II) on the outer surface of quartz sand grew perpendicular to the quartz surface, which might be an imperative once the surface of sand is fully covered with goethite crystals and space is lacking (Figure 3, Dominik et al., 2007). The specific surface area of precipitated goethite was larger than that of adsorbed goethite because crystals were smaller and less crystalline.

2.5.2 Mobilization of colloids

The sorption of P mobilized goethite and soil colloids from all quartz or soil matrices if a critical equilibrium concentration of P_{diss} in supernatants was exceeded (Figure 4). This can be ascribed to more negative zeta potentials (Figure 5), which resulted in a repulsion of colloids from the negatively charged quartz or soil matrix. A reduction of the zeta potential of Fe oxides as a consequence of P sorption has been documented by several authors (Stumm and Sigg, 1979; Puls and Powell, 1992; Celi et al., 1999), but to my knowledge this is the first time that the process of P adsorption and a simultaneous mobilization of Fe oxides from a quartz sand matrix has been described.

Although pH increased due to an addition of P, P sorption governed colloid mobilization. The point of zero charge of goethite is at a pH of $\geq$ 8 (i.a. Scheidegger et al., 1993; Celi et al. 2001; Xu and Axe, 2005). Thus, the increase of pH to values ranging from 5.3 to 6.7 is unlikely to be sufficient to cause the reversal of charge from positive to negative, which resulted in the release of goethite. Furthermore, partial correlation showed that P sorption influenced the surface charge independently from pH, although correlation coefficients without the pH effect were smaller.

I assume that the increasing electrical conductivity did not significantly affect colloid mobilization from soil samples. In the Bw samples exposed to ortho-P

the increase of optical density was levelled off at a P addition of about 2.6 mmol P l^{-1}. However, a significant increase of the electrical conductivity started just above this degree of P addition. The large electrical conductivity of IHP systems was caused by the polyvalence of the IHP-ion at the given pH and not by Na addition (Celi et al., 2001).

Comparing the critical P_{diss} concentrations of soils and model systems, P_{diss} concentrations had to be 40-140 times larger in soils compared to model systems for colloid mobilization. Firstly, this may be due to pH, which was about one order of magnitude smaller in soil systems than in model systems. At small pH values larger total concentrations of P are necessary to reverse the surface charge of goethite (Stumm & Sigg, 1979). Secondly, this finding can be explained with larger concentrations of sesquioxides in soils than Fe concentrations in model systems. Further, sorbed organic matter, which competes with P for sorption sites of oxides (Kaiser & Zech, 1996; Karathanasis, 1999; Kreller *et al.*, 2003) may superimpose the dispersing effect of P adsorption. In an experiment conducted by Lima *et al.* (2000) an increasing addition of P did not shift the surface charge of soil clay particles to more negative values. According to the authors explanation, P sorption mainly occurred by displacing organic compounds and therefore did not change the surface charge. Moreover, the sorption of organic matter as well as already present P in soils may have caused the dispersion of easily dispersible soil colloids before the soils were sampled and the experiment was started.

The amounts of sorbed P related to the surface area of goethite in model systems were larger than reported in literature. Cornell and Schwertmann (2003) summarized the results of several studies and found a maximum P saturation of 2.5 µmol P m^{-2} Fe oxide in acidic to neutral media. Celi et al. (2000) reported a maximum sorption of 5.3 µmol P m^{-2}, which is also smaller than my P saturation values. I checked the existence of traces of Ca^{2+} in the model systems, which may potentially cause the precipitation of apatite, with atomic absorption spectrometry (AAS; Perkin Elmer 1100B, Shelton, USA). Measured Ca^{2+} concentrations, however, were too small to result in the precipitation of apatite. By means of the equilibrium speciation software Visual Minteq (Allison et al., 1991) I was further able to eliminate the possibility of solid Fe(III) phosphate precipitation.

Inositol hexaphosphate dispersed significantly more colloids than ortho-P. The strong dispersing effect of IHP is related to smaller acid dissociation constants of IHP compared to ortho-P, which cause large shifts in surface charge as a consequence of IHP sorption (Celi et al., 2001). The more negative surface charge of colloids released by IHP might also be responsible for their smaller particle size in comparison to colloids released by ortho-P. Particles with a large positive or negative surface charge do not aggregate as fast as particles with a surface charge close to zero (Kretzschmar et al., 1997a).

The two model systems differed significantly in their dispersion behaviour. For the system with adsorbed goethite dispersion as a function of zeta potential was a non-linear process with a sharp increase of dispersed goethite concentrations, if a certain critical limit of P accumulation was exceeded. I attribute this finding to a rather homogeneous accessibility of sorption sites for P and a uniform bonding strength of goethite crystals to the quartz surface. The Bayferrox goethite with a surface area smaller than 20 m^2 g^{-1} is very crystalline with few micropores. Thus, the adsorption of P took place quickly as described by Strauss et al. (1997), who found a significant dependence of sorption kinetics on the crystallinity of goethite. For the sand with precipitated goethite the increase of dispersed particle concentrations with increasing P sorption was more gradual, but also occurred if a distinct P saturation was exceeded. This gradual release of goethite has probably several reasons. First, not all goethite crystals are equally available for P sorption in the massive coating produced by precipitation of goethite on the sand surface. Thus, it might have taken more than 24 h for goethite crystals close to the quartz surface to reach equilibrium with P_{diss}. Indeed, a sorption experiment showed that after 24 h only half of the total P sorption capacity was occupied (data not shown). Furthermore the single goethite crystals are closely connected to each other, maybe even grown together during the precipitation process. Together with the slow sorption kinetics of P, the close association of single crystals might be the reason, why one order of magnitude less goethite was dispersed in the system with precipitated goethite compared to the system with adsorbed goethite.

Also the two soils differed in their dispersion behaviour. Whereas a close relation between zeta potential and the optical density of supernatants could be de-

tected for Bw samples, such a relationship was poor for Bg samples. Similar to the precipitated goethite model system, more intense cross-linking of goethite crystals and a reduced accessibility of single goethite crystals within the oxide coatings of the Bg mottles are probably responsible for this finding. However, maximum optical densities of supernatants were larger for the Bg samples than for the Bw samples (Figure 4). Generally, more potential colloids may have been available in the Bg samples because of larger concentrations of dithionite- and oxalate-extractable Fe and Al (Table 1). Another reason might be the larger organic C content of the Bw samples in relation to their content of Fe and Al oxides (Table 1). In an experiment conducted by Lima et al. (2000), sorption of P shifted the surface charge of clay particles to more negative values for B horizon samples, but not for A horizon samples. According to the authors explanation, P sorption in the A horizon mainly occurred by displacing organic compounds, which did not change the surface charge. Possibly the accumulation of organic C on surfaces of Fe and Al oxides in the Bw horizon prevented a further reduction of their surface charge and hence colloid release. Indeed, the organic C content of colloids released from the Bw samples was larger than the C content of colloids released from the Bg samples.

2.5.3 Potential sorbents of colloidal P released from soil samples

Significant positive correlations between optical density and Fe_{coll}, Al_{coll} and P_{coll} indicate that Fe and Al oxides contribute a significant fraction of released colloids (Table 5). Based on my assumptions described above, Fe_{coll} and Al_{coll} provided most of the sorption capacity for P_{coll} (Table 6). However, not all P_{coll} released from Bw samples could be adsorbed by Fe_{coll} and Al_{coll} with the assumed specific surface areas. The ratios of C_{coll}/P_{coll} were unrealistically small compared to values of 44:1 or 150:1 typically encountered in soils (Guggenberger et al., 1996). Furthermore, C_{coll} and P_{coll} concentrations were not significantly correlated except for the Bw samples exposed to IHP (Table 5). This indicates a subordinate role of organic matter as carrier for P_{coll}. In addition to colloidal oxides, clay minerals might have provided additional sorption capacity for P (Frossard et al., 1995; Celi et al., 1999).

2.5.4 Maximum P_{coll} concentrations and potential environmental relevance

Background concentrations of P_{diss} in agricultural soils are about 0.65 µmol l^{-1} (0.02 mg P l^{-1}), but can reach up to 10 µmol l^{-1} P (0.3 mg P l^{-1}), especially in highly P saturated sandy soils (Siemens et al., 2004). In the experiment with soil samples mobilization of colloids started at an equilibrium concentration of P_{diss} between 2.4 and 72 µmol P l^{-1}. However, it has to be considered that the pH of agricultural soils is at least one order of magnitude larger than the pH of the investigated forest soils, which enhances colloid mobilization even at smaller P_{diss} concentrations. I observed maximum P_{coll} concentrations at P_{diss} concentrations that are 1-2 orders of magnitude larger than P_{diss} concentrations typically encountered in drainage water of subsoils. However, P_{coll} concentrations larger than 3.3 µmol l^{-1}, which would be environmentally relevant if measured in the field, occurred at P_{diss} concentrations of less than 3.3 µmol l^{-1} for Bw samples exposed to IHP. The calculated absolute DPS values 13-21% that are critical for the release of colloids, are within the range of threshold DPS for large P_{diss} concentrations that were reported by Ilg et al. (2005) and by Breeuwsma and Silva (1995). Critical relative increases of DPS for the release of colloids from subsoil samples are small in relation to DPS-values of > 50%, which can be found for highly P-saturated soils (Siemens et al., 2004). Hence, in accordance with field observations (Hens and Merckx, 2001; Motoshita et al., 2003), it has to be considered that the process of P-induced colloid mobilization can possibly play a significant role in soils.

2.6 Conclusions

The adsorption of P releases goethite and soil colloids from coatings of quartz sand and subsoils if a critical P saturation is exceeded, because P sorption reduces the surface charge of goethite and soil colloids. Thus, an accumulation of P in (sub)soils, e.g. as a consequence of excessive fertilization, might enhance the risk of colloid-facilitated export of P to ground- and surface waters. Inositol hexaphosphate mobilizes significantly more colloids at the same P saturation than ortho-P. Therefore organic P, added for example with organic manure, might even have a stronger colloid-mobilizing effect in soils than ortho-P added with mineral fertilizer. Environmentally relevant concentrations of P_{coll} occur at

small P_{diss} concentrations following the addition of IHP and at realistic DPS. Future research should address the effect of other factors such as pH or organic matter on P-induced colloid mobilization.

3 Colloidal and dissolved phosphorus in sandy soils as affected by P saturation

3.1 Abstract

Fertilization exceeding crop requirements causes an accumulation of P in soils, which might increase concentrations of dissolved and P_{coll} in drainage. I sampled soils classified as typic Haplorthods from four fertilization experiments to test i) whether increasing DPS increase concentrations of dissolved and P_{coll}, and ii) if critical DPS levels can be defined for P release from these soils. Oxalate-extractable concentrations of P, Fe and Al were quantified to characterize DPS. Turbidity, zeta potential, P_{diss} and P_{coll}, Fe, Al and C concentrations were determined in water and KCl extracts. While concentrations of P_{diss} decreased with increasing depth, concentrations of water-extractable P_{coll} remained constant. In topsoils 28±17% and in subsoils 94±8% of water-extractable P was bound to colloids. Concentrations of P_{diss} increased sharply for DPS > 0.1. Colloidal P concentrations increased with increasing DPS because of an additional mobilization of colloids and due to an increase of the colloids P contents. Additionally to DPS, ionic strength and Ca^{2+} affected the release of P_{coll}. Hence, using KCl for extraction improved the relationship between DPS and P_{coll} compared to water extraction. Accumulation of P in soils increases not only concentrations of P_{diss} but also the risk of P_{coll} mobilization. Leaching of P_{coll} is potentially important for inputs of P into water bodies because P_{coll} as the dominant water-extractable P fraction in subsoils was released from soils with relatively low DPS.

3.2 Introduction

The eutrophication of surface waters as a consequence of increasing input of P has been of concern for more than 30 years (Schindler, 1971; Lee, 1973). In Germany, 25 to 70% of the total annual P loading to water bodies can be attributed to agricultural diffuse sources mainly because of excessive fertilization of farmlands over several decades (Behrendt and Bachor, 1998; Behrendt et al., 1999; Umweltbundesamt, 2004).

In sandy soils, the DPS is a central factor controlling the concentration of P_{diss} in drainage water and therefore subsurface P leaching (Behrendt and Boekhold, 1993; Breeuwsma and Silva, 1992). The ratio of oxalate extractable P to (Fe+Al) is a good measure of the DPS (van der Zee and van Riemsdijk, 1988; van der Zee and de Haan, 1994). Concentrations of P_{diss} increase sharply, if the DPS exceeds a certain critical value that has been termed the “change point” (Maguire and Sims 2002; McDowell and Sharpley, 2001c). This change point can be related to the nonlinear sorption characteristics of ortho-P to soil (Ryden and Syers, 1977; Barrow, 1983; Koopmans et al., 2002). Several authors have quantified distinct change points for various soils (Celardin, 2003; Nair et al., 2004). However, as Koopmans et al. (2002) pointed out, these change points depend both on experimental conditions, such as the soil to solution ratio, and on soil characteristics. Highly fertilized sandy soils that are poor in the main P sorbents Fe and Al oxides and rich in P, often exceed a critical level of DPS and are therefore vulnerable to P leaching. Such soils are found in areas with high livestock densities, e.g. in the Netherlands, Belgium and the northwestern part of Germany (Breeuwsma and Silva, 1992; De Smet et al., 1996; Leinweber et al., 1997). In these areas, subsurface leaching of P is often equally important as surface erosion for P inputs into surface waters (Driescher and Gelbrecht, 1993).

In addition to P_{diss}, P bound to suspended particles and colloids contributes to P leaching from agricultural soils (Jensen et al., 2000; Hesketh et al., 2001; Hens and Merckx, 2001, Motoshita et al., 2003). Soil colloids are defined as particles ranging from >1nm to <1µm, which remain suspended in water and are therefore mobile (Kretzschmar et al., 1999). Phosphorus may be bound to mineral colloids, such as Fe and Al oxides, or to organic or organo-mineral colloids (Celi et al., 2001, Hens and Merckx, 2002). Colloidal P was in soil water samples may account for 13-95% of total P, but its relevance for P leaching and the processes governing its release from soils are not fully understood (Haygarth et al., 1997; Hens and Merckx, 2001; Shand et al., 2000).

Zhang et al. (2003) reported that application of P to sandy soils packed into columns soils induced the mobilization of P_{coll} and Fe. In accordance with this finding, Siemens et al. (2004) showed that sorption of P caused the release of P_{coll}

from sandy soils in batch experiments. Referring to Celi et al. (1999), Puls and Powell (1992) and Stumm and Sigg (1979), who found that P sorption decreases the surface potential of Fe oxides, they hypothesized that a certain P saturation of the sorbent may mark a change point for the release of P_{coll}, similar to the change point for the mobilization of P_{diss}.

Experience with soil test methods as tools for assessing the risk of P_{diss} export from soil is rapidly growing; however, no data are currently available that relate soil P parameters to the risk of subsurface transport of P_{coll} (Schouwmans and Chardon, 2003).

The objective of this study was to evaluate the impact of P fertilization and the initial DPS on concentrations of dissolved and P_{coll} in sandy soils. I hypothesize that i) increasing DPS not only increases P_{diss} concentrations, but also enhances the release of P_{coll} from soils and ii) a critical level of DPS exists above which concentrations of dissolved and P_{coll} increase sharply. To test these hypotheses, I sampled four long-term fertilization experiments on sandy soils to ensure a wide range of P contents and DPS as a result of different manuring and P fertilization.

3.3 Materials and methods

3.3.1 Sites and agricultural management

I investigated four long-term fertilization experiments in northwest Germany, two of which were located in Dülmen near Münster (Do and Dn), one near Nienburg (N) and the fourth near Hamburg (H; Table 3.1). The climate at all sites is temperate and oceanic, which promotes groundwater recharge. The mean annual precipitation is 650-800 mm, and the average annual temperature is 9.3-9.5°C. Soils are classified as typic Haplorthods. The soil texture is sand to loamy sand at all sites.

The experiments are maintained by two fertilizer companies. Different kinds and amounts of mineral and organic fertilizer were applied during different periods of time with regard to their effect on crop yield. This resulted in different contents of Calcium-acetate-lactate extractable P (CAL-P) in the 0-30 cm depth (Table 3.1). Experiment Dn had control variant. I sampled manure and mineral fertilization treatments to ensure a maximum range of DPS.

3.3.2 Sampling and general characterization of soils

In January 2003, composite samples derived from three corings on each plot were taken for depth intervals of 0-30 cm, 30-60 cm and 60-90 cm. These depth intervals are commonly sampled for soil nutrient analyses in Germany (Untersuchungszentrum NRW, 2004). Soil samples were air dried and sieved to a particle size < 2 mm. Soil pH was measured in water, using a soil to solution ratio of 1:8. The electrical conductivity was determined as a measure for the total electrolyte concentration (both inoLab pH/Cond, WTW, Weilheim, Germany). To quantify the concentrations of exchangeable Ca^{2+}, Mg^{2+} and K^{+}, I extracted 5 g of soil with 25 mL of 1 N ammonium acetate (Thomas, 1982). Calcium, Mg^{2+} and K^{+} concentrations were determined on an atomic absorption spectrometer (AAS; Perkin Elmer 1100B, Shelton, USA).

3.3.3 Degree of P saturation

Oxalate-extractable P, Fe and Al concentrations (P_o, Fe_o, Al_o) were determined by extracting 2 g of soil with 100 mL ammonium oxalate (0.2 M, pH 3.25) for 1 hour in the dark (Schlichting et al., 1995). Iron and Al concentrations were measured using AAS. The detection limits were 0.1 mg l^{-1} for Fe and 1 mg l^{-1} for Al. I measured P concentrations by the method of Murphy and Riley (1962) using a Continuous Flow Analyzer (CFA; Skalar, Erkelenz, Germany). In the CFA P compounds are transferred from the sample flow line to an analyte flow line in a dialysis chamber. Therefore the method minimizes the hydrolyses of organic P compounds during the molybdenum-blue colour reaction (Baldwin, 1998) and measures mainly concentrations of ortho-P. The detection limit was 0.01 mg P l^{-1}. All vessels were rinsed with 0.1 M HNO_3 prior to P analyses. The DPS was calculated according to Breeuwsma and Silva (1992) and van der Zee and de Haan, 1994):

$$DPS = \frac{[P_o]}{0.5([Fe_o]+[Al_o])}, \qquad (1)$$

where $[P_o]$, $[Fe_o]$ and $[Al_o]$ denote the concentrations of elements in mmol kg^{-1}.

Table 3.1: *Characteristics of the long-term fertilization experiments*

Experiment/ Coordinates	Crop rotation	Treatments	P input with mineral fertilizer (kg P ha^{-1} yr^{-1})	P input with organic fertilizer (kg P ha^{-1} yr^{-1})	P-balance* (kg P ha^{-1})	CAL-P† (mg P kg^{-1})	Experiment duration years	Number of replicates
Dülmen	potato (*solanum tuberosum*)	1) control	-	-	-259	47	45	4
old (Do)	rye (*secale cereale*)	2) stable manure (potato)	-	105	1220	88	45	4
7°11´E	oat (*avena sativa*)	3) thomasphosphate‡ + K	39	-	1469	108	45	4
51°46´N		4) stable manure (potato) + thomasphosphate + K	39	105	2968	154	45	4
Dülmen	maize (*zea mays*)	1) triplephosphate	43(maize), 34(wheat, barley)	-	520	82	18	3
new (Dn)								
7°11´E	winter wheat (*triticum aestivum*)	2) triplephosphate + 220 kg N/ha	43,34	-	270	100	18	3
51°46´N	winter barley (*hordeum vulgare*)	3) triplephosphate + stable manure + 220 kg N ha^{-1}	43,34	126	990	112	18	3
		4) triplephosphate + stable manure	43,34	126	1207	140	18	3
Hamburg	summer barley (*hordeum vul-*	1) control	-	-	-142	70	6	4
(H)	*gare*)							
9°25´E	sugar beet (*beta vulgaris*)	2) triplephosphate	22	-	-16	74	6	4
53°31´N	potato (*solanum tuberosum*)	3) Thomaskalk®‡	22	-	-16	87	6	4
	rye (*secale cereale*)	4) triplephosphate	44	-	114	79	6	4
		5) Thomaskalk®‡	44	-	112	79	6	4
Nienburg	winter rye (*secale cereale*)	1) control	-	-	-271	79	15	4
(N)	oat (*avena sativa*)	2) phosphate + potassium "R" §	21 (31 in 1998)	-	13	92	15	4
8°31´E	winter barley (*hordeum vulgare*)	3) Thomaskali®‡	21 (31 in 1998)	-	-7	100	15	4
52°37´N	winter wheat (*triticum aestivum*)	4) phosphate +potassium "R"	42 (31 in 1998)	-	288	109	15	4
	grain maize *(zea mays*)	5) Thomaskali®‡	42 (31 in 1998)	-	279	114	15	4
	triticale	6) Thomaskali®‡	63 (31 in 1998)	-	551	135	15	4

* P-balance: difference between P input (mineral and organic fertilizer) and removal of P (harvest)

† Calcium-acetate-lactate extractable P in the 0-30 cm depth determined by the companies running the experiments to assess the amount of P available to plants in topsoils

‡ made from phosphorus-containing basic slags which accrue during steel production, Thomaskalk® (Thomasdünger GmbH, Düsseldorf) and thomasphosphate contain Ca_3 (PO_4)* x $(CaSiO_4)$, whereas the concentration of phosphate in Thomaskalk® is lower; Thomaskali® (Thomasdünger GmbH, Düsseldorf) is a two component fertilizer made from thomasphosphate and potassium

§ Phosphorus-potassium-fertilizer containing partly solubilized rock phosphate and sulfur

3.3.4 Dissolved and colloidal P

I used the concentration of water-dispersible P as a measure for potentially mobile, P_{coll} (Kaplan et al., 1997). Ten g of soil were shaken end-over-end with 80 mL of deionized H_2O for 24 h. The extracts were centrifuged at 3000 g for 10 minutes. Assuming a density larger than 2 g cm^{-3} and a spherical shape of colloids, the centrifugation treatments should have sedimented particles larger than 8 µm. Thereafter, the extracts were filtered (No 512 ½, Schleicher and Schuell, Dassel, Germany) to remove coarse particles and then filtered through 1.2 µm cellulose acetate filters (Sartorius, Göttingen, Germany) to analyze only particles < 1.2 µm of the colloidal fraction. The first 5 mL of both filtrates were discarded. An aliquot of the filtrate was ultra-centrifuged at 300 000 g for 1 hour to remove colloids (Beckman Optima TL, Unterschleissheim, Germany). Colloidal P was calculated as the difference between the concentration of total P in non ultra-centrifuged and ultra-centrifuged samples. I measured total P concentrations after oxidation and acid hydrolysis of organically bound P by the method of Murphy and Riley (1962) using the CFA. To achieve a complete oxidation, 3.2 M H_2SO_4 and 37 mM $K_2O_8S_2$ were added, the samples were heated to 95°C and irradiated with UV-radiation for 6 minutes without using a dialyte chamber as for the determination of inorganic P_o. The detection limit was 0.01 mg P l^{-1}.

3.3.5 Characterization of colloids

To characterize the released colloids I extracted a randomly chosen set of 16 soil samples per depth. In addition to the parameters mentioned above, I determined the average particle size (High Performance Particle Sizer, HPP 5001, Malvern Instruments, United Kingdom) and the zeta potential (zeta sizer DTS 5200, S/N 34132/35 Malvern Instruments, United Kingdom). The optical density of the filtrate at a wavelength of 525 nm was quantified as a measure of the concentration of colloids (specord photometer, Jena, Germany). Concentrations of Fe and Al were measured in ultra-centrifuged and non-ultra-centrifuged samples to quantify Fe_{coll} and Al_{coll}. Colloidal C concentrations were determined on a TOC analyzer (TOC-Analyzer 5050A, Shimadzu Europa GmbH, Germany).

The effect of ionic strength and electrolyte composition on the release and properties of colloids was tested by extracting a set of five samples, randomly

chosen from each depth, with deionized H_2O and 0.01 M KCl. Potassium chloride was chosen as background electrolyte instead of $CaCl_2$ to avoid the precipitation of apatite and an aggregation of colloids. The same parameters as mentioned above were determined.

3.3.6 Precision

To check the quality of laboratory methods, 12 randomly chosen samples were extracted in duplicate. The analytical repeatability of dissolved and P_{coll} was 91% and 84%, respectively. The repeatability of field replicates was 61% and 50%, respectively. The three sets of 72, 16 and 5 samples from each sampling depth were analyzed in separate analytical runs. The coefficients of variation of dissolved and P_{coll} concentrations between these runs were large (52% and 38%, respectively), because concentrations of water-extractable P were small especially for soil samples in the 30-60 cm and 60-90 depth (samples below detection limit: 16% and 25%, respectively). The concentration of P_{coll} is a calculated parameter, therefore error propagation reduces the repeatability. To account for the limited repeatability between different analytical runs, I compared only values that were determined within the same run.

3.3.7 Calculations and statistical evaluations

Arithmetic means, standard deviations and coefficients of variation were calculated for all variables. Values below detection limit and concentrations of P_{coll}, Fe and Al < 0 were set to zero. In case of large variations of the input parameters total and P_{diss} concentration, error propagation leads to varying quantification thresholds. Setting negative concentrations of composite parameters as P_{coll} concentrations to one half of the respective quantification threshold introduces "artificial" differences into the dataset, which may influence the statistical analysis (Siemens and Kaupenjohann, 2002). For this reason, I preferred setting negative P_{coll} concentrations to zero. I think that this approach is straightforward as it provides a clearly conservative estimate of P_{coll} concentrations. The significance of fertilization effects on concentrations of P_o, P_{coll}, P_{diss} and DPS were tested using the non-parametric Kruskal-Wallis test. I applied the non-parametric Nemenyi test for post-hoc comparisons (Köhler et al., 1996). Parameters were analyzed for correlations by the non-parametric Spearman

statistic. Differences between depths and between concentrations of water extracts and KCl extracts were compared with the non-parametric Wilcoxon-matched- pairs test. All tests, except for the Nemenyi test, were carried out using the STATISTICA 6.0 software (StatSoft, Tulsa, USA). I used the split-line model described by McDowell and Sharpley (2001b) to identify change points of the effect of DPS on other variables. The model consists of two linear regressions separated by a critical value of the independent variable. Change points are regarded as significant if the slopes of the two linear relationships are significantly different. The model was fitted using the nonlinear regression procedure of the SPSS 6.0 software (SPSS, Chicago, USA). The significance level for all tests was defined as $p < 0.05$.

3.4 Results

3.4.1 Effect of fertilization on soil P fractions

In the 0-30 cm soil depth, increasing P fertilization induced an accumulation of oxalate-extractable P (P_o), but the effect was significant only at sites Do and H (Table 3.2). At site H, fertilization with 22 kg P ha^{-1} y^{-1} caused a significantly smaller P_o concentration compared to 44 kg P ha^{-1} y^{-1}. For the 30-60 cm depth, significant differences between the treatments could be detected only at site H. I found no effect of fertilization on P_o concentrations in the 60-90 cm depth.

Similar to P_o concentrations, DPS reflected increasing P balances. However, significant effects were detected only for experiment Do for the 0-30 cm and the 30-60 cm depth. At site H a significantly smaller DPS of treatment 3 (22 kg P ha^{-1} y^{-1} as Thomaskalk®) compared to treatment 2 (22 kg P ha^{-1} y^{-1} as triple-phosphate) was observed for the 30-60 cm depth, which corresponds to the difference between oxalate-extractable P concentrations. I found no effect of fertilization on DPS in the 60-90 cm subsoil layer.

Table 3.2: *Effects of fertilization on soil P fractions and P saturation (DPS)*

site	treatment	P input with mineral fertilizer (kg P ha^{-1} yr^{-1})	P input with organic fertilizer (kg P ha^{-1} yr^{-1})	oxalate-extractable P (mg P kg^{-1})			DPS			dissolved P (mg P kg^{-1})			water-extractable colloidal P (mg P kg^{-1})		
				0-30 cm	30-60 cm	60-90 cm	0-30 cm	30-60 cm	60-90 cm	0-30 cm	30-60 cm	60-90 cm	0-30 cm	30-60 cm	60-90 cm
Do*	1	-	-	251^{a†}	113^{a}	60^{a}	0.23^{a}	0.08^{a}	0.04^{a}	9.2^{a}	0.28^{a}	0.01^{a}	3.3^{a}	2.4^{a}	5.6^{a}
	2	-	105	426^{ab}	194^{a}	51^{a}	0.34^{ab}	0.12^{ab}	0.04^{a}	18.4^{ab}	2.2^{ab}	0.08^{a}	4.3^{a}	5.7^{a}	3.0^{a}
	3	39	-	546^{b}	228^{a}	99^{a}	0.37^{ab}	0.11^{ab}	0.07^{a}	17.3^{ab}	0.67^{ab}	0.04^{a}	7.1^{a}	3.9^{a}	2.7^{a}
	4	39	105	545^{b}	304^{a}	106^{a}	0.44^{b}	0.22^{b}	0.08^{a}	30.0^{b}	8.6^{b}	0.22^{a}	5.3^{a}	6.5^{a}	6.5^{a}
Dn*	1	43 (maize), 34 (wheat, barley)	-	355^{a}	74^{a}	20^{a}	0.33^{a}	0.06^{a}	0.02^{a}	17.1^{a}	1.8^{a}	0.04^{a}	6.7^{a}	5.2^{a}	7.0^{a}
	2	43,34	-	425^{a}	108^{a}	42^{a}	0.32^{a}	0.08^{a}	0.03^{a}	18.8^{ab}	1.4^{a}	0.14^{a}	5.6^{a}	2.8^{a}	5.6^{a}
	3	43,34	126	477^{a}	103^{a}	23^{a}	0.37^{a}	0.09^{a}	0.03^{a}	21.7^{ab}	2.2^{a}	0.12^{a}	6.2^{a}	3.8^{a}	2.7^{a}
	4	43,34	126	473^{a}	126^{a}	31^{a}	0.40^{a}	0.12^{a}	0.04^{a}	23.0^{b}	8.1^{a}	0.11^{a}	9.7^{a}	5.3^{a}	6.7^{a}
H	1	-	-	272^{ab}	91^{ab}	52^{a}	0.27^{a}	0.09^{ab}	0.07^{a}	8.7^{ab}	0.21^{a}	0.12^{a}	0.56^{a}	4.5^{a}	1.6^{a}
	3	22	-	245^{a}	100^{a}	54^{a}	0.23^{a}	0.09^{a}	0.08^{a}	9.6^{ab}	0.13^{a}	0.03^{a}	0.40^{a}	5.9^{a}	2.4^{a}
	2	22	-	259^{ab}	62^{b}	51^{a}	0.26^{a}	0.07^{b}	0.06^{a}	8.5^{a}	0.00	0.04^{a}	3.0^{a}	4.8^{a}	0.88^{a}
	4	44	-	333^{b}	83^{ab}	45^{a}	0.31^{a}	0.08^{ab}	0.07^{a}	12.1^{ab}	0.13^{a}	0.02^{a}	3.5^{a}	5.5^{a}	1.9^{a}
	5	44	-	302^{ab}	87^{ab}	69^{a}	0.28^{a}	0.09^{ab}	0.08^{a}	12.6^{b}	0.15^{a}	0.02^{a}	3.3^{a}	5.8^{a}	1.8^{a}
N	1	-	-	271^{a}	34^{a}	30^{a}	0.19^{a}	0.03^{a}	0.04^{a}	1.1^{a}	0.14^{a}	0.16^{a}	1.9^{a}	1.2^{a}	0.83^{a}
	2	21 (31 in 1998)	-	344^{a}	39^{a}	33^{a}	0.25^{a}	0.04^{a}	0.05^{a}	2.6^{ab}	0.08^{a}	0.2^{b}	1.5^{ab}	1.8^{ab}	0.73^{a}
	3	21 (31 in 1998)	-	298^{a}	36^{a}	31^{a}	0.22^{a}	0.04^{a}	0.04^{a}	1.4^{a}	0.11^{a}	0.28^{b}	2.0^{ab}	1.4^{ab}	0.67^{a}
	4	42 (31 in 1998)	-	366^{a}	43^{a}	28^{a}	0.29^{a}	0.05^{a}	0.04^{a}	2.7^{ab}	0.01^{a}	0.2^{ab}	1.7^{ab}	1.9^{b}	1.03^{a}
	5	42 (31 in 1998)	-	350^{a}	32^{a}	24^{a}	0.28^{a}	0.05^{a}	0.04^{a}	2.4^{ab}	0.03^{a}	0.1^{ab}	1.5^{ab}	1.7^{ab}	1.17^{a}
	6	63 (31 in 1998)	-	460^{a}	67^{a}	21^{a}	0.33^{a}	0.07^{a}	0.03^{a}	3.8^{b}	0.15^{a}	0.2^{ab}	0.6^{b}	1.8^{ab}	0.79^{a}

*Do: Dülmen old, Dn: Dülmen new; H: Hamburg; N: Nienburg

†different superscript letters indicate significance of treatment effect for each depth at individual sites ($p<0.05$)

Dissolved P was the parameter that reacted most sensitive on fertilization. I observed significant effects for the 0-30 cm depth at all sites and for the 30-60 cm depth of experiment Do. In experiments Do, Dn and N, the treatments receiving the highest P input had significantly higher concentrations of P_{diss} compared to the controls. At site H, treatment 3 receiving 22 kg P ha^{-1} y^{-1} as Thomaskalk® had significantly lower concentrations of P_{diss} than treatment 5 receiving 44 kg P ha^{-1} y^{-1}. In subsoils, differences between treatments were less pronounced. Generally, concentrations of P_{diss} decreased sharply with increasing depth. For the 60-90 cm depth, they were often close to the detection limit.

Water-extractable P_{coll} concentrations tended to increase with increasing P fertilization in the 0-30 cm and the 30-60 cm depth, but there was no significant positive effect detectable except for the 30-60 cm depth of treatment 4 at site N receiving 42 kg P ha^{-1} y^{-1} (Table 3.2). In contrast, at site N fertilization with 63 kg P ha^{-1} y^{-1} showed significantly smaller concentrations of P_{coll} than the control in the 0-30 cm depth. Whereas concentrations of P_o, P_{diss}, and DPS decreased with increasing depth, the concentrations of P_{coll} did not change. As a consequence, the fraction of P_{coll} increased from 28±17% of water-extractable P for topsoils to 94±8% for the 60-90 cm depth.

No significant differences between effects of organic and mineral fertilizers could be detected for any soil P fraction or DPS.

3.4.2 Relating dissolved and colloidal P concentrations to P saturation

Dissolved P concentrations were significantly correlated with DPS in the 0-30 cm and the 30-60 cm depths (Figure 3.1). No correlation was detected for the 60-90 cm depth. Fitting the split-line model to the data from site D (experiments Do and Dn) for the 30-60 cm depth, I identified a significant change point of DPS = 0.11±0.01.

Concentrations of P_{coll} were significantly correlated with the soil's DPS in the 0-30 cm and the 30-60 cm depths (Figure 3.2). Again, no significant correlation was detected in the 60-90 cm depth. In contrast to the relation between P_{diss} and DPS, no change point was identified for any depth. The concentration of P_{coll} was positively correlated to the optical density of the extracts chosen as an indicator for the total concentration of colloids (Table 3.3). Similarly, the concentrations of P_{coll} increased with the concentrations of Fe_{coll}+Al_{coll}. In the 0-30 cm

and the 30-60 cm depths, the concentrations of P_{coll} increased with increasing DPS of the colloids, which in turn reflected the DPS of the bulk soil. Concentrations of C_{coll} were not correlated with the concentrations of P_{coll}.

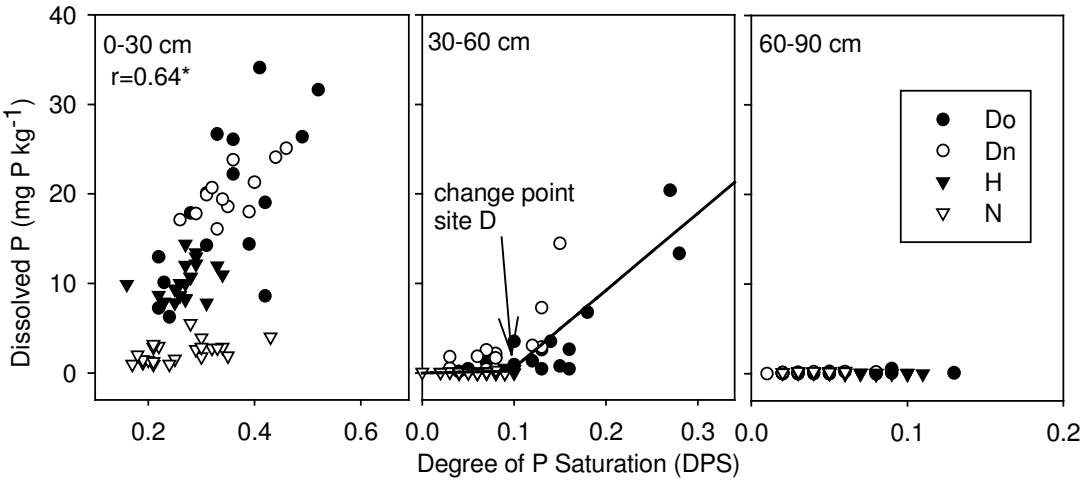

Figure 3.1: *Concentrations of dissolved P as a function of the degree of P saturation; * significant correlation at p < 0.05, r= Spearmans R. The split line was calculated for samples from 30-60 cm depth of the Dülmen site. Do: Dülmen old; Dn: Dülmen new, H: Hamburg, N: Nienburg.*

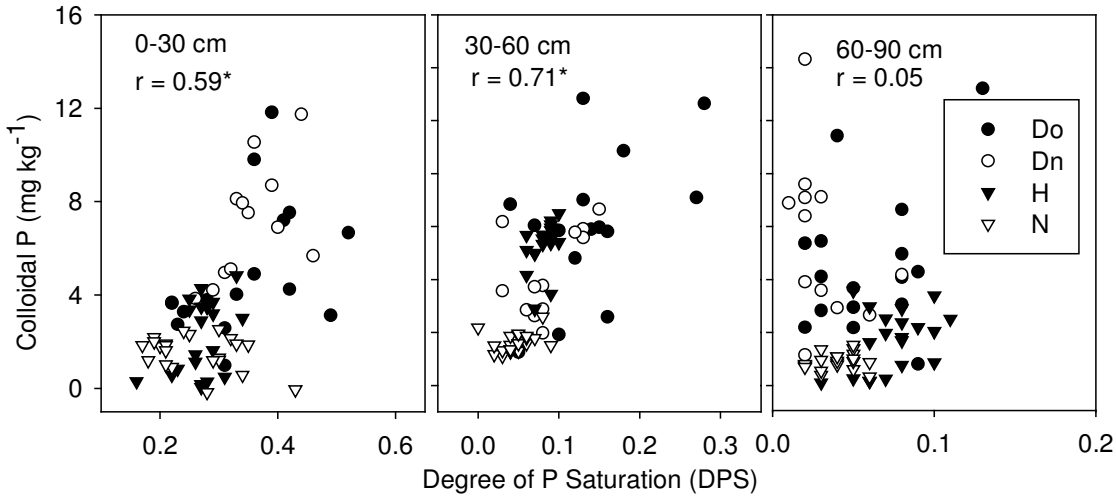

Figure 3.2: *Colloidal P concentrations related to the degree of P saturation; * significant correlation at p < 0.05, r= Spearmans R. Do: Dülmen old; Dn: Dülmen new, H: Hamburg, N: Nienburg.*

Table 3.3: *Coefficients of correlations between colloid characterizing properties (n=16).*

depth	0-30 cm	30-60 cm	60-90 cm
colloidal P concentration - optical density	0.89*	0.53*	0.88*
colloidal P concentration - colloidal Fe + Al concentration	0.88*	0.56*	0.77*
colloidal P concentration - DPS¶ of colloids	0.59*	0.69*	0.11
DPS of soil colloids - DPS of solid phase	0.52*	0.66*	0.25

* significant at $p < 0.05$
¶ DPS= Degree of P saturation

3.4.3 Fertilization effects on pH, ionic strength, and exchangeable cations affecting the stability of colloidal suspensions

The pH varied little because all sampled plots of the four long term experiments are limed regularly. The pH decreased with increasing depth from 6.7 (range: 6.1-7.2) in the 0-30 cm depth to 6.4 (range: 4.9-6.8) in the 30-60 cm depth and 5.9 (range: 4.7-6.7) in the 60-90 cm depth, but differences were not significant. Fertilization hardly affected the pH of the soils in the experiments Dn, H, and N. In experiment Do however, 45 years of fertilization increased the pH to 7.0 (Do3, 105 kg P ha^{-1} y^{-1}) and 7.2 (Do4, 144 kg P ha^{-1} y^{-1}) compared to the control (pH = 6.4).

The electrical conductivity decreased with increasing soil depth from 62±14 µS cm^{-1} in the 0-30 cm depth to 39±13 µS cm^{-1} in the 30-60 cm depth and 26±7 µS cm^{-1} in the 60-90 cm depth. The difference between the 0-30 cm and the 60-90 cm depth was significant. Conductivities were small because the sandy soils were sampled in January after most solutes had been leached. Exchangeable Ca^{2+} concentrations decreased significantly from topsoils to subsoils (839±273 mg kg^{-1} in the 0-30 cm, 361±101 mg kg^{-1} in the 30-60 cm, 312±64 mg kg^{-1} in the 60-90 cm depth). Similarly, K^{+}-concentrations were significantly higher in the plow layer (84±21 mg kg^{-1}) than in the 30-60 cm (51±16 mg kg^{-1}) and the 60-90 cm depth (57±18 mg kg^{-1}). Concentrations of exchangeable Mg^{2+} were approximately 5% of the Ca^{2+}-concentrations in the plow layer (42±18 mg kg^{-1}). In the 60-90 cm depth they were similar to concentrations in the 0-30 cm depth (40±18 mg kg^{-1}), while concentrations in the 30-60 cm depth were significantly smaller (28±11 mg kg^{-1}).

3.4.4 Effects of ionic strength and electrolyte composition on the release of colloids

Masking the effect of ionic strength and exchangeable cations by adding 0.01 M KCl as background electrolyte increased the electrical conductivity of the extracts to 1.43 mS cm^{-1} (Table 3.4). Increasing the total electrolyte concentration reduced the optical density and the concentrations of P_{coll}, Fe+Al and C. This effect was most pronounced for soil samples from the 60-90 cm depth. As a consequence, the optical density, the concentrations of P_{coll} and Fe+Al, as well as the ionic strength and pH, were significantly smaller for samples from the 60-90 cm depth compared to samples from the 0-30 cm depth. The zeta potential was significantly larger for samples from the 60-90 cm depth than for samples from the 0-30 cm depth.

Table 3.4: *Properties of colloids and colloidal suspensions*

depth (cm)	n	extractant	colloidal P (mg P kg^{-1})	colloidal Fe +Al (mg kg^{-1})	colloidal C (mg kg^{-1})	average particle size (nm)	zeta potential (mV)	optical density	pH	conductivity (µS cm^{-1})
0-30	5	H_2O	9.28[†a]	108[a]	57[a]	270[a]	-31.5[a]	0.198[a]	6.6[a]	56.6[a]
		KCl	4.77[b]	52.9[a]	27[b]	294[b]	-18.9[b]	0.118[a]	6.3[a]	1438[b]
30-60	5	H_2O	6.93[a]	220[a]	84[a]	275[a]	-33.2[a]	0.219[a]	6.3[a]	34.6[a]
		KCl	2.72[a]	39[b]	38[a]	428[b]	-20.2[b]	0.074[a]	5.7[b]	1426[b]
60-90	5	H_2O	3.13[a]	439[a]	13[a]	285[a]	-33.1[a]	0.265[a]	5.6[a]	24.8[a]
		KCl	bd[‡b]	8.24[b]	3[b]	1404[a]	2.12[b]	0.002[b]	4.8[b]	1409[b]

[†] arithmetic means; different superscript letters indicate significant differences between water extracts and KCl-extracts of the same depth increment
[‡] bd, below detection limit

The extraction with KCl confirmed the significant relationship between the concentration of water-extractable P_{diss} and the DPS (Figure 3.3). Similar to my findings for water-extractable P_{coll}, the concentrations of KCl-extractable P_{coll} increased linearly with increasing DPS without showing a distinct change point for the release of P_{coll}. In contrast to water-extractable P_{coll}, concentrations of KCl-extractable P_{coll} were closely correlated with the DPS when all three depths were pooled (Figure 3.3). Concentrations of Fe_{coll}+Al_{coll} were also significantly

related to DPS. The concentration of KCl-extracted colloids increased with increasing DPS as indicated by the optical density. Similar to the extraction with water, DPS of colloids was closely related to the bulk soil DPS.

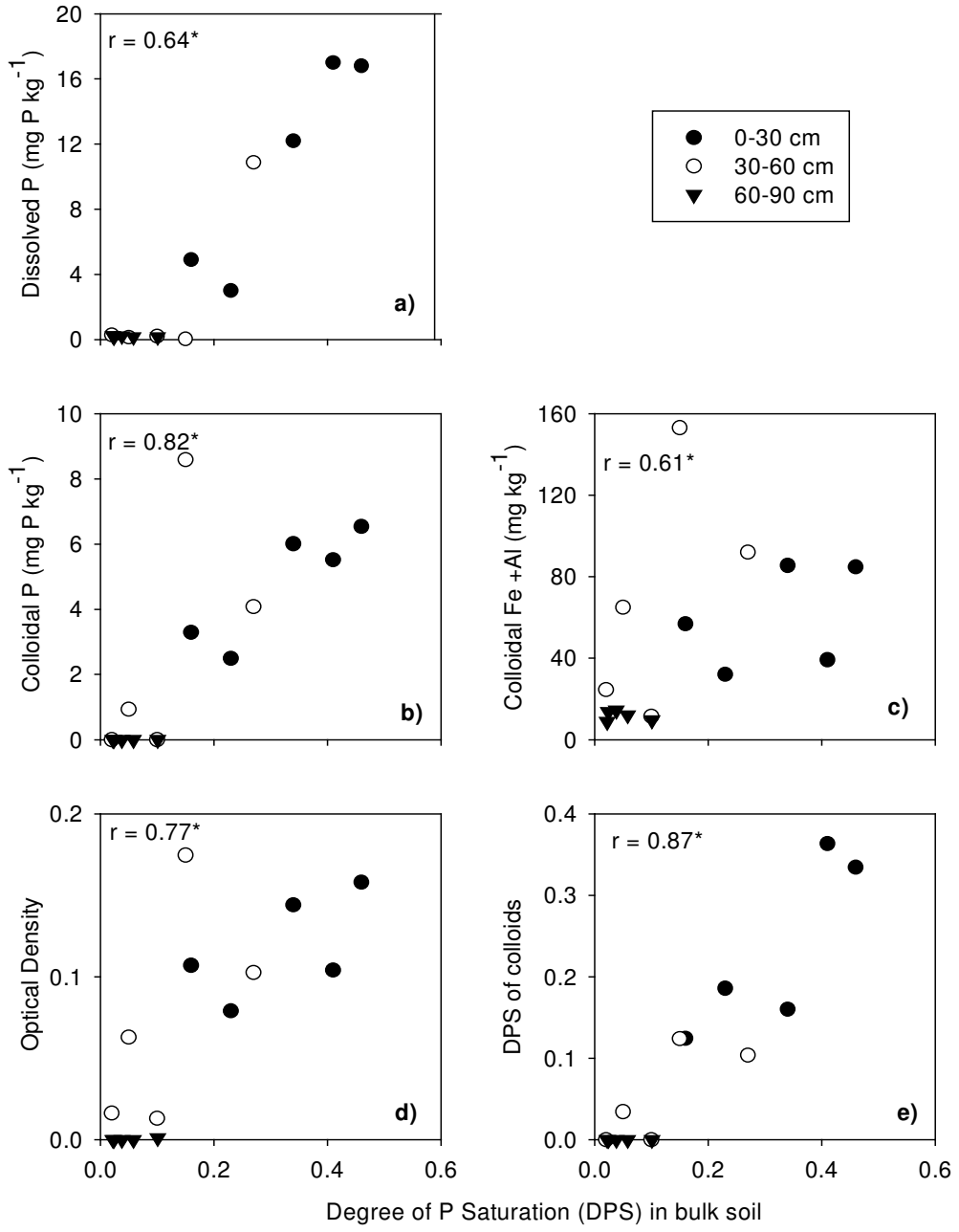

Figure 3.3: *Effect of the degree of P saturation on concentrations of dissolved P, colloidal P, colloidal Fe and Al, P saturation of colloids and optical density in KCl extracts; * significant correlation at $p < 0.05$.*

3.5 Discussion

3.5.1 Effect of fertilization on soil P fractions

Fertilization and application of manure had a stronger effect on the concentration of inorganic P_o, water-extractable P_{diss} and the P saturation in experiment Do compared to the other sites, which can easily be related to the large P accumulation in the soil of this experiment (Table 3.1). Interestingly, the nearly two-fold P balance of treatment 4 compared to treatment 3 as a consequence of the addition of manure was not reflected in significant differences in soil P fractions or DPS. Compared to P_o concentrations and DPS, the concentration of P_{diss} was more sensitive to P fertilization. For the Hamburg site, a small difference of 254 kg P ha^{-1} between the P balances of fertilized and unfertilized plots resulted in a significant increase of P_{diss} concentrations. Similar results were reported by Anderson and Wu (2001), who found that bicarbonate- and water-extractable P were more sensitive to different amounts of slurry application than total and oxalate-extractable P. These results are in conflict with the observation of Neyroud and Lischer (2004), however, that aggressive extracting agents such as oxalate were better related to P accumulation than "mild" agents.

The concentration of water-extractable P_{diss} decreased sharply from topsoil to subsoil, which is in accordance with depth profiles of P_{diss} concentrations reported by Siemens et al. (2004) for sandy soils of northwestern Germany. It is noteworthy that DPS never exceeded the critical value of 0.25 in the subsoils, which indicates leaching of P_{diss} concentrations larger than 100 µg l^{-1} potentially enhancing eutrophication of surface waters is unlikely at all sites. The critical value of 0.25 has been identified as tolerable for similar sandy soils of the Netherlands (Breeuwsma and Silva, 1992; van der Zee and van Riemsdijk, 1986, 1988; van der Zee and de Haan, 1994).

3.5.2 Relating dissolved P concentrations to P saturation

I found a significant change point of P saturation for samples from the 30-60 cm depth of the Dülmen Podzol, above which concentrations of P_{diss} increased sharply (experiments Do and Dn; Figure 3.2). Principally, the value of this change point as well as the slopes of the two linear regressions below and above the change point are soil specific and depend on the soil's sorption ca-

pacity, the soil's P affinity and experimental conditions such as the considered range of soil P or the soil to solution ratio (Koopmans et al. 2002). In fact, the increase in P_{diss} concentrations with increasing DPS in the 0-30 cm depth at site N seems to be small compared to the increase at the other sites (Fig. 2, 0-30 cm). Furthermore, part of the scatter of the relationship between DPS and P_{diss} in samples from the 30-60 cm depth might be caused by sampling varying fractions of Podzol B horizons and C horizons when taking samples from a fixed depth increment. However, the change point of DPS ≈ 0.10, which was determined for the 30-60 cm depth of the Dülmen site has some relevance for the other sites as well as for the other soil depths, as pooling the data from all sites and depths resulted in a similar change point of ≈ 0.10. The apparent robustness of the change point value under given experimental conditions allowed several authors to derive common DPS values as indicators of P leaching for sets of soils (Celardin, 2003; Maguire and Sims, 2002; McDowell et al., 2002) or even combinations of topsoil and subsoil horizons from different soils (Nair et al., 2004).

The critical DPS value of 0.1 that I found is smaller than the critical value of 0.25 and also smaller than the value of 0.20 that was reported by Nair et al. (2004) for sandy soils from the Suwannee river basin, Florida. In the case of the Dutch reference value, this difference might be attributed to the different ways that were used to identify critical values of P saturation. Whereas a description of the sorption and desorption process was used in the Netherlands to identify a P saturation corresponding to a critical P_{diss} concentration of 100 µg P l^{-1} (van der Zee et al., 1988; Schoumans and Groenendijk, 2000), I used a statistical model to separate two regions of P saturation without defining a critical target concentration of P_{diss}. Overall, my findings confirm the results of Maguire and Sims (2002), McDowell et al. (2002), Nair et al. (2004) and Siemens et al. (2004), which suggest that DPS is the most important factor controlling the concentration of P_{diss} in non-calcerous soils of temperate and subtropical climates.

3.5.3 Colloidal P and P saturation

The significant increase of P_{coll} concentrations with increasing DPS (Fig. 2) might be related i) to an increasing P concentration of individual colloidal parti-

cles or ii) to an additional release of colloids from the soil. In the first case, increasing P concentrations of individual colloids might be the consequence of increasing P_{diss} concentrations and sorption equilibria. In fact, the concentration of P_{coll} was correlated to the DPS of colloids, which reflected the bulk soil DPS (Table 3.3). However, water-extractable concentrations of P_{coll} were also positively correlated to the optical density and to the concentration of Fe_{coll}+Al_{coll} (Table 3.3). Both correlations indicate that additional colloids were released by an increasing DPS of the bulk soil. Hence, both processes seem to contribute to the increase of P_{coll} concentrations with increasing DPS. However, the fact that P_{coll} was released from subsoils with small DPS and the fact that the relations between concentrations of P_{coll} and DPS were not uniform for all depths show that DPS is not the only factor that controls the release of water-extractable P_{coll}. Similarly, the fact that P_{coll} concentrations were significantly smaller in the 0-30 cm depth receiving the highest P inputs compared to the control in experiment N (Table 3.2) indicates that factors other than P addition might influence the concentration of P_{coll}. Effects of other factors controlling the stability of colloidal suspensions like ionic strength or electrolyte composition might add considerable variability to the relation between DPS and water-extractable P_{coll}, which reduces the suitability of the extraction of P_{coll} with water to study the effect of P saturation or P accumulation on the risk of P_{coll} leaching.

3.5.4 Effects of pH, ionic strength and electrolyte composition on concentrations of colloidal P

It is well known that pH, ionic strength and electrolyte composition (in particular Ca^{2+}) significantly influence colloid mobilization and stability of colloidal suspensions (Kretzschmar et al., 1993; Heil and Sposito, 1993; Kretzschmar et al., 1999). In my case, it is unlikely that the pH had a pronounced effect on the release of water-extractable P_{coll}, because differences among pH values within a given depth increment were small and not significant. The significant decrease of ionic strength, Ca^{2+} and, to a lesser extent, Mg^{2+} concentrations from topsoils to subsoils might explain the high mobilization of colloids despite low DPS in subsoils. Furthermore, organic C increases the aggregation of soil particles in topsoils and may therefore influence the release of colloids (Goldberg et al., 2000). Higher concentrations of C_{coll} in soil samples from the 0-30 cm and the

30-60 cm depth compared to the 60-90 cm depth at a given DPS might reflect the aggregation of primary particles by organic matter in the topsoils (Table 3.4).

By adding KCl as background electrolyte, I masked the effect of low ionic strength on the release of P_{coll}. Consequently, DPS became the most important factor for the release of KCl-extractable P_{coll} as pooled concentrations of P_{coll} were closely correlated to DPS for all depths (Figure 3.3). Similar to my findings regarding water-extractable P_{coll}, the increase of P_{coll} concentrations might be related to the additional release of colloids as well as to increasing P concentration of single colloids because the optical density and the DPS of colloids increased with increasing DPS of the bulk soil (Figure 3.3). Generally, my results correspond to the findings of Zhang et al. (2003) and Siemens et al. (2004) that P additions or increasing P saturation induce the release of colloids and P_{coll} from soils. However, in contrast to Siemens et al. (2004) who reported a non-linear relationship between the concentration of KCl-extractable P_{coll} and DPS, I found a rather linear relationship (Figure 3.3) without a significant change point. In the sandy soils of this study this might reflect a more heterogeneous distribution of colloids with different characteristics in the sandy soils of this study, which are released at different DPS.

3.6 Conclusions

The DPS of oxalate-extractable Fe and Al oxides controls the concentration of P_{diss} in the sandy soils I investigated and increases the concentration if DPS $\geq$ 0.1. Water-extractable P_{coll} is a significant, in subsoils the dominating fraction of P that is potentially mobile. Concentrations of P_{coll} increase with increasing DPS without showing a critical level of P saturation for the release of P-containing colloids, which means that mobilization of P_{coll} might be already enhanced by P accumulation at low levels of P saturation. Furthermore, the release of P_{coll} is controlled by multiple factors including high DPS, small concentrations of exchangeable Ca^{2+} and small total electrolyte concentrations. Consequently, extraction methods masking the effects of electrolyte concentration and composition by using a background electrolyte are superior to extractions with water for studying the effect of P accumulation on P_{coll} in soils.

4 Comparing unsaturated colloid transport through columns with differing sampling systems

4.1 Abstract

Methodological difficulties of colloid sampling in the vadose zone are limiting our knowledge regarding the relevance of colloid transport for groundwater contamination. I compared the colloid sampling efficiency of five different lysimeters in a column experiment (9 cm length, 8 cm diameter) using ^{59}Fe labeled goethite: Polyester membranes with a pore diameter of a) 1.2 µm and b) 10 µm, c) porous glass plates with 16 µm pore diameter, d) wick samplers, and e) zero-tension lysimeters. Four replications of each lysimeter type were tested with concentrations of 0.1 mg l^{-1} and 10 mg l^{-1} goethite. The irrigation rate was 58 mm h^{-1}, which caused an average transport velocity of 240 mm h^{-1}. Compared to nitrate a tendency of accelerated transport of goethite in the sand columns was observed. The mean recovery of ^{59}Fe over all lysimeters was 30.7%±6.7% for the small and 3.4%±3.5% for the large colloid input concentration. For the small goethite concentration no differences between lysimeter systems were detected. In contrast, the lysimeters performed differently at large concentrations: zero-tension and 10 µm membrane lysimeters showed the largest (9.1% and 6.8%), wick lysimeters the smallest colloid recovery (0.7%), which was related to trapping of colloids in the wick. I conclude that membranes of 10 µm pore size and zero-tension lysimeters are superior for colloid sampling, but results of the latter may be biased towards an overestimation of colloid transport because of water saturation at the lysimeter/soil interface.

4.2 Introduction

Colloids are potentially important carriers for strongly sorbing pollutants and nutrients in soils (Kretzschmar et al., 1999). For example, Flury et al. (2002) and Cherrey et al. (2003) found that Cesium (Cs) sorbed to clay mineral colloids was hardly retarded or filtered in the unsaturated zone. Similarly colloidal transport of heavy metals such as mercury (Hg), cadmium (Cd) and zinc (Zn) or pes-

ticides as atrazine appears to be even more important than transport of dissolved species (Saiers, 2002; Guine et al., 2003; Barton and Karathanasis, 2003). Thus, many studies focus on processes of mobilization, transport and immobilization of colloids in laboratory experiments. To evaluate the role of colloids in soils, quantification of colloid transport under field conditions is also necessary. However, only few data are available about the extent of colloid dislocation at soil profile scale and at larger scales, e.g. in watersheds or over a longer time period (Kretzschmar et al., 1999; Heathwaite et al., 2005). This is mainly attributed to methodological difficulties of colloid sampling under unsaturated conditions.

To date colloids from natural soils are sampled by extracting soils in the laboratory with various solutions and separating dissolved and colloidal phase afterwards (Rhea et al., 1996; Sequaris and Lewandowski, 2003). However, most of these methods produce artifacts, e.g. by shaking, and therefore provide only a relative measure of colloid concentrations. They do not reflect the actual concentrations and mobility of colloids in soil solution under field conditions. Under field conditions various kinds of lysimeters are used to collect colloids via seepage water sampling (Gasser et al., 1994, Kaplan et al., 1997; Worall et al., 1999). The most frequently used lysimeter types are wick samplers, suction plates and zero-tension lysimeters. However, as Thompson and Scharf (1994) noted, not all types of lysimeters are equally suited for colloid sampling. Filtration and trapping of colloids in porous suction plates or cups with an average pore diameter of few micrometers as well as in fiberglass wicks may tamper colloid sampling (Grossmann and Udluft, 1991; Czigany et al., 2005). Additionally, installation of lysimeters may disturb the surrounding soil and lysimeters, especially zero-tension lysimeters, might influence the flow of water in the soil (e.g. Abdou and Flury, 2004), which in turn might affect colloid transport. Thompson and Scharf (1994) recommended specially constructed zero-tension lysimeters to sample and monitor colloid concentrations in the field. These lysimeters consist mainly of a sampling cup, which is connected to the soil surface by a tube and covered by a 150 μm polyester membrane, and are installed below an excavated and afterwards replaced soil core. However, the authors did not demonstrate the superior performance of their system compared to oth-

ers. Czigany et al. (2005) e.g. found, that fiberglass wicks are also suitable for colloid sampling, but only under certain conditions, particularly at high pH.
The objective of my study was to quantify the colloid-sampling efficiency of five different lysimeter systems (with a 1.2 µm membrane, a 10 µm membrane, a porous plate, a wick and zero-tension) under unsaturated conditions. I used ^{59}Fe labeled goethite as colloids.

4.3 Materials and methods

4.3.1 Lysimeter and column design, instrumentation

I tested colloid permeability of five collection systems, which are commonly used in soil sciences , each with four replications:

- membrane, pore size 1.2 µm, polyester (Pall, Portsmouth, England)
- membrane, pore size 10 µm, polyester (Franz Eckert GmbH, Waldkirch, Germany)
- membrane, pore size 200 µm, polyamide (Franz Eckert GmbH, Waldkirch, Germany)
- porous plate, nominal maximum pore size 16 µm, thickness 5 mm, sintered borosilicate (No. 50904, ROBU, Hattert, Germany), hydraulic conductivity: 17 mm h^{-1}.
- wick, 1.3 cm diameter, length 50 cm, glass fiber, 8 µm diameter (No. 1381, Pepperell Braiding Co., East Pepperell, MA, USA)

The collection systems were fixed at the bottom of plexiglass columns with a length of 30 cm and an inner diameter of 8 cm (Figure 4.1). A 30 cm hanging water column in a silicone tube (0.3 cm inner diameter) generated suction for porous plates, 1.2 µm and 10 µm membranes. The volume of water in the hanging tube was negligible compared to the volume of water in the columns. Therefore the tubes did not influence transport parameters of the tracer or colloids. Fiberglass wicks are self-priming and act as a hanging water column according to the height difference of the wick without external application of suction (Boll et al., 1992). The 200 µm membrane lysimeters drained freely into the sampler and is denoted as zero-tension lysimeter in the following. I tested the 20 columns in two runs with different colloid concentrations. One replicate of each

lysimeter type appeared in both runs and the remaining three replicates were randomly distributed.

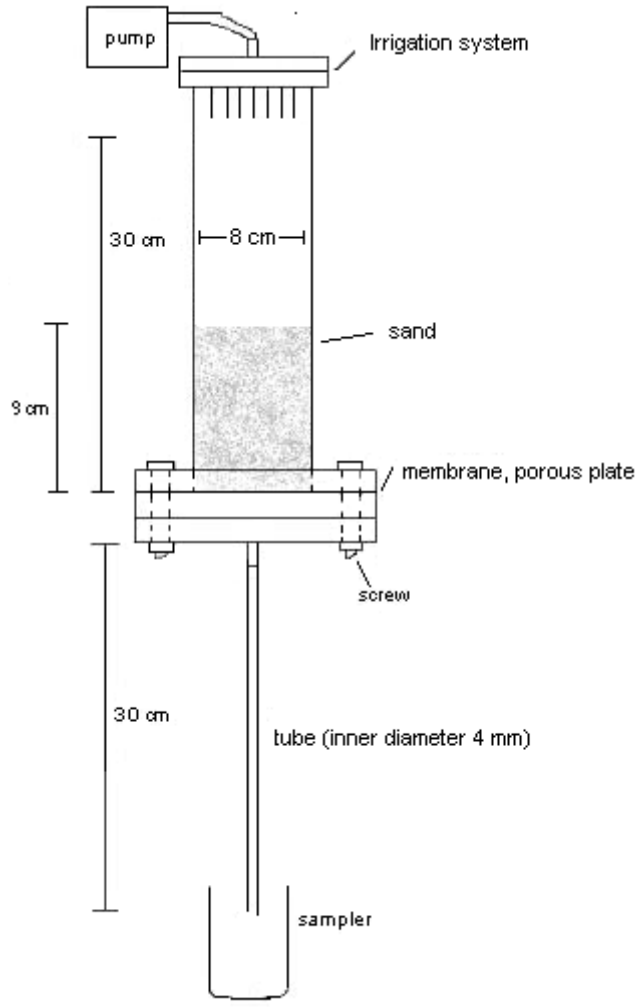

Figure 4.1: *Column with a membrane lysimeter. The tube acts as a hanging water column, ensuring unsaturated conditions.*

In a pre-experiment I tested columns filled up to a level of 25 cm with quartz sand (grain size of 0.2-0.6 mm). However, no colloids were found in the outflow of the columns and therefore the set up of the experiment was changed. For the main experiment I filled up the columns to a level of 9 cm with quartz sand (Dorsilit, Germany) of a grain size of 0.6-1.2 mm. The pore volume was 0.42 m^3 m^{-3} and the saturated conductivity 3460 cm d^{-1}. The sand had a very steep water retention curve with water contents of 0.30 m^3 m^{-3} at a matrix potential of -1 kPa and 0.04 m^3 m^{-3} at -2 kPa. Prior to use, the sand was heated up to 1000°C for 2

for 2 h to remove organic matter and washed with 1 M hydrochloric acid (HCl) for 24 h to remove lime residues. Afterwards I replaced the acid by flushing the treated sand with deionized water and conditioned the sand with a 200 µM sodium dihydrogen phosphate (NaH_2PO_4) solution for 24 h. A pH of 6.7 was adjusted with sodium hydroxide (NaOH).

On top of the columns an irrigation system was installed, which consisted of a plexiglass block containing 45 cannulae with an inner diameter of 0.4 mm at the bottom side (Figure 4.1). Peristaltic pumps fed the columns with solution. An automatic sampler collected column outflow.

4.3.2 Colloid suspension

I synthesized goethite by oxidation of Fe(II) ($FeSO_4*7H_2O$) with H_2O_2 at a pH of 7 according to Mikutta et al. (2006). Goethite was washed, until the water had an electrical conductivity of 10 µS cm^{-1}, freeze-dried and goethite aggregates were ground. X-ray diffraction analysis (D5050, Siemens, Germany) showed a pure goethite without contamination. Electron microscopic pictures showed crystals with an average size of 80 nm (S520, Hitachi, USA). The specific surface area was 144.8 m^2 g^{-1} (Autosorb-1, Quantachrome Instruments, Odelzhausen, Germany).

Two batches of goethite were irradiated with neutron radiation for 55 h in the research reactor of the Hahn-Meitner-Institut (HMI, Berlin, Germany) and allowed to decay for three days. Upon irradiation, ^{56}Fe was transformed to ^{59}Fe to some extent. Decay of ^{59}Fe to stable Co^{59} emits β- and γ-radiation. The half-life of ^{59}Fe is 45.1 d (Metcalfe, 1976). Resulting activities after irradiation were $1.1*10^7$ (1^{st} batch) and $1.6*10^6$ Bq (2^{nd} run).

I suspended the two batches of Goethite in 1 l and 0.5 l of 80 µM NaH_2PO_4 and kept them in an ultrasonic bath for 30 min to break up agglomerates. Following ultrasonic treatment, the first batch of goethite suspended in NaH_2PO_4 solution was stirred for 24 h. Because of technical reasons, the second batch of goethite suspension was shaken end-over-end for 15 h. I filtrated the suspensions with a 1.2 µm cellulose acetate filter (Sartorius, Göttingen, Germany) to analyze only particles < 1.2 µm of the colloidal fraction. The resulting suspensions had an activity of 12.3 Bq ml^{-1} in the 1^{st} batch (equivalent to 0.1 mg goethite l^{-1}) and 338

Bq ml^{-1} in the 2nd batch (equivalent to 10 mg goethite l^{-1}). For a non-radioactive, equally treated goethite I measured an average particle size of approximately 400 nm after filtration (High Performance Particle Sizer, Malvern Instruments, UK).

The resulting adsorption of phosphate shifts the isoeletric point of goethite from pH 7-8 down to approximately pH 4 (Stumm and Sigg, 1979). Therefore phosphate-covered goethite colloids were negatively charged in my experiment, which I conducted at pH 6.5-7 (Puls and Powell, 1992). The zeta-potential of a non-radioactive, equally-treated goethite at pH 6.5 was -29.8 mV (DTS 5200 Zetasizer 2000, Malvern Instruments, UK). I supposed the negatively charged colloids to be repelled from the phosphate-covered sand matrix and therefore to be more mobile than goethite colloids without adsorbed phosphate.

4.3.3 Column experiment

I irrigated the columns in a steady state, unsaturated flow modus with an average irrigation rate of 58 mm h^{-1} (in the pre-experiment 2.5 mm h^{-1}). Irrigation rates ranged from 51 to 65 mm h^{-1}. Before application of the goethite suspension, columns were irrigated with 80 µM NaH_2PO_4 solution until constant water contents and flow rates were established for each individual column. I applied 26 mg NO_3 l^{-1} in the first run and 99 mg NO_3 l^{-1} in the second run as conservative tracer in the colloid suspension. Irrigation for application of tracer and colloids took 5 min, afterwards I continued irrigation with the background electrolyte (80 µM NaH_2PO_4). Each run lasted 1.5 h. During the first third of each run, samples were collected every minute, during the second third every two minutes and during the last third every six minutes.

The outflow was determined gravimetrically for each sample. I detected nitrate with a photometer at a wavelength of 203 nm (Specord 200, Carl Zeiss Technology, Jena, Germany). The detection limit was 0.32 mg NO_3 l^{-1}. The radioactivity of the samples was determined with a germanium (Ge) detector (Canberra Industries, Meriden, USA) and the data processed with an analog-digital-converter (7070 ADC, FAST Comtec Datensysteme GmbH, Oberhachingen, Germany) and a MCD/PC operating software (FAST Comtec Datensysteme). The detector recorded γ-radiation at 1098 MeV and 1292 MeV. I considered only the signal at 1098 MeV, because transition probability was larger than for

the peak at 1292 MeV. Integration time of the first run was 1200 s and of the second run only 500 s, because of the larger activity.

After the irrigation experiment I selected one column of each lysimeter type from the second run with large colloid concentrations to separate the sand into three layers in order to determine the radioactivity: upper, middle and lower part. Similarly, one wick was cut into three sections. A defined amount of active goethite solution mixed with uncontaminated sand or wick was used for calibration. Unfortunately, it was not possible to determine the activity of porous plates and membranes because the inhomogeneous distribution of ^{59}Fe hindered proper calibration. Sand and wick samples were measured in a Ge detector (Canberra Industries, Meriden, USA) using an integration time of 500 s.

4.3.4 Adsorption of goethite to sand

To check if goethite colloids sorb to the quartz sand, samples of 7 g of phosphate-covered sand were shaken for 15 h end-over-end with 50 ml of phosphate-covered goethite suspensions with increasing concentrations (5-400 Bq ml^{-1}). Afterwards I decanted the solution and measured the activity in the supernatant. Adsorption of goethite colloids to sand was negligible.

4.3.5 Calculations and statistical evaluations

I conducted a stationary experiment with constant flow conditions. Transport of solutes through a homogeneous porous medium can be described with the convection-dispersion-equation (CDE) (Wierenga and van Genuchten, 1989; Vanclooster et al., 1993). Deposition of colloids can be described by an additional first-order deposition term. Colloid deposition occurs either directly at the water-solid or at the air-water interface. Commonly remobilization back to solution is small and can be neglected (Schäfer et al., 1998). The CDE for colloid transport with a first-order deposition term is:

$$\frac{\partial c}{\partial t} = D\frac{\partial^2 c}{\partial x^2} - v\frac{\partial c}{\partial x} - \mu_d c \qquad (1)$$

where c (x, t) is the colloid concentration in mg l^{-1}, D the hydrodynamic dispersion coefficient in $mm^2\ h^{-1}$, v the average transport velocity in mm h^{-1} and μ_d the coefficient of deposition in h^{-1}. I fitted D and v for nitrate and D, v and μ_d for colloids. All parameters were fitted simultaneously using the measured break-

through curves of the tracer and the colloids with the software CXTFIT 2.1 (Toride et al., 1998).

Statistic calculations were done using STATISTICA 6.0 software (StatSoft, Tulsa, USA). All data were tested for normality with the Shapiro-Wilk's W-test (Shapiro et al., 1968) and for homogeneity of variances using the Levene's test (Sachs, 1982). I checked the significance of differences between mean values with the Tukey-test (Winer et al., 1991). Not normally distributed data were tested with the non-parametric Kruskal-Wallis H-test (Winer et al., 1991) and the Mann-Whitney U-Test (Dineen and Blakesley, 1973). Parameters of nitrate and goethite transport were compared with the parametric paired t-test and the non-parametric paired Wilcoxon-test (Sprent and Smeeton, 2001). I used a level of significance of $p < 0.05$ for all tests.

4.4 Results

In the pre-experiment with medium sand, longer columns and smaller flow rates I found no goethite colloids in the outflow of all columns. Therefore I decided to conduct the experiment with coarser sand, shorter columns and higher flow rates. In the latter experiment one of the 10 µm membrane lysimeters failed, probably because of an incorrect application of tracer and colloids. No nitrate and no ^{59}Fe could be detected in the outflow of this column although water flowed through the column. Therefore I took only three lysimeters of this type into account. In one 10 µm membrane lysimeter and one porous plate lysimeter water did not flow through continuously, therefore only few samples were collected.

4.4.1 Water regime and nitrate transport

Nitrate breakthrough curves were fitted with CXTFIT with an average R^2 of 0.72±0.24 for 10 µm membrane, 0.98±0.01 for wick, 0.86±0.06 for zero-tension, 0.92±0.08 for porous plate and 0.95±0.02 for 1.2 µm membrane lysimeters. Exemplary breakthrough curves and fits of every lysimeter type for both applied colloid concentrations are shown in Figure 4.2 and 4.3. A pronounced tailing for nitrate could be observed, but a mobile-immobile model approach (Cherrey et al., 2003) did not improve the fit. Average nitrate recovery was 102%, ranging from 90 to 108% with one exception of 145% for a 10 µm membrane column in

the first run (Table 4.1). I ascribe recoveries above 100% to irregularities of peristaltic pumps, which probably delivered slightly more than the calculated amount of solution. The recoveries did not differ significantly between the lysimeter types. The coefficients of dispersion varied between 970 and 2910 $mm^2\ h^{-1}$. Transport velocity ranged between 156 and 415 mm h^{-1} (Table 4.1). Transport parameters of nitrate did not differ significantly between the two runs.

Table 4.1 *Hydrodynamic and tracer parameters of the columns; standard deviations in parenthesis*

type of lysimeter	transport velocity (v) mm h^{-1}	coefficient of dispersion (D) $mm^2\ h^{-1}$	recovery of tracer %
1.2 µm membrane	415 (77)	1940 (1300)	102 (5.5)
10 µm membrane	264 (156)	1220 (1070)	117 (24)
porous plate	261 (130)	967 (899)	96.5 (2.7)
Wick	193 (156)	1340 (1560)	106 (2.4)
zero-tension	253 (55)	2910 (630)	94.2 (4.4)

4.4.2 Colloid transport

Similar to nitrate transport, colloid breakthrough showed a pronounced tailing that was not described satisfactory by the CDE-model (Figure 4.2-3). For two of three wick lysimeters in the second run no meaningful colloid breakthrough curves could be fitted, because only few samples contained colloids in small concentrations. Fitted transport parameters of these two columns were not used, but I included the columns in calculations of mass balances. Also other columns had small colloid concentrations in the outflow and fitting was only possible with a correlation coefficient < 0.9 for most of the columns. The coefficient of dispersion ranged from 533 to 3260 $mm^2\ h^{-1}$. Transport velocity varied within 240 and 393 mm h^{-1} (Table 4.2).

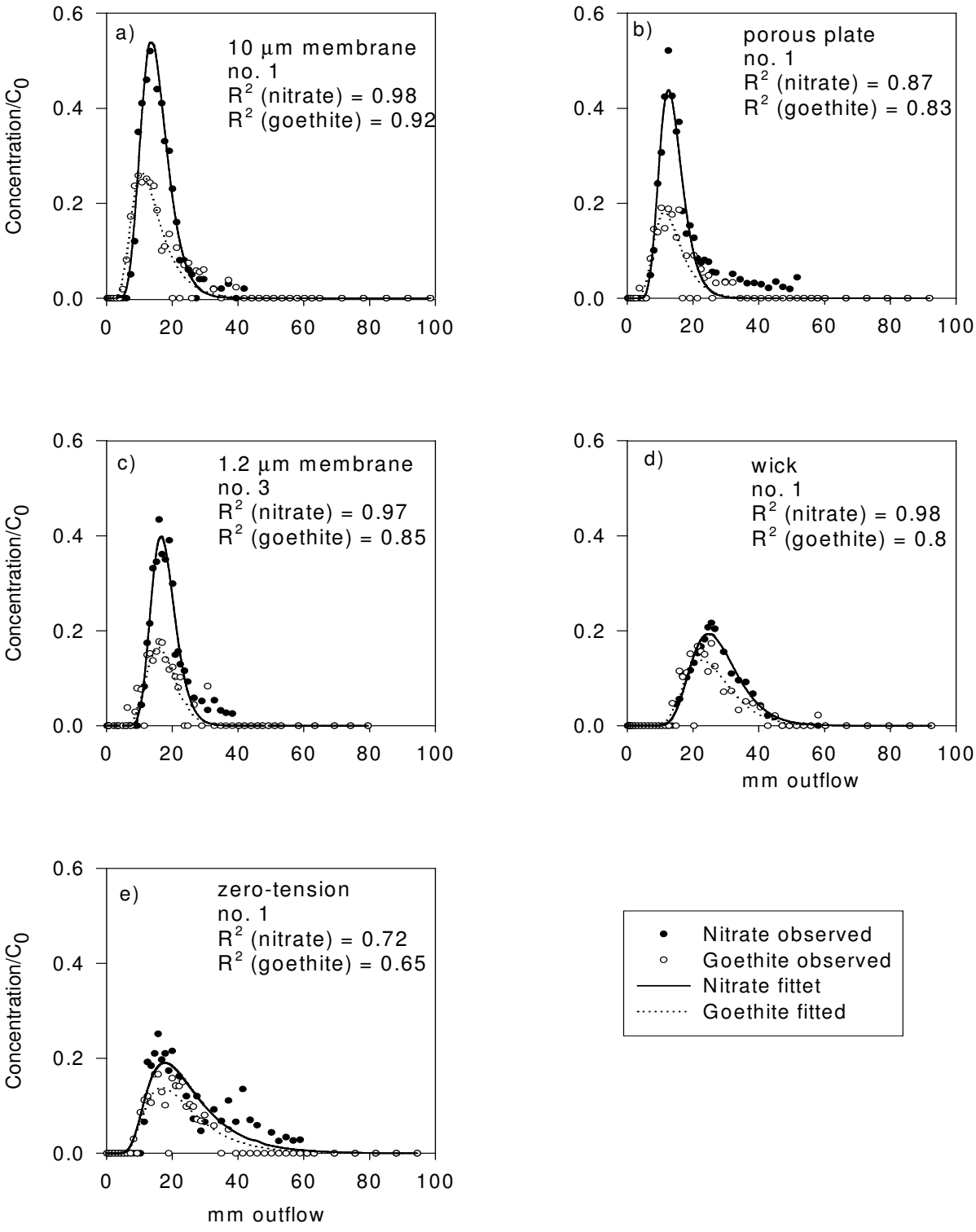

Figure 4.2 a)-e): *Exemplary nitrate and goethite breakthrough curves of all lysimeter types (small colloid concentration applied). Curves were fitted with the convection-dispersion-equation.*

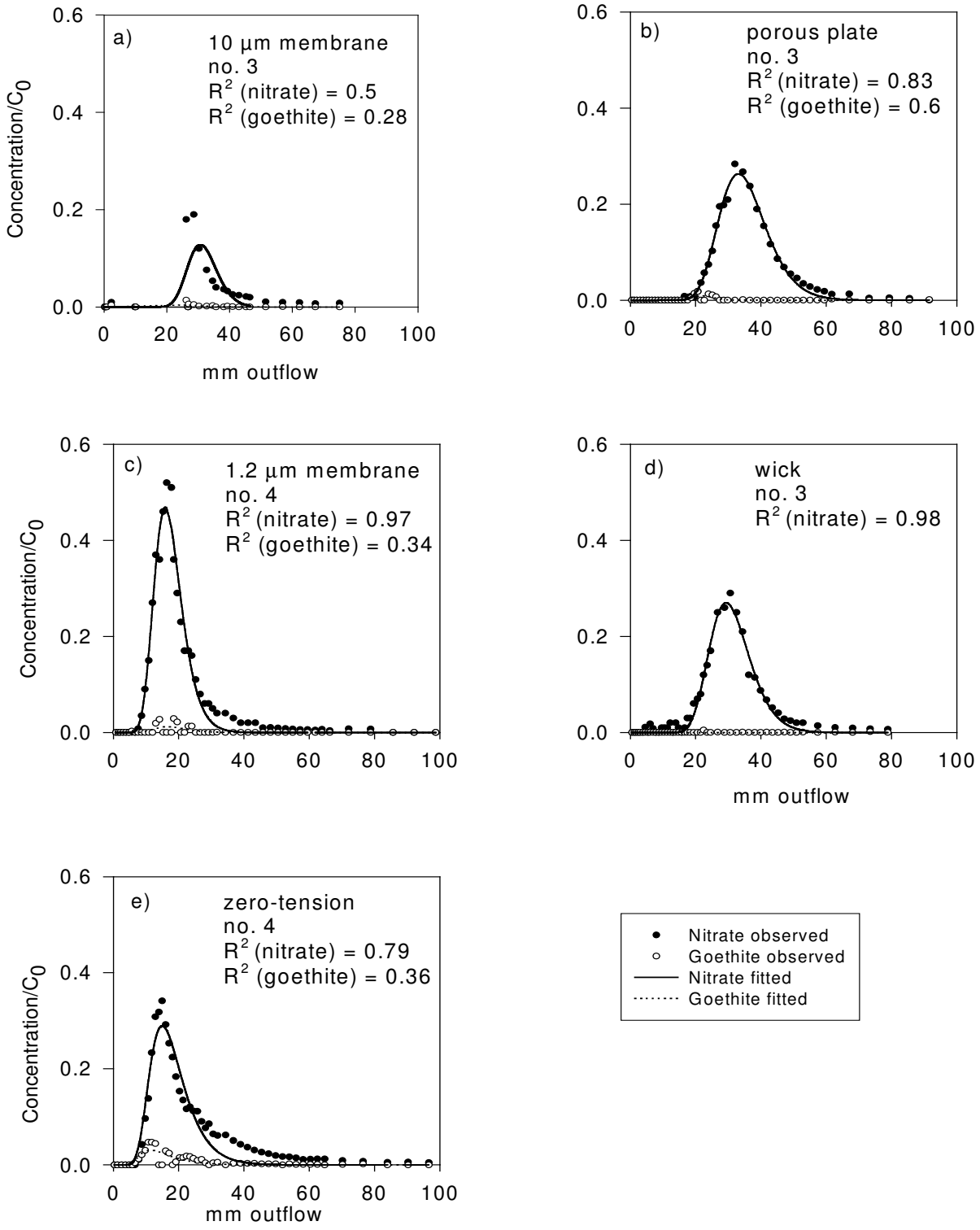

Figure 4.3 a)-e): *Exemplary nitrate and goethite breakthrough curves of all lysimeter types (large colloid concentration applied). Curves were fitted with the convection-dispersion-equation.*

Table 4.2: *Mean values of transport velocities, coefficient of dispersion, recovery and coefficient of deposition of colloids; standard deviations in parenthesis (where no standard deviation is denoted, I had only one replication in that run)*

type of lysimeter	transport velocity (v)	coefficient of dispersion (D)	recovery		coefficient of deposition (μ)	
	mm h^{-1}	mm^2 h^{-1}	%		h^{-1}	
			small colloid concentration	large colloid concentration	small colloid concentration	large colloid concentration
1.2 μm membrane	351 (111)†	3260 (3090)	28.7 (2.5)	2.3	5.2 (1.1)	12
10 μm membrane	240 (173)	2900 (2590)	36.9 (9.8)	6.8	2.8 (0.88)	4.6
porous plate	381 (113)	1290 (2040)	28	1.4 (0.78)	4.4	21.1 (11)
Wick	259 (62)	533 (669)	31	0.7 (0.2)	0.75	19.8
zero-tension	393 (111)	1510 (1210)	28.7 (12)	9.1 (0.52)	4.4 (4.2)	13 (8.1)
overall average			*30.7 (6.7)*	*3.4 (3.5)*	*3.9 (2.3)*	*15.9 (8.7)*

Colloid breakthrough peaks tended to occur before the nitrate breakthrough in all lysimeter types except wick lysimeters. Figure 4.4 shows exemplarily one cumulative breakthrough curve of each lysimeter type as percentage of the total amount recovered. To compare nitrate and colloids, the amount of both is related to the total cumulative amount in the outflow. Goethite particles passed the column faster than nitrate. On average the cumulative breakthrough of colloids reaches the value of 25% of the total amount recovered 1.8±0.3 mm before nitrate. A bias resulting from differing precisions of measurement between nitrate and goethite was tested and can be excluded. However, differences between transport parameters for colloids and nitrate were not significant.

The transport velocities v and dispersion coefficients D were not significantly different for the smaller and larger colloid concentration, however, the recovery and hence the first-order deposition rate coefficient μ was (Table 4.2). For the small colloid concentration, μ was significantly smaller and therefore recovery larger than in the second run. Further, functioning of the lysimeter types was different at different colloid concentrations: While recoveries were similar for all

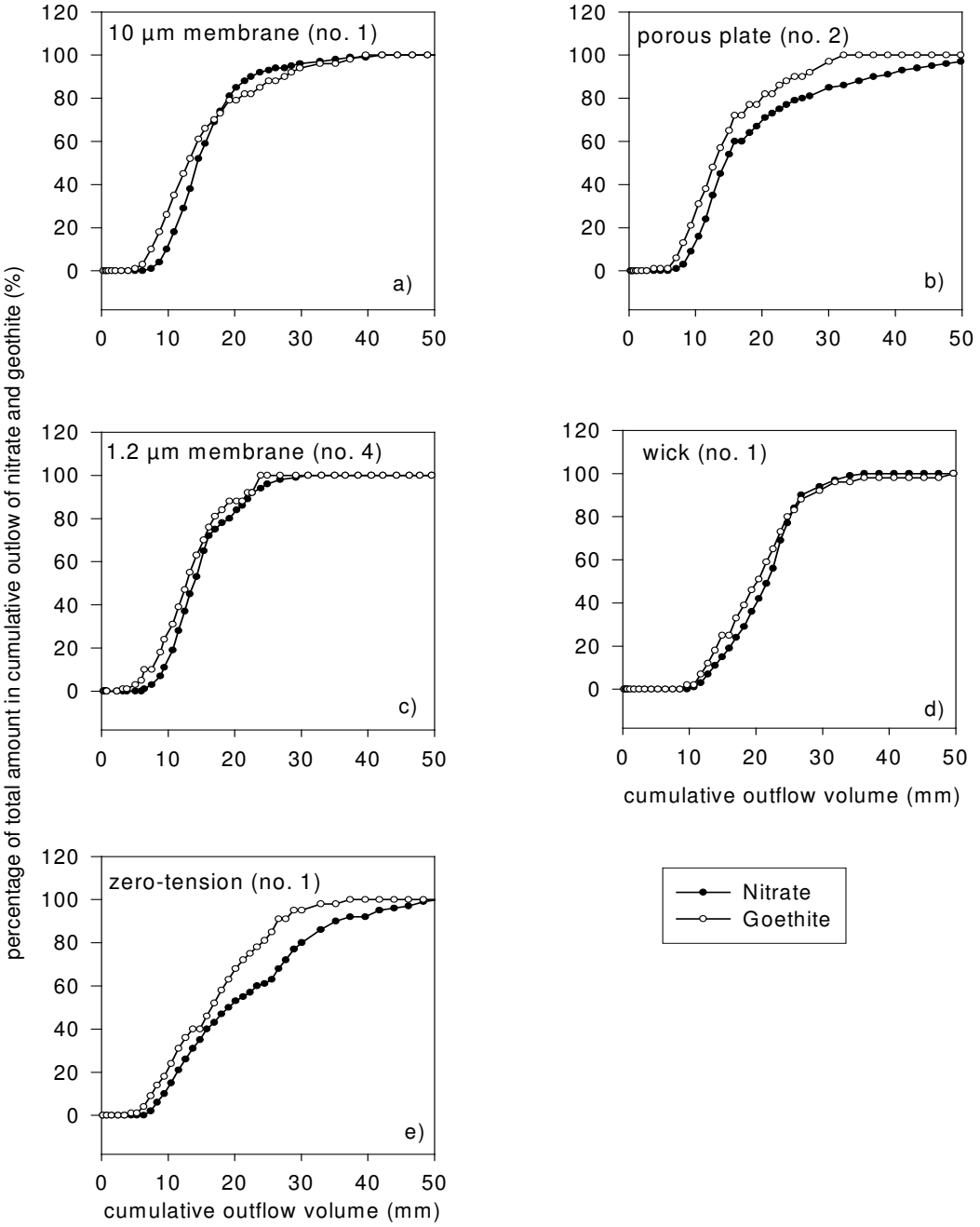

Figure 4.4 a)-e): *Cumulative breakthrough curves (in percentage of the total amount in the outflow) of nitrate and goethite. Goethite tends to move faster through the sand than nitrate.*

lysimeter types for the small colloid concentration, results differed after application of the larger colloid concentration. Membranes of 10 µm pore size and zero-tension lysimeters showed above-average recoveries of ^{59}Fe in drainage whereas recoveries of wick, 1.2 membrane and porous plate lysimeters were below average (Table 4.2).

By measuring the ^{59}Fe activity in different segments of the columns of the second run I established depth profiles, which illustrated the retention of colloids in the sand (Figure 4.5). In all examined columns the majority of colloids was retained within the upper 0-3 cm of the sand column. In the zero-tension lysimeter column I detected no colloids in the lowest depth interval (Figure 4.5 e, 6-9 cm). The total recovery of ^{59}Fe (sand, leachate and wick) was 99%±19%.

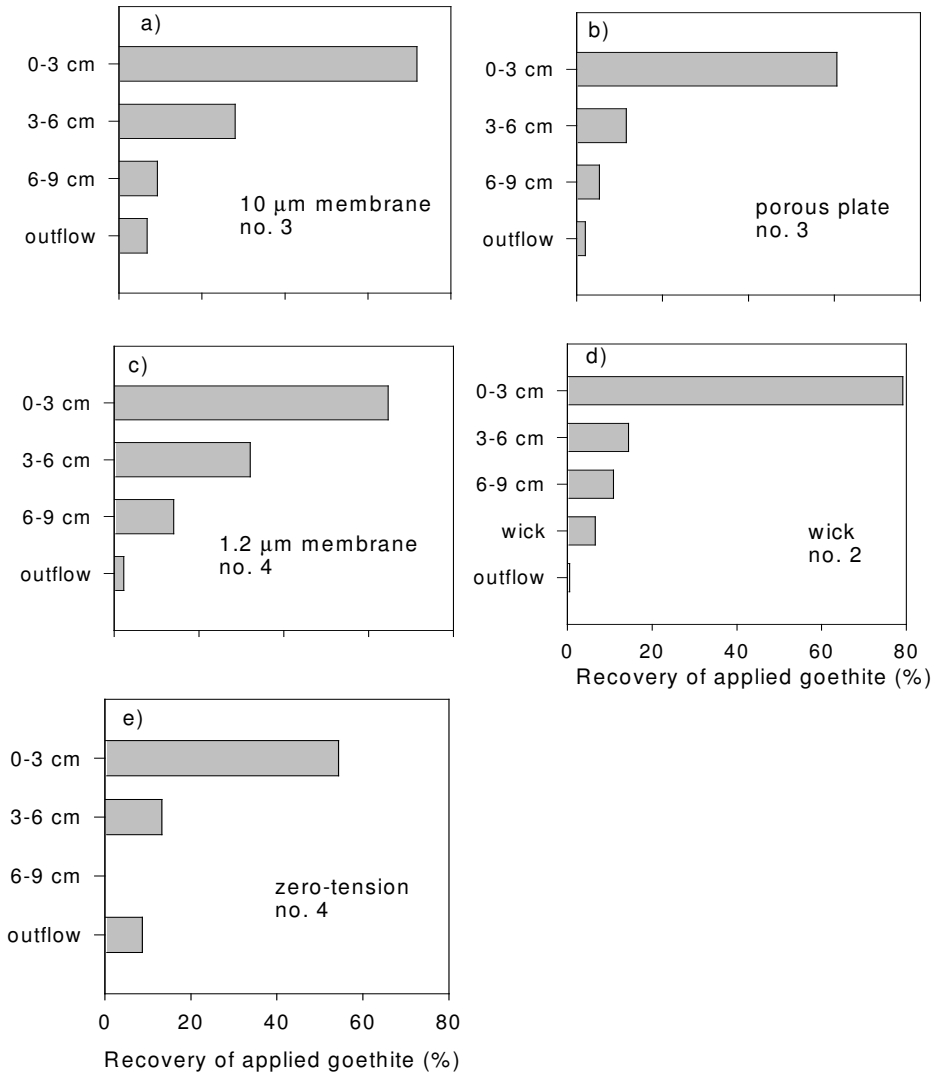

Figure 4.5 a)-e): *Depth profiles of colloids in sand, wick and outflow (second run with large colloid concentrations). The accumulation of ^{59}Fe in the top-three centimeters of the sand illustrates that unsaturated sand was a good filter for Goethite colloids. Note the absence of colloids in the sand directly above the zero-tension lysimeter, which is probably related to saturated conditions above the lysimeter/soil interface. Colloids were trapped in the wick.*

4.5 Discussion

4.5.1 Water regime and nitrate transport

The recovery of nitrate in drainage was satisfactory for all lysimeter systems. Probably because of saturated conditions in the lower part of the column, zero-tension lysimeters had a larger dispersion coefficient than the other systems: Water was retained above the lysimeter and diffusion could take place resulting in an equilibration of nitrate concentration gradients (Abdou and Flury, 2004).

I assume a gradient of water content between upper and lower part of the columns, because of the steep water retention curve of the coarse sand. Water contents directly above the lysimeters are influenced by the lysimeters themselves, which is a natural characteristic of the collection systems and therefore also valid under field conditions. Therefore effects of differing hydraulic conditions in the sand columns and effects of the lysimeters themselves on colloid transport can not be separated from each other. In contrast to other systems, in a zero-tension lysimeter system water has to accumulate above the collection system until atmospheric pressure is reached before water can flow off (Abdou and Flury, 2004). But also the systems with membranes and porous plates influence the water content above the lysimeter depending on the difference between the conductivity of the membranes and the plate compared to the conductivity of sand. Due to the low unsaturated hydraulic conductivity of the coarse sand, the influence of the lysimeter on the hydraulic conditions is not as pronounced as in finer sands or silty materials.

4.5.2 Colloids

In the pre-experiment all colloids were retained in the column, because of i) the length of the column (25 cm) and/or ii) the small grain size of the sand. This confirms the efficiency of slowly percolating sand filters for the removal of colloids (Gimbel and Nahrstedt, 2004).

In my presented experiment with coarse sand and short columns, however, an accelerated transport of goethite compared to nitrate was observed, independent of the sampling system used (Figure 4.4). According to Keller et al. (2004) and Sirivithayapakorn and Keller (2003) accelerated transport can be assigned to a size-exclusion effect: colloids move faster through porous media because

they travel through wider pores compared to a dissolved tracer. However, the effects are small and the statistical evaluation of transport parameters did not confirm significant differences of transport velocities and dispersion coefficients between goethite and nitrate, which I ascribe to the homogeneous pore system and the shortness of columns used in the experiment. Tailing of nitrate and colloid breakthrough curves can not be caused by reactions with sand, because nitrate behaves like a conservative tracer and adsorption of goethite with sand was tested and can be excluded. The exchange of nitrate and goethite between mobile and immobile regions of the pore system can be another reason for tailing (Cherrey et al., 2003). However, application of a mobile-immobile model of solute transport did not improve the goodness of fit.

I observed smaller recoveries at large colloid concentration and larger recoveries at small colloid concentration, although deposition should be independent from the applied colloid concentration and is assumed to follow a first-order kinetic rate law (Kretzschmar et al., 1997b). Differing recoveries occur if hydraulic conditions, e.g. the flow rate, vary: Larger flow rates cause larger water contents within the columns and therefore a smaller deposition of colloids (Cherrey et al., 2003; Mays and Hunt, 2005). But none of the hydraulic parameters differed between the two runs (Table 4.1). Li et al. (2004) observed a decreasing colloid deposition with increasing transport distance. This finding would correspond to my result if the effect is related to decreasing colloid concentrations along the transport path. Colloid concentrations may decrease due to straining, i.e. the deposition of colloid particles in down-gradient pores, which are too small to allow particle passage (Bradford et al., 2004). The effect might be enhanced by pore clogging, because initially deposited colloids make the pores smaller and smaller. An effect of differing particle sizes on varying deposition of colloids in the two runs cannot be excluded, because I was not able to check the particle size of radioactive goethite colloids. Differing particle size distributions would strongly influence colloid migration (Bradford et al., 2004). Furthermore, it cannot be ruled out that the stability of colloidal suspension was lowered due to the larger colloid concentration or slightly larger ionic strength in the second run because of larger nitrate concentration (Kretzschmar and Sticher, 1997; Saiers and Lenhart, 2003).

Differences between lysimeter systems did not appear at small colloid concentrations and small deposition rate. Obviously filtration caused by different lysimeter systems did not significantly influence the outflow of colloids under these conditions. Large colloid concentrations and large deposition rates, however, might have increased filtration by membranes, porous plates, and wicks. Compared to the porous plate, for 1.2 μm and the 10 μm membrane lysimeters it is not very likely that relevant concentrations of colloids were deposited directly in the thin membranes. In the lowest depth segment the 1.2 μm membrane system showed the largest colloid concentration compared to the other systems (Figure 4.5 c). I assume that colloids accumulate at the surface of the membrane, because of a filtration effect of the lysimeter. For the 10 μm membrane colloid concentration in the lowest depth segment was smaller and recoveries in the outflow larger, because it did not filter as much colloids as the 1.2 μm membrane (Figure 4.5 a). In the second run I had only one 10 μm membrane column. Anyway, I assume that the result is reliable, because standard deviations of other column replications in this run were small compared to the measured recovery. The retention of colloids in fiberglass wicks corresponds to the findings of Czigany et al. (2005), who observed a recovery smaller than 5% for ferrihydrite transport through wicks at pH 7. They ascribe colloid retention to physicochemical deposition inside the wick, which was probably the reason for fragmentary breakthrough curves of wick samplers in my study. The zero-tension lysimeters column retained no colloids in the lowest column segment at all. As I argued above, water saturation is larger in the lower part of this column. Under saturated conditions, colloid deposition is smaller and colloids are more mobile (Cherrey et al., 2003). Additionally no barrier as e.g. a porous plate or a wick retained colloids. This might explain the larger recovery of zero-tension lysimeters in the outflow compared to 1.2 μm membrane, porous plate, and wick lysimeters in the second run.

4.6 Conclusion

Generally, my experiments confirm the large filtration efficiency of sand under unsaturated conditions. Especially at realistic flow rates of less than 10 mm h^{-1}, negatively charged goethite was hardly mobile in the medium sand. Transport

velocity and dispersion of colloidal goethite particles were similar to a conservative tracer and accelerated transport due to size exclusion was small. Colloid retention and deposition was not independent of the colloid concentration, which is in conflict with a first-order deposition rate model for colloid transport. Wick samplers were effective filters for goethite colloids, which disqualifies them for colloid sampling. Among the tested systems, zero-tension lysimeters and membranes of 10 µm pore size appeared superior for sampling of colloids because they showed largest recoveries of ^{59}Fe in drainage, when large goethite concentrations were applied. However, water saturation above the soil/lysimeter interface of zero-tension systems may cause a bias towards an overestimation of colloid transport.

5 Colloid-facilitated phosphorus leaching as influenced by P accumulation in sandy soils

5.1 Abstract

Colloidal P may significantly contribute to P leaching from soils. In an experiment with undisturbed soil columns I investigated whether an increasing P saturation enhances the leaching of P_{coll} from sandy soils. Furthermore I hypothesized that large concentrations of P_{coll} occur at the onset of leaching events and that P_{coll} mobilized from topsoils is retained in subsoils. Columns were collected in northeastern Germany at a former disposal site for liquid manure and at a long-term fertilization experiment in Thyrow. Soils were of varying P saturation and depth (0-25 cm and 0-40 cm). After irrigation I measured the concentrations of P_{diss}, P_{coll}, Fe_{coll}, Al_{coll}, and C_{coll}, optical density, zeta potential, pH and electrical conductivity of the outflow. Colloidal P concentrations ranged from 0.46 to 10 µmol l^{-1} and contributed between one and 37% to total P leaching. Significantly larger concentrations of P_{coll} were leached from the Werbellin subsoil characterized by a large DPS than from a subsoil of a slope containing less P. In contrast, P_{coll} concentrations in drainage from P-rich and P-poor Thyrow plots were similar. Concentrations of colloids and P_{coll} were not particularly large at the onset of irrigation. Colloids mobilized from topsoils were not retained in subsoils. Colloidal P significantly contributed to P leaching at the two sites. However, my results for the Thyrow site illustrated that an accumulation of P in sandy soils does not necessarily induce an increased leaching of P_{coll}.

5.2 Introduction

Between 1955 and 1995 fertilization in Germany caused a P accumulation of nearly 1000 kg ha^{-1} in agricultural soils (Bach et al., 2000). Especially in regions densely stocked with cattle, pigs or poultry, P accumulation in soils can be large (Leinweber et al., 1997). An increasing P saturation of soils increases the risk of P leaching (Behrendt and Boekhold, 1993). For sandy soils van der Zee and van Riemsdijk (1988) introduced the ratio of oxalate-extractable P to Fe + Al, which are the main sorbents for P in sandy soils (Beek, 1978), as a measure of the DPS. Concentrations of P_{diss} commonly increase sharply if the DPS exceeds

a certain critical value (Maguire and Sims 2002; McDowell and Sharpley, 2001). In areas, where soils with a large DPS are abundant, the leaching of P may be equally important for P inputs into surface waters as erosion (Driescher and Gelbrecht, 1993).

In addition to P_{diss}, P_{coll} contributes to P leaching (Motoshita et al., 2003; Heathwaite et al., 2005). Colloids are defined as particles ranging from > 1nm to < 1µm, which remain suspended in water and are therefore mobile (Kretzschmar et al., 1999). Colloidal P in soil water samples may account for up to 80% of total P and may be associated with organic matter, Fe and Al (Shand et al., 2000; Hens and Merckx, 2001). Several factors such as ionic strength, pH and macropore flow affect the mobilization and transport of P_{coll} (de Jonge et al., 2004; Hens and Merckx, 2001, Stamm et al., 1998). Especially right after the beginning of heavy irrigation or rainfall events, colloids and P_{coll} are mobilized and above-average concentrations are leached, which is called “first-flush effect” (de Jonge et al., 2004; Schelde et al., 2006). This effect is explained with the mobilization of particles that are only slightly associated with macropore walls and are easily detached by flowing water.

Ilg et al. (2005) showed in batch experiments that P_{coll} concentrations, similar to P_{diss} concentrations, can be positively correlated with DPS. In batch experiments conducted by Siemens et al. (2004) large concentrations of P_{coll} were related to large DPS and the sorption of P induced a release of P_{coll} from soil samples. The sorption of P can modify the surface charge of P-sorbents to more negative values (Stumm and Sigg, 1979). Thus, the originally positive or neutral surface charge of Fe and Al oxides may change from positive or neutral to negative (Puls and Powell, 1992). A shift of surface potentials to values below -20 mV thereby triggers the release of P-containing Fe oxides from negatively charged quartz sand matrices (Ilg et al., 2007). To what extent the influence of P saturation on the mobilization of P_{coll} actually affects the leaching of P_{coll} from undisturbed soils was not in the focus of scientists yet.

The leaching of P_{diss} usually decreases with increasing soil depth due to sorption to less P saturated subsoils (Butler and Coale, 2005). Hence, also the leaching of P_{coll} may decrease with increasing soil depth, because P from highly

P-saturated topsoil colloids might re-adsorb to the subsoil matrix due to equilibration.

The objective of this study was to evaluate the leaching of P_{diss} and P_{coll} in undisturbed sandy soils of different soil P saturation. I hypothesize that i) an increasing DPS not only increases P_{diss} concentrations, but also enhances the release and leaching of P_{coll} from soils; ii) the majority of P_{coll} is mobilized in the beginning ("first flush"), and iii) P_{coll} concentrations leached from subsoils are smaller than those leached from topsoils, because P_{coll} mobilized in topsoils is retained in subsoils. To test these hypotheses, I conducted an irrigation experiment with undisturbed soil columns from soils of different DPS and depths.

5.3 Materials and methods

5.3.1 Soils

I sampled soil columns from two sites located in the federal state Brandenburg in northeastern Germany. The climate at both sites is temperate and oceanic-continental. Mean annual precipitation is 500-600 mm and the average annual temperature is 8.2-8.9°C. Site Thyrow (52°16´ northern latitude and 13°12´ eastern longitude) is a static nutrient deficiency experiment, a long-term fertilization experiment of the Humboldt University of Berlin. The soil type is an albeluvisol and soil texture is loamy sand. Since 1937 there is a crop rotation of potatoes, silage maize and spring barley. I sampled a variant fertilized with 30000 kg manure ha^{-1} and a^{-1}, 24 kg mineral P ha^{-1} and a^{-1}, lime, N and K and a P-deficiency variant fertilized with lime, N and K only (Baumecker et al., 2002). Site Werbellin (52°54´ northern latitude and 13°42´ eastern longitude), which is permanently monitored by the Landesumweltamt Brandenburg, was a disposal site for organic manure for several decades until 1989. Additionally, the site is fertilized with mineral P. The soil type is a cambisol and soil texture is loamy sand. Since 1992 there is a crop rotation of silage maize, winter rye and fallow (Landesumweltamt Brandenburg, unpublished data). I sampled soil columns from a depression, where organic manure accumulated during the time of disposal and from a slope position, where less manure accumulated than in the depression (Table 1). The P-rich Thyrow variant and the former manure disposal site were selected for the experiment because they were expected to be

especially susceptible for P-induced colloid leaching from sandy soils in the sense of a worst case scenario.

Table 5.1: *General characteristics of soils at the two research sites. The Werbellin site was used for a disposal of manure, which accumulated in the depression. The Thyrow site is used for a long-term fertilization trial, which includes a P-deficiency variant (P-poor) and a variant that is intensively fertilized with manure and mineral P (P-rich).*

		Werbellin		Thyrow	
	depth	depression	slope	P-rich	P-poor
pH		4.4[(a)]	5.2	5.8	6.1
C_{org} (g kg^{-1})	0-30 cm	4.38[(a)]	8.33	6.27	3.86
DPS	0-30 cm	68 (21)^{C}[(b)]	50 (6)^{C}	64 (7)^{AC}	28 (1)^{BC}
(%)	30-60 cm	32 (8)^{AD}	14 (5)^{BD}	21 (4)^{AD}	4 (2)^{BD}
dispersible P	0-30 cm	176 (144)	104 (67)	1320 (456)^{A}	696 (192)^{B}
(µmol P kg^{-1})	30-60 cm	27.6 (34)	7.8 (10)	632 (288)	nm

[(a)] data for Thyrow from Baumecker et al. (2002) and for Werbellin from Landesumweltamt Brandenburg (unpublished)

[(b)] A and B indicate significant differences between identical depth segments of two P variants, C and D indicate significant differences between the two depth segments of one fertilization variant

nm: not measured

Oxalate-extractable P, Fe and Al concentrations were determined by extracting 2 g of soil with 100 ml ammonium oxalate (0.2 M, pH 3.25) for 1 hour in the dark according to Schlichting et al. (1995, p. 148). I determined Al by atomic absorption spectrometry (flame furnace, Model 1100B, PerkinElmer, USA). The detection limit was 37 µmol Al l^{-1}. Iron concentrations were measured photometrically at a wavelength of 562 nm using the method of Dominik and Kaupenjohann (2000) with a detection limit of 0.3 µmol Fe l^{-1}. I measured ortho-P concentrations photometrically according to the method of Murphy and Riley (1962) at a continuous flow analyzer (Skalar, Erkelenz, Germany) with a detection limit of 0.55 µmol P l^{-1}. All vessels were rinsed with 0.1 M HNO_3 prior to P analyses.

The DPS in (%) was calculated according to Breeuwsma and Silva (1992):

$$DPS = \frac{[P_o]}{0.5([Fe_o]+[Al_o])} * 100 \qquad (1)$$

where $[P_o]$, $[Fe_o]$ and $[Al_o]$ denote the concentrations of oxalate extractable elements in mmol kg^{-1}.

To determine potentially dispersible P I extracted 10 g of soil with 80 ml of 0.01 M KCl and rotated the samples end-over-end for 24 h at 10 rpm according to Ilg et al. (2005). Often deionized water is used to extract potentially dispersible colloids (e.g. Kaplan et al. 1997). However, in the study of Ilg et al. (2005) 0.01 M KCl was superior to detect differences between soils regarding the release of colloids because it masks the effect of variations of ionic strength. In contrast to deionized water or a dilute rain-like solution, the ionic strength of 0.01 M KCl extracts resembles the one of column leachate while avoiding a potential precipitation of apatite or an effective flocculation of colloids, which might be caused by 0.01 M $CaCl_2$. After filtration through 1.2 µm cellulose acetate filters (Sartorius, Göttingen, Germany) dispersible P was determined as the difference between total P in a non-ultracentrifuged aliquot and dissolved total P in the supernatant in an aliquot after ultracentrifugation at 300'000 g for 15 min (Beckman Optima TL, Unterschleissheim, Germany, further methodological details see Ilg et al., 2005).

5.3.2 Column experiment

I pounded stainless steel tubes of 40 cm length and an inner diameter of 13.5 cm into the soil and excavated them to obtain soil columns. I observed no compaction of soils during this procedure, because the columns were sharp-edged and had a sufficient diameter to easily penetrate the soil. I collected a total of 16 soil columns from the plough horizon (0-25 cm) and 16 columns from the plough horizon plus 15 cm subsoil (0-40 cm), resulting in four replicates for each variant. Estaimated pore volumes were about 1600 ml for 0-25 cm columns and 2500 ml for 0-40 cm columns. Columns were fixed with silicone onto zero-tension lysimeters consisting of a plexiglass block with a stainless steel wire gauze having a pore size of 200 µm. After comparing different lysimeter types, Ilg et al. (2007) recommended zero-tension lysimeters to sample colloids in

seepage water. Furthermore, the installation and handling of zero-tension lysimeters is fast and simple (Thompson and Scharf, 1994). On top of the columns an irrigation gear was installed, which consisted of a plexiglass block containing 137 cannulae with an outer diameter of 0.4 mm (Sterican BL/LB, size 20, Braun Melsungen AG, Germany). Mariotte's bottles fed the columns with an artificial solution similar to the composition of unpolluted rainwater in Germany (Umweltbundesamt, unpublished). The irrigation water contained 51 µmol NH_4NO_3 l^{-1}, 9 µmol $(NH_4)_2SO_4$ l^{-1}, 11 µmol $CaCl_2$*2 H_2O l^{-1}, 1.5 µmol $K_2S_2O_7$ l^{-1}, 4 µmol $MgSO_4$*7 H_2O l^{-1} and 12 µmol Na_2SO_4 l^{-1}. The pH was adjusted to 5 with diluted HNO_3. The electrical conductivity was 23 µS cm^{-1}.

I irrigated the columns in intervals of 15 minutes irrigation and 15 minutes break to avoid ponding until 850 ml of drainage were collected. The design of the experiment was rather targeted on the simulation of a heavy rainfall event under field conditions comparable to the field experiments conducted by Schelde et al. (2006) than on conducting a "classical column experiment" with input-output balances. Therefore, less than one pore volume of rainwater was applied. The average irrigation rate was 17 mm h^{-1} according to the definition of a heavy rainfall event (Keil, 1950). From the beginning of outflow I sampled column outflow in four fractions of 100 ml, 250 ml, 250 ml, and 250 ml volume. The volume of the first fraction was smaller to avoid a possible masking of a "first flush phenomenon" due to dilution. Samples were taken to the laboratory right after the experiment and completely analyzed within three days.

A common problem associated with the use of zero-tension lysimeters is the formation of saturated conditions at the lower end of the soil column. Saturated conditions might enhance the mobility of colloids, which means that zero-tension columns tend to overestimate the actual export of colloids (Ilg et al. 2007). Another potential artifact is the formation of reducing conditions as a consequence of saturated conditions, which might induce the transformation of Fe oxides. However, the formation of reducing conditions in the columns was prevented by the large flow rates that were applied. First, the large flow rates restricted the total leaching time to approximately 4 hours. Second, the intense irrigation ensured the percolation of the soil column with oxygen-rich water.

5.3.3 Treatment and analyses of outflow samples

Leachates were filtered through 1.2 µm cellulose nitrate filters (Sartorius, Göttingen, Germany) to collect only colloidal particles. Before filtration solutions were slightly colored, but visibly clear and quickly passed the filter. No clogging of filters was observed. The first 5 ml of the filtrate were discarded. An aliquot of the filtrate was ultra-centrifuged with either 110'000 g for one hour or 300'000 g for 15 min to remove colloids (Sorvall OTD 65B, Du Pont, Wilmington, USA and Beckman Optima TL, Unterschleissheim, Germany). Assuming a density >2 g cm^{-3} and a spherical shape of colloids, both ultracentrifugation treatments should have settled particles >20 nm. I calculated concentrations of P_{coll}, Fe_{coll}, Al_{coll} and C_{coll} as the difference between concentrations in non-ultra-centrifuged (total P) and ultra-centrifuged (P_{diss}) samples.

In soil solutions I measured pH and electrical conductivity (inoLab pH/Cond, WTW, Weilheim, Germany). Furthermore, I determined the zeta potential of the colloids (zeta sizer DTS 5200, S/N 34132/35 Malvern Instruments, United Kingdom). I measured the optical density of filtrated outflow samples as an indirect measure of colloid concentrations at a wavelength of 525 nm according to Kretzschmar et al. (1997a) with a detection limit of an absorbance of 0.008 (specord photometer, Jena, Germany). Colloidal C concentrations were determined using a TOC analyzer (TOC-Analyzer 5050A, Shimadzu Europa GmbH, Duisburg, Germany) with a detection limit of 0.16 mmol C l^{-1}.

Total Fe, Al and P concentrations in the filtrated outflow samples were measured after digestion with peroxodisulfate using a modified procedure after Rowland and Haygarth (1997): 7 ml of sample were mixed with 1.4 ml solution consisting of 150 mmol $K_2O_8S_2$ l^{-1} and 180 mmol H_2SO_4 l^{-1} and autoclaved at 121 °C for one hour. Afterwards I added 1 ml of 188 mmol ascorbic acid l^{-1} and boiled the samples at 100 °C for another hour.

5.3.4 Calculations and statistical evaluations

Arithmetic means, medians and standard deviations were calculated for all parameters. Measured values below detection limit were set to half of the detection limit for further calculations and concentrations of P_{coll}, Fe_{coll}, Al_{coll} and C_{coll} < 0 were set to zero. To detect a first flush-effect I tested differences between

the four fractions of each column type for significance with the non-parametric Wilcoxon-test. For further comparisons of sites, variants, and soils depths I calculated the median of the four fractions of each replicate. Differences within one site between topsoil and topsoil + subsoil samples and between the two variants were tested with the non-parametric Mann-Whitney-U-test. The same test was used to detect differences between site Werbellin and Thyrow. All tests were carried out using the STATISTICA 6.0 software (StatSoft, Tulsa, USA). I defined the level of significance for all tests as $p < 0.05$.

5.4 Results

5.4.1 P status of soils

The DPS ranged for site Werbellin from 14% to 68% and for site Thyrow from 4% to 64% (Table 1). Topsoils had significantly larger DPS values than subsoils. For site Thyrow the plot receiving P fertilization had a significantly larger DPS than the P-poor plot. For site Werbellin, subsoil DPS were significantly larger at the depression than at the slope. Dispersible P concentrations varied between 8 and 176 µmol P kg^{-1} soil for Werbellin and 632 and 1320 µmol P kg^{-1} soil for Thyrow (Table 1). Thyrow had larger dispersible P concentrations than Werbellin. For both sites dispersible P concentrations were larger on the plots with larger DPS.

5.4.2 General characteristics of column outflow and colloids

I found no significant differences between the four fractions of drainage collected from each column.

The stability of colloidal suspensions strongly depends on pH (Stumm and Sigg, 1979), with high pH values commonly favoring the leaching of colloids. The pH of drainage from columns of the Werbellin soil tended to be higher for 40 cm columns (slope: 4.6, depression: 4.9) than for 25 cm columns (slope: 4.2; depression: 4.6), reflecting a slow acidification as a consequence of a reduced management of the soil after 1989. Furthermore, the pH of drainage from the columns collected at the depression was slightly higher than the pH of leachate from columns taken from the slope, which is probably the consequence of larger inputs of base cations with manure in the depression. Comparing the two sites,

the pH of outflow from the Thyrow columns (pH 6.0-6.8) was larger than the pH from the Werbellin columns due to the application of lime, but differences were not significant. Among columns from Thyrow, the outflow from the 40 cm columns of the P-poor plots had a significantly larger pH (6.7) than the outflow of columns collected from the P-rich plots (6.0).

Except for high pH, a low ionic strength supports the mobilization and transport of colloids (Kretzschmar et al., 1999). The average electrical conductivity of drainage from Werbellin columns ranged from 671 µS cm^{-1} to 1140 µS cm^{-1}. Compared to leachate from 40 cm columns from Werbellin, the outflow of 40 cm columns from Thyrow had significantly larger average electrical conductivities of 1017 µS cm^{-1} for the P-poor plot and 1563 µS cm^{-1} for the P-rich plot.

While the small concentration of colloids in leachate from Werbellin columns prevented the determination of meaningful values of optical densities, colloid concentrations in drainage from Thyrow columns caused average optical densities between 0.012 and 0.032. The drainage from 25 cm columns of the P-poor plot was more turbid (0.021±0.005) than drainage from the 40 cm columns (0.012±0.005).

The surface potential of colloids, measured as zeta potential, is a critical parameter that determines the separation distance of colloids and hence their deposition and mobilization. Similar to optical densities, the zeta potential of suspended colloids in leachate from Werbellin columns could not be determined due to small colloid concentrations. Average zeta potentials of colloids released from Thyrow columns ranged from -9.8 mV to -13 mV. Colloids leached from P-poor columns had a slightly more negative zeta potential (-13±1.4 mV) than colloids leached from P-rich columns (-11.9±1.6 mV).

Colloids are often mobilized in soils by large flow rates during storm flow events (Schelde et al., 2006). The flow rate of the columns varied between 10.3 and 24.6 mm h^{-1}, with an average of 17.4 mm h^{-1}. The Thyrow columns had significantly larger flow rates than Werbellin columns. I found no differences between the two depth segments and no correlation between the flow rates of columns and the optical density in column outflow.

5.4.3 P leaching from columns and composition of colloids

For Werbellin columns from the slope position I found significantly larger P_{diss} concentrations in the outflow of 25 cm than in 40 cm columns (Table 2). Comparing the two sites, P_{diss} concentrations in the drainage of the Thyrow columns were significantly larger than those of Werbellin columns. Among Thyrow columns, those from plots receiving P fertilization had significantly larger P_{diss} concentrations than those from P-poor plots. For the P-poor variant, leached P_{diss} concentrations were significantly larger for the 25 cm columns than for the 40 cm columns.

Colloidal P concentrations in the outflow of columns originating from the depression in Werbellin were significantly larger in 40 cm columns than in 25 cm columns. Furthermore, P_{coll} concentrations leached from columns collected at the depression were significantly larger than those leached from columns collected at the slope. No significant differences between Thyrow and Werbellin columns could be detected. Also, I found no significant differences for Thyrow columns between the variants or between the two depth segments.

In addition to P_{coll} and P_{diss} concentrations I calculated their proportion in relation to total P in drainage water. For both sites the P_{coll} fraction of total P was smaller than the P_{diss} fraction. Among Werbellin columns, the 40 cm columns had a significantly larger proportion of P_{coll} than the 25 cm columns. For Thyrow, the 40 cm columns of the P-rich plot had a significantly smaller proportion of P_{coll} than 40 cm columns of the plot receiving no P fertilization.

Colloidal Fe concentrations in the drainage water of Werbellin columns were significantly smaller compared to Fe_{coll} concentrations leached from Thyrow columns. For Thyrow columns Fe_{coll} concentrations from 40 cm columns were significantly larger for the P-poor plot compared to the P-rich plot.

The drainage of 25 cm columns from Werbellin contained large concentrations of C_{coll}. Concentrations of C_{coll} from Thyrow columns were significantly smaller than those from Werbellin. Average ratios of C_{coll} to P_{coll} ranged from 6 to 65 for Thyrow columns and from 69 to 80 for the 25 cm columns collected at Werbellin. For site Thyrow I found significant correlations between the optical density on the one hand and Al_{coll} and Fe_{coll} concentrations on the other hand (Figure

1). No strong correlations, however, were detected between P_{coll} concentrations and concentrations of Fe_{coll}, Al_{coll}, or C_{coll}.

Table 5.2: *Phosphorus concentrations in the outflow of soil columns and the composition of leached colloids; values denote arithmetic means of four soils columns. Standard deviations are given in parentheses. Averages and standard deviations were derived from median values of four fractions of leachate collected from each soil column.*

		depth	dissolved P	colloidal P	colloidal Al	colloidal Fe	colloidal C	colloidal fraction of total P
		cm			µmol l^{-1}			%
Werbellin	depression	25	50.3 (36.6)	1.6 (0.5)$^{C(a)}$	nd	0.29 (0.57)	275.0 (257)	6 (4)^{C}
		40	14.3 (9.26)	6.8 (3.2)^{AD}	nd	0.17 (0.21)	nm	37 (15)^{D}
	slope	25	15.6 (6.3)^{C}	1.3 (0.6)	0.2 (0.4)	0.08 (0.12)	403.0 (395)	10 (4)^{C}
		40	3.7 (1.2)^{D}	1.4 (0.8)^{B}	0.1 (0.1)	0.07 (0.14)	nm	26 (7)^{D}
Thyrow	P-rich	25	247.0 (89.7)^{A}	10.4 (17.4)	nd	2.35 (4.51)	21.8 (36)	1.4 (0.2)
		40	203.0 (70.2)^{A}	3.2 (6.4)	nd	1.00 (0.69)^{A}	90.1 (43.5)	4 (6)^{A}
	P-poor	25	43.1 (9.4)^{BC}	0.5 (0.9)	3.1 (6.2)	8.28 (3.01)	14.4 (28.8)	1.4 (0.2)^{C}
		40	13.7 (324.0)^{BD}	2.9 (2.1)	28.3 (25.3)	16.10 (10.6)^{B}	69.8 (67.8)	19 (13)^{BD}

$^{(a)}$ A and B indicate significant differences between identical depth segments of two P variants, C and D indicate significant differences between the two depth segments of one fertilization variant; nd: not detectable, nm: not measured.

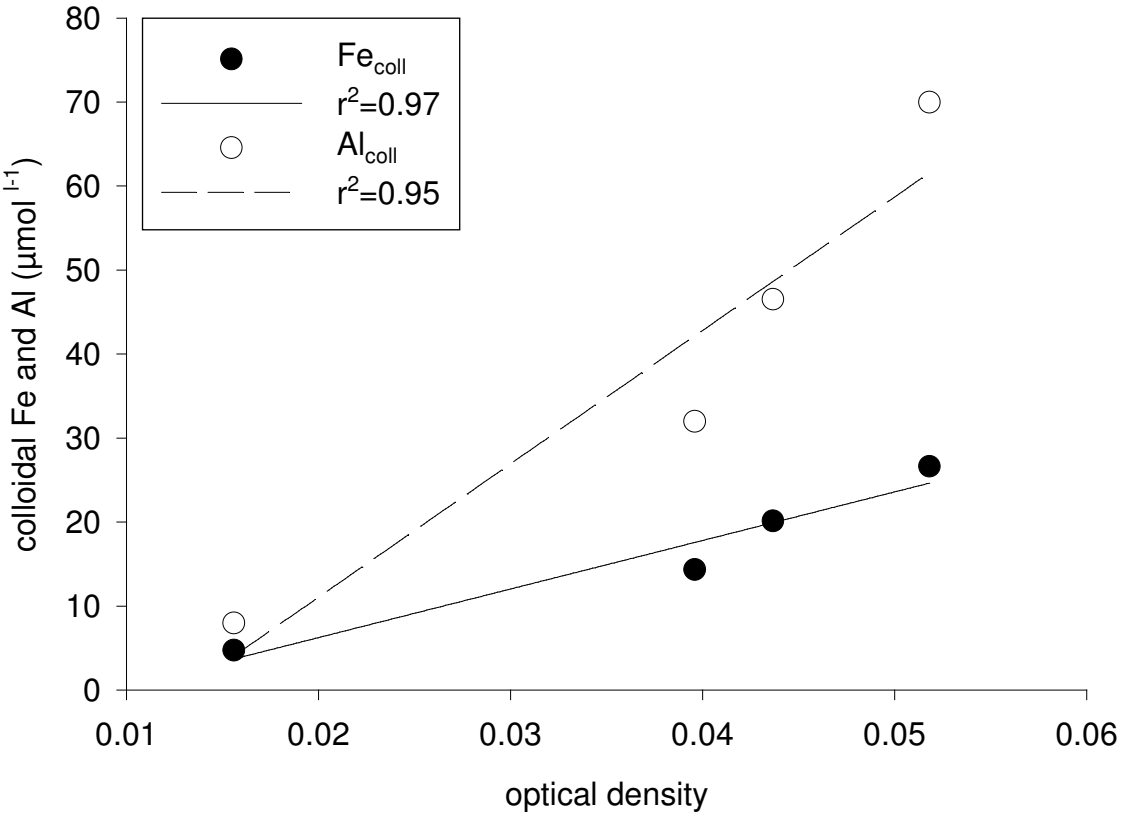

Figure 5.1: *Relations between optical density and concentrations of colloidal Fe and Al for drainage from 40 cm columns collected at the P-poor plot in Thyrow; each data point is the mean of four leachate fractions collected from one soil column.*

5.5 Discussion

Large DPS values combined with a silty to sandy texture, as observed on both sites, could be seen as "worst case" for a potential leaching of P_{diss} (Nair et al., 2004) and for a P-induced mobilization and leaching of P_{coll} (Siemens et al., 2004). Dispersible P concentrations of site Thyrow (Table 1) were in a range comparable to data from Ilg et al. (2005), whereas for site Werbellin dispersible P concentrations were smaller at similar DPS values. This might be due to low pH values of site Werbellin, which decreased the release of colloids.

In the drainage of most columns P_{diss} concentrations exceeded the critical threshold of 100 µg P l^{-1} (~ 3 µmol P l^{-1}) for groundwater, above which the eutrophication of surface waters is enhanced (Breeuwsma et al., 1995). For the fertilization variant of Thyrow, P_{diss} concentrations were more than one order of magnitude above the critical threshold. Similar results were reported by Nelson

et al. (2005), who found more than 18 mg P l^{-1} in acid sandy soils with DPS values exceeding 100%. An accumulation of P as a consequence of fertilization and manure disposal increased P_{diss} concentrations at both sites. Although the DPS of topsoils were similar for Thyrow and Werbellin (64% vs. 68%) I found five times larger concentrations of P_{diss} in Thyrow. In contrast to site Werbellin, the soil in Thyrow is fertilized every year with mineral fertilizer and manure. Manure disposal at Werbellin dates back to the years before 1989, therefore P forms in soil may be aged and thus be sorbed more strongly. Vanderdeelen (1995), Buehler et al. (2002) and Kitayama et al. (2004) found that P was less mobile because of stronger sorption with increasing time after P application and in older compared to younger soils. Furthermore, liquid manure disposal in Werbellin led to an accumulation of organic P, which might sorb preferentially and stronger to the soil than ortho-P (Leytem et al., 2002).

The extent of P leaching commonly decreases with increasing depth due to sorption to less P-saturated subsoils (Butler and Coale, 2005). However, I observed this effect only for the slope site in Werbellin and for the P-poor plots in Thyrow. In the highly P-saturated variants also subsoils had a large DPS and P originating from topsoils could not be sorbed as effectively as in the variants containing less soil P. A lack of P retention in subsoils due to large DPS down to great soil depths was also reported for a plaggic anthrosol fertilized with manure and mineral fertilizer (Siemens et al., 2004). Together with the large flow rates large soil DPS and large P_{diss} concentrations leached from the soil columns collected at the P-rich Thyrow plot and the Werbellin depression illustrated that the experiment indeed represented a kind of worst case scenario for a P-induced leaching of colloids from sandy soils.

Similar to P_{diss} concentrations P_{coll} concentrations exceeded critical P concentrations in the column outflow of the Werbellin depression variant (40 cm) and of the P-rich Thyrow variant (25 cm). Shand et al. (2000) and Hens and Merckx (2002) also observed P_{coll} concentrations > 3-4 µmol P l^{-1} in soil solutions. In my experiment P_{coll} contributed between one and 37% to P leaching, which is in the same range as found by Haygarth et al. (1997) and Ulen (2004).

My results regarding the effect of P accumulation and hence large DPS on the leaching of P_{coll} were equivocal. While P_{coll} concentrations leached from the de-

pression columns were significantly larger than P_{coll} concentrations leached from columns collected at the Werbellin slope, P_{coll} concentrations leached from P-rich and P-poor Thyrow columns were similar. Therefore my first hypothesis stating that a larger DPS causes an increasing mobilization and transport of P_{coll} is not clearly supported. These findings of the column experiment are in contrast to results of batch experiments that unequivocally demonstrated the colloid-releasing effect of P accumulation or P addition (Siemens et al., 2004; Ilg et al., 2005). Also, dispersible P concentrations of site Thyrow were significantly larger in the P-rich variant with a larger DPS than in the P-poor variant. Ilg et al. (2007) observed a pronounced release of colloids in batch experiments when P-accumulation decreased zeta potentials of colloids below -20 mV. The fact that zeta potentials of colloids released from the Thyrow columns were considerable higher than -20 mV might partly explain the lacking effect of DPS on the concentration of leached colloids for this site. Another important difference between the present column experiment and the batch experiments was physical disturbance and an input of energy by shaking. The absence of physical disturbance in the column experiment might have prevented the release of colloids. Another reason might be that the release of colloids is in part a transient phenomenon restricted to a period of time right after an addition of P. The combination of physical disturbance and P addition might explain the findings of Zhang et al. (2003), who conducted an experiment with disturbed columns and observed a mobilization of Fe oxide colloids directly after P application.

Furthermore, a possible impact of P saturation on colloid mobilization and transport for Thyrow columns might have been covered by other factors that influenced colloid mobilization and transport such as electrical conductivity and pH. Significantly larger electrical conductivities and significantly lower pH values of leachate from the P-rich Thyrow columns compared to the P-poor columns both counteracted the release and leaching of colloids, which was illustrated by significantly smaller Fe_{coll} concentrations. Differences in pH between the leachate of the P-rich and P-poor Thyrow columns might have been accentuated by an artifact of the experimental conditions. At high partial pressures of CO_2 in soil air, large concentrations of carbonic acid dissolve in soil solution. The concentration of carbonic acid in equilibrium with soil air CO_2 increases

strongly with increasing pH. Therefore, a part of the dissolved CO_2 escaped from leachate after leaving the soil column due to the lower atmospheric partial pressure of CO_2, which in turn increased pH. This increase of pH due to an outgassing of dissolved CO_2 was probably smaller for soil columns from the P-rich Thyrow plot than for columns from the P-poor plot.

Also differing water saturations and flow rates within the columns may have influenced colloid transport. Probably because of a slightly coarser soil texture Thyrow columns had larger flow rates than Werbellin columns. However, the non-significant correlation between flow rate and optical density indicated no dominant impact of flow rates on colloid transport.

Colloidal P concentrations leached from 40 cm columns were often larger than P_{coll} concentrations leached from 25 cm columns (Table 2). Thus, I had to reject my hypothesis that P_{coll} leached from topsoils was retarded in subsoils. In contrast to a retention of colloids in the subsoil, my results indicated an additional mobilization of colloids. The additional release of colloids may have been caused by P_{diss} leached from topsoils that was sorbed to oxides in the subsoil and changed their surface charge, which caused their release.

The colloidal fraction of total P increased significantly in 40 cm columns compared to 25 cm columns except for the P-rich variant of Thyrow (Table 2). Thus, the relevance of P_{coll} for P leaching increased with increasing depth. Also, Ilg et al. (2005) observed that the fraction of P_{coll} of total KCl-extractable P increased with increasing depth.

The strong correlation between Fe_{coll}, Al_{coll} and optical density suggest that Fe- and Al oxides (Figure 1) were an important fraction of the colloids leached from the Thyrow soil columns. Similar correlations were already detected by Ilg et al. (2005) in batch experiments with various soils from fertilization trials. However, the absence of significant correlations between P_{coll} on the one hand, and Fe_{coll} and Al_{coll} on the other hand implies that Fe and Al oxides were probably not the only carriers of P_{coll}. This finding is in contrast to results of Ilg et al. (2005), who found a close relationship between P_{coll} concentrations and Fe_{coll}+Al_{coll} concentrations. In addition to Fe and Al oxides, clay minerals and to some extent organic matter may have been additional sorption partners for P_{coll} (Frossard et al., 1995; Celi et al., 1999). Small C_{coll}/P_{coll} ratios together with a lack of correla-

tion between P_{coll} concentrations and C_{coll} concentrations yet point to a limited relevance of organic matter as carrier of P_{coll} at the research sites. Furthermore, P_{coll} could be comprised of high-molecular polyphosphates of colloidal size. It is known, that polyphosphates may persist in soils for several weeks before they are hydrolyzed to orthophosphate (McBeath et al., 2006) so that humic and fulvic acids may contain up to 16% of all P as polyphosphates (Makarov et al., 1997). Direct observations of the elemental composition of single colloids with e.g. scanning electron microscopy coupled with energy-dispersive X-ray analysis (SEM/EDX) might provide more insight into the binding partners and composition of P_{coll} in future studies given that the P concentration is large enough to be detected with EDX.

Contrary to other studies (e.g. de Jonge et al., 2004, Schelde et al., 2006) I found no first flush-effect of colloid mobilization, which may be related to the zero-tension lysimeters used in my column experiment. The hydraulic gradient in the lysimeter was disrupted, because water was retained above the lysimeter/soil interface and ran off only after reaching atmospheric pressure (Abdou and Flury, 2004). Although colloid deposition under such saturated conditions is smaller and colloids are more mobile (Cherrey et al., 2003), the outflow of colloids may have been decelerated and so a first flush effect was partly blurred. Additionally the volume of 100 ml for the first fraction might have been too large to record a first flush effect.

5.6 Conclusions

In addition to the dissolved fraction, P_{coll} significantly contributed to P leaching from the investigated sandy soils. Concentrations leached from the soil columns were not significantly larger right after the onset of irrigation than during the rest of the flow event. In the subsoil with the largest DPS, P_{coll} leached from topsoils was not retained, but additional P_{coll} was mobilized. Strong correlations between optical density on the one hand and Fe_{coll} and Al_{coll} on the other hand suggest that Fe- and Al oxides were a significant fraction of colloids leached from the Thyrow columns. A lack of strong correlations between P_{coll}, Fe_{coll} and Al_{coll} concentrations yet indicates that Fe- and Al oxides were not the exclusive carriers of P_{coll}. While the accumulation of P in the depression of the Werbellin site was

related to an increased leaching of P_{coll} from subsoils, P_{coll} concentrations in drainage from P-rich and P-poor soils from Thyrow were similar. An accumulation of P in sandy soils hence does not inevitably induce the leaching of P_{coll}.

6 Extended summary, general conclusions and outlook

6.1 Extended summary

Subsurface losses of P contribute to the translocation of P from terrestrial to aquatic ecosystems and may enhance the eutrophication of surface waters. Fertilization exceeding crop requirements causes an accumulation of P in soils. The resulting P saturation is a central factor controlling the concentration of P_{diss} in drainage water and therefore subsurface P leaching, especially from sandy soils. In addition to P_{diss}, P_{coll} significantly contributes to P leaching from soils. Because the sorption of P to dispersible solids such as Fe and Al oxides may change their surface charge, P might contribute to the mobilization and mobility of colloids itself.

The objective of my thesis was to clarify the process of P-induced colloid mobilization. The thesis was split into four individual sub-studies with five hypothesis, of which the results are summarized in the following:

a) The sorption of P to Fe oxides, which are sorbed or precipitated to a quartz sand matrix, causes the dispersion of Fe oxides from the matrix. There is a critical threshold of P accumulation for the release of Fe oxide colloids. (Chapter 2)

In a batch experiment I added increasing P concentrations to i) goethite adsorbed to fine quartz sand and ii) goethite precipitated on coarse quartz sand. The addition of P caused the mobilization of colloidal goethite above an equilibrium concentration of P_{diss} of 0.01-0.03 mg P l^{-1}. The critical P saturation corresponded to a zeta potential of about -20 mV of dispersed goethite. One order of magnitude less goethite was dispersed from precipitated goethite compared to adsorbed goethite, because precipitated goethite crystals were less accessible for P.

b) The threshold of P accumulation estimated in pure systems consisting of P, goethite and quartz is also valid for the P-induced release of colloids from sandy soils. Dominant colloidal sorbents for P in soils are Fe and Al oxides. (Chapter 2)

Soil samples from a cambisol (Bw-horizon) and from a gleysol (mottles of the Bg-horizon), both originating from the same catena, were exposed to increasing concentrations of P. The addition of P caused the release of colloids in this batch experiment, but larger P concentrations (0.07-2.22 mg P l^{-1}) than in the quartz-sand experiment were necessary to induce dispersion. This critical P_{diss} concentrations corresponded to P saturations between 13% and 25%. For the Bw samples, dispersion was triggered by a surface charge of less than -20 mV similar to the model systems. For the Bg samples, however, no distinct critical zeta potential was found. More colloids were released from the Bg samples than from the Bw samples, probably because of larger total Fe and Al concentrations and a smaller C-saturation of colloids. Colloids consisted mainly of Fe and Al oxides, which provided most of the capacity necessary for sorption of P_{coll}.

c) Organically-bound P, an important fraction of total P in organic manure and soils, enhances the dispersion of Fe oxides and soil colloids more effectively than inorganic P. (Chapter 2)

This hypothesis was tested in the batch experiments described above comparing ortho-P and IHP, which is one of the most abundant and stable organic P forms in soils. In both batch experiments adsorption of IHP reduced the zeta potential of colloids more effectively than adsorption of ortho-P. Therefore, IHP was the more efficient dispersing agent and caused the release of larger colloid concentrations compared to ortho-P.

d) The accumulation of P in sandy soils enhances the release of P_{coll} from soils and there is a critical degree of P saturation above which concentrations of P_{coll} increase sharply. (Chapter 3)

I extracted a sample collective from several fertilization experiments differing in DPS to determine colloid mobilization depending on long-term accumulation of P in fertilized soils. Colloidal P concentrations in supernatants increased with

increasing DPS because of an additional mobilization of colloids and due to an increase of the colloids P contents. Whereas P_{diss} concentrations increased sharply for a DPS $\geq$ 0.1, released P_{coll} concentrations increased linearly with increasing DPS without a critical level of DPS for the release of colloids. On the one hand this result indicates that a mobilization of P_{coll} might be already enhanced by a P accumulation at low levels of P saturation. On the other hand the large variability of Fe and Al oxides in arable soils as well as the interference with other factors affecting dispersion than DPS might cause multiple threshold values of DPS for the release of colloids rather than a single threshold value.

e) Comparing the colloid-sampling efficiency of five different lysimeter systems. (Chapter 4)

In the column experiment presented in chapter 4 I investigated the colloid-sampling efficiency of five different lysimeter systems (1.2 µm membrane, 10 µm membrane, porous plate, wick and zero-tension) to select an optimal sampling system for the column experiment of chapter 5. The experiment was conducted under unsaturated conditions using ^{59}Fe labeled goethite as model colloid. Most of the applied ^{59}Fe was retarded in the unsaturated sand column well above the lysimeter surface. The mean recovery of ^{59}Fe in column outflow over all lysimeters was 30.7%±6.7% for a small and 3.4%±3.5% for a large colloid input concentration. For the small goethite concentration no differences between lysimeter systems were detected. In contrast, the lysimeters performed differently at the large goethite concentration: zero-tension and 10 µm membrane lysimeters showed the largest (9.1% and 6.8%), wick lysimeters the smallest recovery of colloids in outflow (0.7%), which was related to trapping of colloids in the wick. I conclude that membranes of 10 µm pore size and zero-tension lysimeters are superior for colloid sampling, but results of the latter may be biased towards an overestimation of colloid transport because of water saturation at the lysimeter/soil interface.

f) An increasing P saturation of soil increases the leaching of P_{coll} under field conditions. (Chapter 5)

Columns with undisturbed sandy soils were irrigated with artificial rain solution to investigate the mobility and transport of P_{coll} depending on the soil P satura-

tion status (Chapter 5). Colloidal P concentrations in drainage ranged from 0.01 to 0.31 mg l^{-1} and contributed between 1 and 37% to total P leaching. Leaching of P_{coll} was not significantly affected by the soil's DPS. Strong correlations between optical density on the one hand and Fe_{coll} and Al_{coll} on the other hand suggest that Fe- and Al oxides were a significant fraction of colloids leached from the Thyrow columns.

6.2 General discussion and conclusions

6.2.1 P-induced mobilization of colloids and colloidal P

In the batch experiment with model systems (Chapter 2) I could clearly prove the process of P-induced mobilization of colloids and P_{coll}. However, the more I approximated my experimental design to natural conditions, the more the process of P-induced colloid mobilization was masked by other factors. This means that the required number of replicats that are necessary to prove the effect of soil processes strongly increases under field conditions.

In the batch experiment with soils (Chapter 2) the P-induced colloid mobilization was clearly visible, but about 1-2 orders of magnitude larger equilibrium concentrations of P_{diss} were necessary to induce the process than in the experiment with model systems. The pH of the two soils was smaller than of the two model systems. At small pH values larger concentrations of P are necessary to reverse the surface charge of minerals such as goethite (Stumm and Sigg, 1979). Further, the model systems consisted only of quartz, goethite and P, whereas the soils contained also other sorbents for P such as clay minerals and organic matter. The sorption capacity of these sorbents for P varies widely depending on their composition. Furthermore, other processes than only P sorption influenced the surface charge of potential colloids and superimposed the dispersing effect of P. From my point of view, the most important of these processes was the sorption of organic matter to oxides, which competes with P for sorption sites and influences the mobilization and stabilization of colloids, too (Kretzschmar et al. 1993; Karathanasis, 1999; Kaiser and Zech, 1996; Kreller, 2003). A sorption of P may have occurred by replacing sorbed organic matter. Thus, at small concentrations P sorption did not change the surface charge of its sorbents (Lima et al., 2000). Further, the pool of potentially dispersible col-

loids may have been diminished, because a C-induced mobilization of colloids occurred before the experiment.

In natural soils from the fertilization experiments (Chapter 3), I observed a mobilization of colloids and P_{coll} with increasing P saturation. Compared to the batch experiment with soils, in which P was added (Chapter 2), colloid mobilization took place at lower equilibrium concentrations of P_{diss} (Figure 6.1a), which I ascribe to a larger pH of the soils from the fertilization experiments compared to the forest soils described in chapter 2. However, also other factors such as a larger concentration of potentially dispersible colloids or an influence of C have to be taken into account.

In the system closest to field conditions, which was the column experiment described in chapter 5, I found no significant correlation between P saturation and the mobility of colloids. In comparison to the batch experiments the physical disturbance and input of energy by shaking are missing in this experiment. The absence of physical disturbance in the column experiment might have prevented the release of colloids. Additionally I added no P to the system as did Zhang et al. (2003), who conducted an experiment with disturbed columns and observed a mobilization of Fe oxide colloids directly after P application. The combination of physical disturbance and P addition might explain the mobilization of colloids observed by Zhang et al. (2003).

In figure 6.1b the relation between zeta potential and optical density for all experiments is shown. In the batch experiment with model systems and for the Bw soil described in chapter 2, dispersion was triggered by a surface charge of less than -20 mV. Comparing these results with results for the soils from the fertilization experiments (Chapter 3) this value can be confirmed. In the experiment with undisturbed soil columns a slight dispersion of colloids was observable at a zeta potential of about -15 mV. Thus, a critical zeta potential of about -20 mV seems to be a central prerequisite for the release of colloids in the investigated soils under the applied conditions. Sequaris and Lewandowski (2003) also found zeta potentials, which were more negative than -16 mV for the release of colloids in batch experiments.

Another eye-catching topic emanates from figures 6.1a and 6.1b: compared to the other experiments the model system with adsorbed goethite described in

chapter 2 has by far the largest dispersion of colloids. The goethite in this system is only adsorbed to the quartz surface by shaking at a selected pH (Scheidegger et al., 1933), whereas in soils Fe oxides grow on the surface of silicates, a process, which may last from months up to millenia (Cornell and Schwertmann, 2003). Thus, the model system with precipitated goethite on quartz sand as described by Dominik et al. (2007) should be preferred as the more appropriate model system for Fe oxides sorbed to a soil matrix.

6.2.2 Is there a change point of P saturation for the P-induced mobilization of colloids?

The surface charge of oxides and thus their aggregation and attachement are influenced by adsorption of P in a strongly non-linear way (Stumm and Sigg, 1979). Due to this non-linear relationship a threshold of P accumulation or P saturation in soils for the release of colloids can be expected. In the batch experiment with an addition of P (Chapter 2) I observed that the P-induced colloid mobilization started above a distinct equilibrium concentration of P_{diss}. But no statistically significant change point of P saturation in non of the systems could be proven, because either the curve progression was too different from a split line model or standard deviations were too large because the chosen amount of samples was too small. Furthermore, the critical P concentrations differed between the four investigated systems and the two applied P forms, because obviously colloid mobilization depends on several factors: the characteristics of sorbents (e.g. Fe oxides with different specific surface areas and/or other differing properties); the attachment of sorbents to the soil matrix (compare the two model systems of chapter 2); and also on other factors generally influencing colloid mobilization such as saturation of colloids with organic matter and pH. In the batch experiment described in chapter 3, in which I investigated topsoils and subsoils without an addition of P, I also found no significant change point of P saturation for the mobilization of colloids. This observation together with the small DPS values calculated in chapter 2 might indicate a mobilization of P_{coll} at low levels of P saturation already.

In the case of P_{diss}, concentrations in drainage water depend solely on the saturation of sorbents, i.e. with an increasing P saturation the concentrations in P_{diss} in drainage water increases. Above a distinct point of P saturation concentra-

tions of P_{diss} sharply increase (McDowell and Sharply, 2001c; Nair et al., 2004), which is attributed to a lack of sorption sites. In the case of colloid mobilization not a lack of sorption capacity causes colloid release, but the change in surface charge, which depends on more factors than only P saturation.

6.2.3 Mobilization versus mobility and transport of colloids and colloidal P

The proven process of P-induced colloid mobilization does not necessarily result in an increased amount of colloids and P_{coll} leached to groundwater. Of course, colloid mobilization is an essential precondition for the leaching of colloids (if colloids are not imported from non-soil sources such as organic manure) and P sorption stabilizes colloidal suspensions under common soil conditions (Puls and Powell, 1992). However, mobilized colloids are stable in soil solution just as long as physico-chemical conditions of the soil (e.g. P saturation and pH) support this. Mobilized colloids may flocculate or resorb to the soil matrix in deeper soil layers, if chemical conditions change there. Such conditions can be a decreasing P saturation of the soil matrix: P desorbs from colloids and sorbs to the soil matrix. As a consequence, the surface charge of colloids becomes less negative and they coagulate or sorb to the soil matrix themselves. Other colloid-influencing factors, which change as a function of soil depth, are the water regime (the larger the soils water content, the more mobile are colloids), ionic strength and ionic composition of soil solution, pH, organic matter content and others (Grolimund et al., 1996; Motoshita et al., 2003). However, if colloids are transported via preferential flow paths as observed by Stamm et al. (1998) and Laubel et al. (1999), they are less susceptible to changing soil chemical conditions on their way to groundwater. Siemens et al. (2004) investigated Plaggic Anthrosols and found at one site large P saturations even in subsoils, which makes this soils quite susceptible for i) the mobilization of P_{coll}, but also for ii) the transport of P_{coll} down to groundwater.

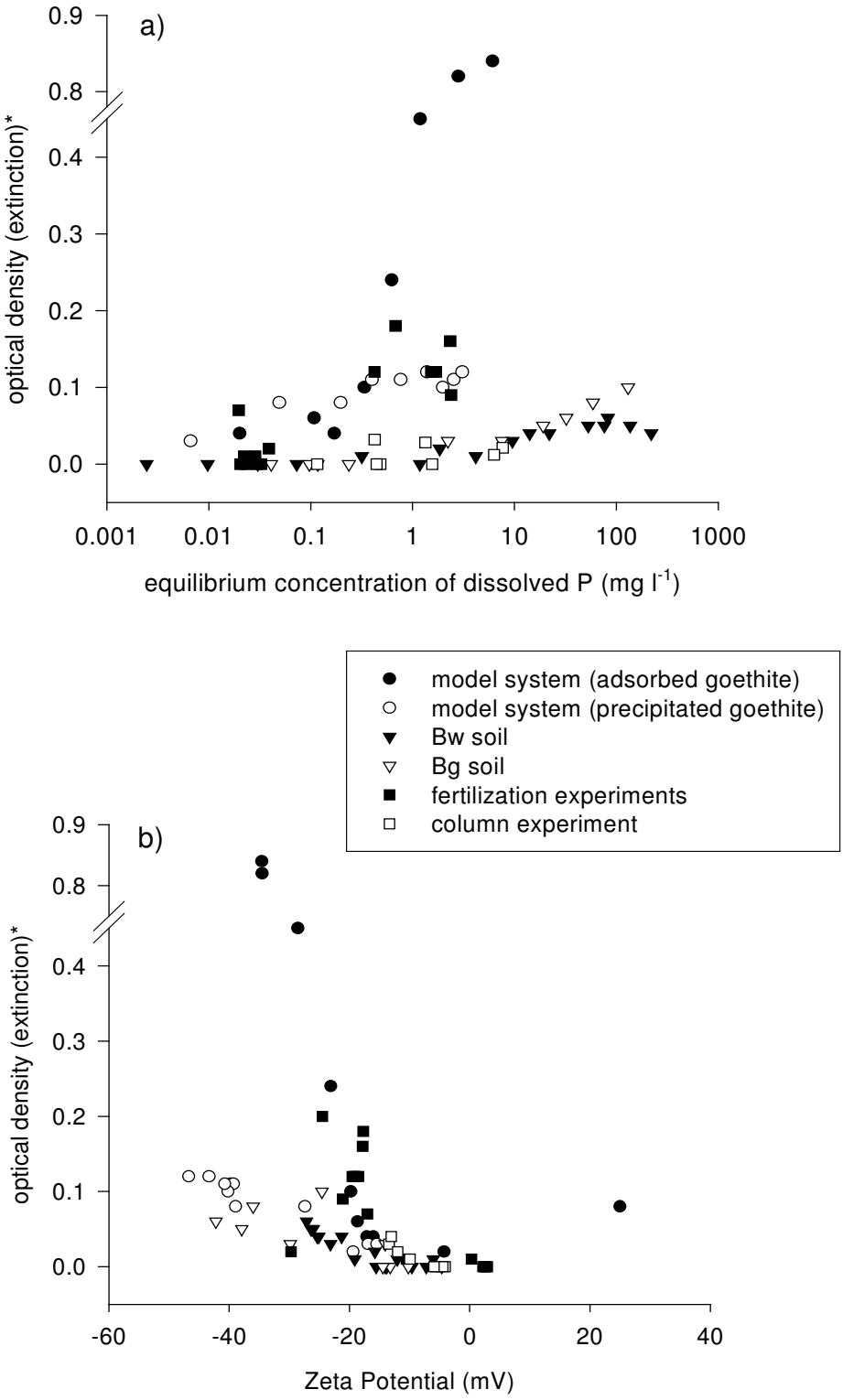

Figure 6.1 a)+b): *Mobilization of colloids depending on a) the equilibrium concentrations of dissolved P and b) the zeta potential of dispersed colloids in the batch systems or in the column outflow; *optical density in supernatants of batch experiments and column outflow.*

Thus, the P-induced mobilization of colloids is not only a process taking place in topsoils with large P saturations. My results indicate that additional colloids in subsoils may be mobilized as happened in the experiment with undisturbed soil columns (Chapter 5), in which I found larger colloid concentrations in columns with top- and subsoils than in columns containing only topsoils. One explanation for this observation might be that P_{diss}, which is transported from top- to the subsoil, sorbs to the soil matrix and mobilizes colloids there.

I strongly suppose that the process of P-induced mobilization of colloids and P_{coll} plays a role not only under well-controlled laboratory conditions, but also in the field. However, with my experimental design I could not prove the relevance for the leaching of P_{coll} in soils. Obviously other factors such as pH or ionic strength play a more important role and cover the influence of P saturation on the mobility of colloids. Anyway, the experiment with undisturbed soil columns (Chapter 5) shows that leaching of P_{coll} significantly contributes to P leaching from agriculturally used sandy soils. Concentrations of up to 0.32 mg P l^{-1} measured in this experiment are above the critical concentration of 0.2 mg total P l^{-1} in seepage water for the eutrophication of surface waters given by Auerswald et al. (2002). Compared to P_{coll} concentrations and fractions of total P given in table 1.2, my results of the column experiment (0.01-0.32 mg P l^{-1} and 1-37% P_{coll} in soil solution) are within the range of other studies dealing with P_{coll} leaching in soils.

6.2.4 Comparison of inorganic and organic P concerning the P-induced mobilization of colloids and colloidal P

In the two batch experiments with added P (Chapter 2) I could show that IHP has a stronger colloid-mobilizing effect than ortho-P. Colloids with sorbed IHP had smaller zeta potentials and were therefore more stable than colloids with sorbed ortho-P, which is in accordance with sorption experiments of Celi et al. (2000, 2001). Organic manure contains between 3 and 15 g organic P kg^{-1}, of which 2-70% consist of free and complexed IHP. Especially organic manure originating from monogastric animals such as pigs contains a large percentage of IHP. Because of its stability, IHP accumulates more than other organic P compounds and can comprise 20-80% of total P in soils (Barnett et al., 1994; Celi et al., 2000; Turner et al., 2002). These findings give a reason for concern

that an accumulation of organic P in soils as a consequence of excessive manure application might trigger the mobilization of P_{coll} more than an accumulation of inorganic P along with mineral fertilization.

6.2.5 Management recommendations

Because I could neither prove nor quantify the environmental relevance of P-induced mobilization of colloids and P_{coll}, I am not able to give any concrete management recommendations, e.g. for P-fertilization, to minimize P-induced leaching of P_{coll}. In sandy soils it is recommendable to measure P saturation as done by van der Zee and de Haan (1994) to assess the risk of leaching of P_{diss}. However, for the soils, which I examined in my study, P saturation did not provide information about the risk of colloid mobilization and P_{coll} leaching. Instead, the estimation of the zeta potential was a more informative parameter for assessing the risk of colloid mobilization, mobility and transport: For a zeta potential at < -20 mV measured in the supernatant an increasing risk of colloid mobilization and transport had to be assumed.

6.2.6 Methodological approaches to investigate colloid mobilization and transport in soils

Batch experiments versus column experiments: Batch experiments can be valuable for the investigation of processes such as colloid mobilization, because i) processes can be identified and characterized; ii) conditions of the experiments can be easily defined and factors such as the water flow regime of a soil can be excluded; iii) batch experiments are cheap, easy to conduct and, thus, large amounts of samples can be investigated with an acceptable expenditure of time and money (Haag and Matschonat, 2001). Under field conditions, mechanical forces such as raindrop impact or ploughing are known to support the mobilization of colloids. Compared to theses forces the physical impact of shaking during batch experiments is much larger. Therefore, colloidal concentrations measured in batch experiments have to be corrected or can be only a relative measure. They cannot be compared directly with field conditions (Blume et al., 2005). Furthermore, only colloid mobilization processes can be investigated, but not the transport and leaching of colloids.

In contrast to batch experiments column systems are dynamic experimental techniques. They are well suited to consider the influence of water flux and physical attributes of the porous media on colloid transport (EPRI report, 1991). Although being more expensive and more difficult to carry out than batch experiments, column experiments are a comparatively simple alternative to field studies. They are closer to real field conditions than batch experiments and allow quantitative estimations (Higgo et al., 1993; Heyer et al., 1995). However, transport of colloids or dissolved substances in columns might be influenced by factors, which do not emerge in the field, such as fringe effects of the column itself or an additional mobilization of colloids because of disturbances while gaining soil columns in the field (Bunn et al., 2002).

Simple systems versus complex systems: My thesis did by far not clarify all open question concerning the process of P-induced colloid mobilization. Anyway, I believe that the chosen step-by-step approach was very useful to elucidate this physico-chemical process: first to investigate the process in synthetic systems, which were as simple as possible and consisted only of the relevant components. Second a simple soil system (in my case two subsoils with low P saturation and low organic C content), which I manipulated by addition of P as I did with the two synthetic systems. Third I chose topsoils and subsoils for a batch experiment, which I did not manipulate any more by P addition, because all the soils had a different natural P saturation status. In the end, the column experiment with undisturbed soils and without any manipulation by P addition was closest to field conditions, under which I investigated the process of P-induced colloid mobilization.

Investigating only simple systems, artifacts can be easily induced and the relevance of the observed phenomenon in real ecosystems can be misinterpreted or is often overestimated (Madsen, 1988; Schindler, 1998). Vice versa in field site experiments processes behind the investigated phenomenon can be “invisible” because other, non-quantifiable factors influence the ecosystem, as probably happened in my experiment with undisturbed soil columns. Therefore, Haag and Matschonat (2001) recommend a stepwise integration of more complexity towards ecosystem conditions, starting from simple experimental systems. The authors differentiated seven types of experimental set-ups with in-

creasing complexity. On their scale I conducted my experiments starting with type one (synthetic model systems) up to type four (column experiment with undisturbed soil). To draw more valuable conclusions concerning the environmental relevance of soil processes such as P-induced colloid mobilization, experiments closer to natural conditions have to be conducted: direct field observations, e.g. sampling drainage water with suitable lysimeters or from drains, either with or without a direct manipulation of the investigated eco-system.

6.3 Outlook

With this study I could prove the process of P-induced colloid mobilization in simple batch experiments. However, under more natural conditions of column experiments the process was masked by other factors. Therefore, future research should create an experimental design to clarify, whether the process has an environmental relevance for P leaching from soils. Such an experimental design, e.g. further column studies or field measurements, should comprise more sites than in my column study with comparable soil properties, but different DPS. Also manipulation experiments can give more information such as P application on columns as described by Zhang et al. (2003) or P application in the field (Pennock, 2004). With manipulative field experiments one could ascertain, whether transient conditions (for example P fertilization or plowing) initiate and/or support the process of colloid mobilization. In this context it could be additionally found out, if there is a critical level of P saturation for colloid mobilization or if the process takes place on a more gradual scale.

Once the environmental relevance is known, the contribution of P-induced colloid mobilization on P leaching from soils to groundwater should be quantified. For this purpose, experiments and measurements have to be up-scaled and approximated to natural field conditions and to ecosystem-scale as far as possible. As next step a valuable risk assessment is possible and, if required, prognoses and management recommendations can be made (Haag and Matschonat, 2001).

Furthermore, future research could address the interactions and the influence of other factors such as pH or organic matter on P-induced colloid mobilization. Therefore, at first these processes should be clarified on a scale of batch ex-

periments, similar to the experiments of my thesis, and then in more complex systems such as column or field experiments.

In the work presented, the stronger mobilization effect of organic P could only be proven for one organic P compound (IHP) and under well-defined laboratory conditions. Therefore it should be investigated, if this stronger mobilization effect is also valid under more natural conditions such as in column experiments. More than only one organic P compound has to be taken into account and finally, organic and mineral fertilization should be compared, e.g. in field manipulation experiments.

7 References

Abdou, H.M. and M. Flury. 2004. Simulation of water flow and solute transport in free-drainage lysimeters and field soils with heterogeneous structures. Eur. J. Soil Sci. 55:229-241.

Agbenin, J.O. and H. Tiessen. 1995. Phosphorus forms in particle-size fractions of a toposequence from northeast brazil. Soil Sci. Soc. Am. J. 59:1687-1693.

Alaily, F. and A. Brande. 2002. Bodenentwicklung am Rande oligotropher Moore im Raum Berlin. J. Plant Nutr. Soil Sci. 165:305-312.

Allison, J.D., D.S. Brown and K.J. Novo-Gradac. 1991. MINTEQA2/PRODEFA2, a geochemical assessment model for environmental systems. Users Manual. United States Environmental Protection Agency, Office of Research and Development, Washington.

Anderson, G. 1980. Assessing organic phosphorus in soils. In: The role of phosphorus in agriculture (ed. F.E. Khasawneh) ASA, Madison. pp.411-43.

Anderson, M.A., M.I. Tejedor-Tejedor, R.R. Stanforth. 1985. Influence of aggregation on the uptake kinetics of phosphate by goethite. Environ. Sci. Technol. 19:632-637.

Anderson, R. and L. Wu. 2001. Agronomic measures of P, Q/I parameters and lysimeter collectable P in subsurface horizons of a long-term slurry experiment. Chemosphere 52:171-178.

Auerswald, K., N. Claassen, W. Römer and W. Werner. 2002. VDLUFA-Standpunkt: Mögliche ökologische Folgen hoher Phosphatgehalte im Boden und Wege zu ihrer Verminderung. Mitteilgn. Dtsch. Bodenkl. Gesellsch. 98:75-80.

Bach, M., H. Behrendt, H.G. Frede. 2000. Agricultural nutrient balances. Conference paper of the workshop “Nitrogen and phosphorus discharge/losses into surface waters” held and published by the German Federal Environmental Agency.

Baldwin, D.S. 1998. Reactive “organic” phosphorus revisited. Water Res. 32:2265-2270.

Barnett, G.M. 1994. Phosphorus forms in animal manures. Bioresource Technol., 49:139-147.

Barrow, N.J. 1983. A mechanistic model for describing the sorption and desorption of phosphate by soil. J. Soil. Sci. 34:733-750.

Barton, C.D. and A.D. Karathanasis. 2003. Influence of soil colloids on the migration of atrazine and zinc through large soil monoliths. Water Air Soil Poll. 143:3-21.

Baumecker, M., F. Elmmer and W. Koehn. 2002. Statischer Nährstoffmangelversuch (Versuch 4.03, Standort Thyrow). In: Koehn, W. and C. Bergwald: Ergebnisreport 2001/2002. Humboldt University of Berlin, Institute of Plant Production – experimental station.

Beek, J. 1978. Phosphate retention by soil in relation to waste disposal. Doctoral Dissertation, Agricultural University, Wageningen.

Behrendt, H. and A. Boekhold. 1993. Phosphorus saturation in soils and groundwaters. Land Degrad. Rehabil. 4:233-243.

Behrendt, H. and A. Bachor. 1998. Point and diffuse load of nutrients to the Baltic Sea by river basins of north east Germany (Mecklenburg-Vorpommern). Water Sci. Tech. 38:147-155.

Behrendt, H., M. Kornmilch, R. Korol, M. Stronska and W.G. Pagenkopf. 1999. Point and diffuse nutrient emissions and transports in the Odra basin and its main tributaries. Act. Hydrochim. Hydrobiol. 27:274-281.

Blume, T., N. Weisbrod and J.S. Selker. 2005. On the critical salt concentrations for particle detachment in homogeneous sand and heterogeneous Hanford sediments. Geoderma. 124:121-132.

Boll, J., T.S. Steenhuis and J.S. Selker. 1992. Fiberglass wicks for sampling of water and solutes in the vadose zone. Soil Sci. Soc. Am. J. 56:701-707.

Bradford, S.A., M. Bettahar, J. Simunek and M.T. van Genuchten. 2004, Straining and attachment of colloids in physically heterogeneous porous media. Vadose Zone J. 3:384-394.

Brady, N.C. and R.R. Weil. 2002. The nature and properties of soils. 13th ed. Prentice Hall. Upper Saddle River.

Breeuwsma, A. and S. Silva. 1992. Phosphorus fertilization and environmental effects in The Netherlands and the Po region, Italy. Rep. 57, DLO The Winard Staring Centre. Wageningen, the Netherlands.

Breeuwsma, A., J.G.A. Reijerink and O.F. Schoumans, O.F. 1995. Impact of manure on accumulation and leaching of phosphate in areas of intensive livestock farming, in Steele, K.: Animal waste and the land-water interface. CRC Press. pp. 239-249.

Brezesinski, G. and H.-J. Mögel. 1993. Grenzflächen und Kolloide. Spektrum Akademischer Verlag. Heidelberg.

Brunauer, S., P.H. Emmett and E. Teller. 1938. Adsorption of Gases in Multimolecular Layers. J. Amer. Chem. Soc. 60:309.

Buehler, S., A. Oberson, I.M. Rao, D.K. Friesen and E. Frossard. 2002. Sequential phosphorus extraction of a 33P-labeled oxisol under contrasting agricultural systems. Soil Sci. Soc. Am. J. 66:868-877.

Buffle, J., R.R. de Vitre, D. Perret and G.G. Leppard. 1989. Physico-chemical characteristics of colloidal iron phosphate species formed at the oxic-anoxic interface of an eutrophic lake. Geochim. Cosmochim. Acta 53:399-408.

Bunn, R.A., R.D. Magelky, J.N. Ryan and M Elimelech. 2002. Mobilization of natural colloids from an iron oxide-coated sand aquifer. Effect of pH and ionic strength. Environ. Sci. Techn. 36:314-322.

Butler, J.S. amd F.J. Coale. 2005. Phosphorus leaching in manure amended atlantic coastal plain soils. J. Environ. Qual. 34:370-381.

Celardin, F. 2003. Evaluation of soil P-test values of canton Geneva/Switzerland in relation to P loss risks. J. Plant Nutr. Soil Sci. 166:416-422.

Celi, L., S. Lamacchia, F.A. Marsan and E. Barberis. 1999. Interaction of inositol hexaphosphate on clays: adsorption and charging phenomena. Soil Sci. 164:574-585.

Celi, L., S. Lamacchia and E. Barberis. 2000. Interaction of inositol phosphate with calcite. Nutr. Cycl. Agroecosys. 57:271-277.

Celi, L., E. Barberis and F.A. Marsan. 2000. Sorption of phosphate at high concentrations. Soil Sci. 165:657-664.

Celi, L., M. Presta, F. Ajmore-Marsan and E. Barberis. 2001. Effects of pH and electrolytes on inositol-hexaphosphate interaction with goethite. Soil Sci. Soc. Am. J. 65:753-760.

Chardon, W.J., O. Oenema, P. Delcastilho, R. Vriesema, J. Japenga and D. Blaauw. 1997. Organic phosphorus in solutions and leachates from soils treated with animal slurries. J. Environ. Qual. 26:372-378.

Chen, B., J. Huston and E. Becket. 2000. The effect of surface coatings on the association of orthophosphate with natural colloids. Sci. Total Environ. 263:23-35.

Cherrey, K.D., M. Flury and J.B. Harsh. 2003. Nitrate and colloid transport through coarse Hanford sediments under steady state, variable saturated flow. Water Res. Res. 39:1165.

Choudhury, F.A. 1988. Distribution of total, inorganic and organic phosphate with respect to soil particle size. Thai J. Agric. Sci. 21:149-155.

Cornell, R.M. and U. Schwertmann. 2003. The iron oxides. VCH, Weinheim, Plate 16/I number D and pp. 267 ff.

Czigany, S., M. Flury, J.B. Harsh, B.C Wiliams and J.M. Shira. 2005. Suitability of fiberglass wicks to sample colloids from vadose zone pore water. Vadose Zone J. 4:175-183.

Dalal, R.C. 1977. Soil organic phosphorus. Adv. Agr. 29:83-117.

Daniel, T.C., A.N. Sharpley and J.L. Lemunyon. 1998. Agricultural phosphorus and eutrophication: A symposium overview. J. Environ. Qual. 27:251-257.

de Jonge, L.W., P. Moldrup G.H. Rubaek, K. Schelde and J. Djurhuus. 2004a. Particle leaching and particle-facilitated transport of phosphorus at field scale. Vadose Z. J. 3:462-470.

de Jonge, L.W., C. Kjaergaard and P. Moldrup. 2004b. Colloids and colloid-facilitated transport of contaminants in soils: An introduction. Vadose Zone J. 3:321-325.

De Smet, J., G. Hofman, J. Vanderdeelen, M. van Meirvenne and L. Baert. 1996. Phosphate enrichment in the sandy loam soils in West-Flanders, Belgium. Fert. Res. 43:209-215.

DeNovio, N.M., J.E. Saiers and J.N. Ryan. 2004. Colloid Movement in unsaturated porous media: recent advances and future directions. Vadose Zone J. 3:38-351.

Dineen, L.C. and B.C. Blakesley. 1973. Generator for sampling distribution of Mann-Whitney U statistics. J. Royal Stat. Soc. Ser. C- Applied Statistics 22:269-273.

Dolfing, J., W.J. Chardon and J. Japenga. 1999. Association between colloidal iron, aluminum, phosphorus and humic acids. Soil Sci. 164:171-179.

Dominik, P. and M. Kaupenjohann. 2000. Simple spectrophotometric determination of Fe in oxalate and HCl soil extracts. Talanta 51:701-707.

Dominik, P., Ilg K., Siemens J. and Kaupenjohann M. 2007. Goethite precipitation on quartz sand under soil-like conditions. Geochim. Cosmochim. Acta. submitted.

Dorich, R.A., D.W. Nelson and L.E. Sommer. 1985. Estimating algal available phosphorus in suspended sediments by chemical extraction. J. Environ. Qual. 13:400-405.

Driescher, E. and J. Gelbrecht. 1993. Assessing the diffuse phosphorus input from subsurface to surface waters in the catchment area of the lower river Spree (Germany). Water Sci. Tech. 28:337-347.

Electric Power Research Institute (EPRI). 1991. Use of Batch and Column Methodologies to Assess Utility Waste Leaching and Subsurface Chemical Attenuation. Technical Results. EN-7313. Palo Alto, USA.

Elimelech, M., M. Nagai, C.H. Ko and J.N. Ryan. 2000. Relative insignificance of mineral grain zeta potential to colloid transport in geochemically heterogeneous porous media. Environ. Sci. Tech. 34, 2143-2148.

Flury, M., J.B. Mathison and J.B. Harsh. 2002. In situ mobilization of colloids and transport of cesium in Hanford sediments. Environ. Sci. Techn. 36:5335-5341.

Food and Agriculture Organisation of the United Nations (FAO). 2006. World Reference Base for Soil Resources. www.fao.org. Rome.

Frossard, E., M. Brossard, M.J. Hedley and A. Metherell. 1995. Reactions controlling the cycling of P in soils. In: Phosphorus in the global environment, editors: H. Tiessen. John Wiley & Sons, LTD. Scope. 107-138.

Gasser, U.G., S.J. Juchler and H. Sticher. 1994. Chemistry and speciation of soil water from serpentinitic soils: importance of colloids in the transport of Cr, Fe, Mg and Ni. Soil Sci. 158:314-322.

Gerke, J. 1992. Orthophosphate and organic phosphate in the soil solution of four sandy soils in relation to pH-evidence for humic-Fe-(Al-) phosphate complexes. Commun. Soil Sci. Plant Anal. 23:601-612

Gimbel, R. and A. Nahrstedt. 2004. Grundlagen der Tiefenfiltration. Pp. 117-118. In: DVWG Deutsche Vereinigung des Gas- und Wasserfaches e.V. Wasseraufbereitung – Grundlagen und Verfahren. Oldenbourg Industrieverlag München Wien (in German).

Goldberg, S., I. Lebron and D.L. Suarez. 2000. Soil Colloidal Behaviour, p. B-2208. In M.E. Sumner (ed.) Handbook of soil science. CRC Press LLC, Boca Raton.

Grolimund, D., M. Borkovec, K. Barmettler and H. Sticher. 1996. Colloid-facilitated transport of strongly sorbing contaminants in natural porous media: A laboratory column study. Environ. Sci. Tech. 30:3118-3123.

Grossl, P.R. and W.P. Inskeep. 1991. Precipitation of dicalcium phosphate dihydrate in the presence of organic acids. Soil Sci. Soc. Am. J. 55:670-675.

Grossmann, J. and P. Udluft. 1991. The extraction of soil water by the suction-cup method: a review. J. Soil Sci. 42:82-93.

Gschwend, P. and M.D. Reynolds. 1987. Monodisperse ferrous phosphate colloids in an anoxic groundwater plume. J. Contam. Hydrol. 1:309-327.

Guggenberger, G., B.T. Christensen, G. Rubæk. and W. Zech. 1996. Land-use and fertilization effects on P forms in two European soils: resin extraction and ^{31}P-NMR analysis. Europ. J. Soil Sci. 47:605-614.

Guine, V., J. Martins and J.P. Gaudet. 2003. Facilitated transport of heavy metals by bacterial colloids in sand columns, J. Phys. IV 107:593-596.

Guzel, N. and H. Ibrikci. 1994. Distribution and fractionation of soil phosphorus in particle-size separates in soils of western turkey. Commun. Soil Sci. Plant. Anal. 25:2945-2958.

Haag, D. and G. Matschonat. 2001. Limitations of controlled experimental systems as models for natural systems: a conceptual assessment of experimental practices in biogeochemistry and soil science. Sci. Total Environ. 277:199-216.

Han, N. and M.L. Thompson. 1999. Soluble organic carbon in a biosolids-amended mollisol. J. Environ. Qual. 28:622-658.

Hartung, J. and B. Elpelt. 199. Multivariate Statistik. 5th edition. R. Oldenbourg Verlag München Wien. pp. 198-201.

Haygarth, P.M., M.S. Warwick and W.A. House. 1997. Size distribution of colloidal, molybdate reactive phosphorus in river waters and soil solution. Wat. Res. 31:439-443.

Haygarth, P.M. and S.C. Jarvis. 1999. Transfer of Phosphorus from Agricultural Soils. Adv. Agr. 66:195-247.

He, Q.H., G.G. Leppard, C.R. Paige and W.J. Snodgrass. 1996. Transmission electron microscopy of a phosphate effect on the colloid structure of iron hydroxide. Wat. Res. 30:1345-1352.

Heathwaite, L., P. Haygarth, R. Matthews, N. Preedy and P. Butler. 2005. Evaluating colloidal phosphorus delivery to surface waters from diffuse agricultural sources. J. Environ. Qual. 34:287-298.

Heckrath, G., P.C. Brookes, P.R. Poulton and K.W.T. Goulding. 1995. Phosphorus leaching from soils containing different phosphorus concentrations in the broadbalk experiment. J. Environ. Qual. 24:904-910.

Heil, D. and G. Sposito. 1993. Organic matter role in illitic soil colloids flocculation. I. Counter ions and pH. Soil Sci. Soc. Am. J. 57:1241-1246.

Hens, M. and R. Merckx. 2001. Functional characterization of colloidal phosphorus species in the soil solution of sandy soils. Environ. Sci. Technol. 35:493-500.

Hens, M. and R. Merckx. 2002. The role of colloidal particles in the speciation and analysis of “dissolved” phosphorus. Wat. Res. 36:1483-1492.

Hesketh, N., P.C. Brookes and T.M. Addiscott. 2001. Effect of suspended soil material and pig slurry on the facilitated transport of pesticides, phosphate and bromide in sandy soils. Eur. J. Soil Sci. 52:287-296.

Heyer, R. and H.J. Stan. 1995. Comparison of the leaching behavior of alachlor and its metabolites under field and laboratory conditions. Int. J. Environ. An. Ch. 58:173-183.

Higgo, J.J.W., G.M. Williams, I. Harrison, P. Warwick, M.P. Gardiner and G. Longworth. 1993. Colloid transport in a glacial sand aquifer - laboratory and field studies. Colloid. Surface. A. 73:179-200.

Ilg, K., J. Siemens and M. Kaupenjohann. 2005. Colloidal and dissolved phosphorus in sandy soils as influenced by phosphorus saturation. J. Environ. Qual. 34:926-935.

Ilg, K., E. Ferber, H. Stoffregen, A. Winkler, A. Pekdeger, M. Kaupenjohann, J. Siemens. 2007. Unsaturated colloid transport through columns with differing sampling systems. Soil Sci. Soc. Am. J. 71:298-305.

Ilg, K., P. Dominik, J. Siemens and M. Kaupenjohann. 2007. Phosphorus-induced mobilisation of colloids – model systems and soils. Europ. J. Soil Sci. submitted.

Inskeep, W.P. and J.C. Silvertooth. 1988. Inhibition of hydroxyapatite precipitation in the presence of fulvic, humic and tannic acids. Soil. Sci. Soc. Am. J. 52:941-946.

James, D.W., J. Kotuby-Amacher, G.L. Anderson and D.A. Huber. 1996. Phosphorus mobility in calcareous soils under heavy manuring. J. Environ. Qual. 25:770-775.

Jensen, M.B., T.B. Olsen, H.C. Bruun Hansen and J. Magid. 2000. Dissolved and particulate phosphorus in leachate from structured soil amended with fresh cattle faeces. Nutr. Cyc. Agroecosys. 56:253-261.

Johnson, P.R. 1999. A comparison of streaming and microelectrophoresis methods for obtaining the zeta potential of granular porous media surfaces. J. Colloid Interface Sci. 209:264-267.

Kaiser, K. and W. Zech. 1996. Nitrate, sulfate and biphosphate retention in acid forest soils affected by natural dissolved organic carbon. J. Environ. Qual. 25:1325-1331.

Kaplan, D.I., P.M. Bertsch, D.C. Adriano and W.P. Miller. 1993. Soil-borne mobile colloids as influenced by water flow and organic carbon. Environ. Sci. Techn. 27:1193-1200.

Kaplan, D.I., P.M. Bertsch and D.C. Adriano. 1997. Mineralogical and physicochemical differences between mobile and nonmobile phase in reconstructed pedons. Soil Sci. Soc. Am. J. 61:641-649.

Karathanasis, A.D. 1999 Subsurface migration of copper and inc mediated by soil colloids. Soil Sci. Soc. Am. J. 63:830-838.

Karathanasis, R. and D.M.C. Johnson. 2006. Stability and transportability of biosolid colloids through undisturbed soil monoliths. Geoderma 130:334-345.

Keil, K. 1950. Handwörterbuch der Meteorologie. Knapp, Frankfurt/Main.

Keller, A.A., S. Sirivithayapakorn and C.V. Chrysikopoulos. 2004. Early breakthrough of colloids and bacteriophage MS2 in a water-saturated sand column. Wat. Resour. Res. 40:no. W08304.

Kitayama, K., S.I. Aiba, M. Takyu, N. Majalap and R. Wagai. 2004. Soil phosphorus fractionation and phosphorus-use efficiency of a bornean tropical montane rain forest during soil aging with podozolization. Ecosystems 7:259-274.

Köhler, W., G. Schachtel and P. Voleske. 1996. Biostatistik p. 182, 2nd edition, Springer-Verlag, Berlin, Heidelberg.

Koopmans, G.F., R.W. McDowell, W.J. Chardon, O. Oenema and J. Dolfing. 2002. Soil phosphorus quantity-intensity relationships to predict increased soil phosphorus loss to overland and subsurface flow. Chemosphere 48:679-687.

Koopmans, G.F., W.J. Chardon and C. van der Salm. 2005. Disturbance of water-extractable phosphorus determination by colloidal particles in a heavy clay soil from the Netherlands. J. Environ. Qual. 34:1446-1450.

Kreller, D.I., G. Gibson, W. Novak, G.W. van Loon and J.H. Horton. 2003. Competitive adsorption of phosphate and carboxylate with natural organic matter on hydrous iron oxides as investigated by chemical force microscopy. Colloid. Surface. A. 212:249-264.

Kretzschmar, R., W.P. Robarge and S.B. Weed. 1993. Flocculation of kaolinitic soil clays: effect of humic substances and iron oxides. Soil Sci. Soc. Am. J. 57:1277-1283.

Kretzschmar, R. and H. Sticher. 1997. Transport of humic coated iron oxide colloids in a sandy soil: influence of Ca^{2+} and trace metals. Environ. Sci. Tech. 31:3497-3504.

Kretzschmar, R., D. Hesterberg and H. Sticher. 1997a. Effects of adsorbed humic acid on surface charge and flocculation of kaolinite. Soil Sci. Soc. Am. J. 61:101-108.

Kretzschmar, R., K. Barmettler, D. Grolimund, Y. Yan, M. Borkovec and H. Sticher. 1997b. Experimental determination of colloid deposition rates and colloid efficiencies in natural porous media. Water. Resour. Res. 33:1129-1137.

Kretzschmar, R., M. Borkovec, D. Grolimund and M. Elimelech. 1999. Mobile subsurface colloids and their role in contaminant transport. Adv. Agr. 66:121-193.

Kronvang, B., M. Bechmann, H. Lundekvam, H. Behrendt, G.H. Rubaek, O.F. Schoumans, N. Syversen, H.E. Andersen and C.C. Hoffmann. 2005. Phosphorus losses from agricultural areas in river basins: effects and uncertainties of targeted mitigation measures. J. Environ. Qual. 34:2129-2144.

Landesumweltamt Brandenburg. 1991. Daten der Bodendauerbeobachtungsfllächen 11 und 12 in Werbellin (data not published), http://www.mluv.brandenburg.de/info/lua.

Laubel, A., O.H. Jacodsen, B. Kronvang, R. Grant and H.E. Anderson. 1999. Subsurface drainage lost of particles and phosphorus from field plot experiments and a tile-drained catchment. J. Environ. Qual. 28:576-584.

Lee, F.G. 1973. Role of phosphorus in eutrophication and diffuse source control. Wat. Res. 7:111-128.

Leinweber, P., F. Lünsmann and K.U. Eckhardt. 1997. Phosphorus sorption capacities and saturation of soils in two regions with different livestock densities in northwest Germany. Soil Use Manage. 13:82-89.

Leytem, A.B., R.L. Mikkelsen and J.W. Gilliam. 2002. Sorption of organic phosphorus compounds in atlantic coastal plain soils. Soil Sci. 167:652-658.

Li, X., T.D. Scheibe and W.P. Johnson. 2004. Apparent decrease in colloid deposition rate coefficients with distance of transport under unfavorable deposition conditions: a general phenomenon. Environ. Sci. Tech. 38:5616-5625.

Liang, L. and J.J. Morgan. 1990. Chemical aspects of iron oxide coagulation in water: laboratory studies and implications for natural systems. Aquat. Sci. 52:32-55.

Lienemann, C.P., M. Monnerat, J. Dominik and D. Perret. 1999. Identification of stochiometric iron-phosphorus colloidal produced in an eutrophic lake. Aquat. Sci. 61:133-149.

Lima, J.M., S.J. Anderson and N. Curi. 2000. Phosphate-induced clay dispersion as related to aggregate size and composition in hapludoxs. Soil Sci. Soc. Am. J. 64:892-897.

Lookman, R., P. Grobet, R. Merckx and K. Vlassak. 1994. Phosphate sorption by synthetic amorphous aluminium hydroxides: a ^{27}AL and ^{31}P solid-state MAS NMR spectroscopy study. Europ. J. Soil Sci. 45:37-44.

Madsen, E.L. 1998. Epistemology of environmental microbiology. Environ. Sci. Techn. 32:429-439.

Maguire, R.O. and T.J. Sims. 2002. Measuring agronomic and environmental soil phosphorus saturation and predicting phosphorus leaching with Mehlich 3. Soil Sci. Soc. Am. J. 66:2033-2039.

Makarov, M.I., T.I. Malysheva, L. Haumaier, L.G. Alt and W. Zech. 1997. The forms of phosphorus in humic and fulvic acids of a toposequence of alpine soils in the northern Caucasus. Geoderma 80:61-73.

Makris, K.C., J.H. Grove and C.J. Matocha. 2006. Colloid-mediated vertical phosphorus transport in a waste-amended soil. Geoderma. 136:174-183.

Mayer, T.D. and W.M. Jarrell. 1995. Assessing colloidal forms of phosphorus and iron in the Tualatin river basin. J. Environ. Qual. 24:1117-1124.

Mays, D.C. and J.R. Hunt. 2005. Hydrodynamic aspects of particle clogging in porous media. Environ. Sci. Techn. 39:577-584.

McBeath, T.M., R.J. Smernik, E. Lombi and M.J. McLaughlin. 2006. Hydrolysis of pyrophosphate in a highly calcareous soil: A solid-state phosphorus-31 NMR study. Soil Sci. Soc. Am. J. 70:856-862.

McDowell, R.W. and A.N. Sharpley. 2001a. Soil phosphorus fractions in solution: influence of fertilizer and manure, filtration and method of determination. Chemosphere 45:737-748.

McDowell, R.W., A.N. Sharpley. 2001b. Phosphorus losses in subsurface flow before and after manure application to intensively farmed land. Sci. Total Env. 278:113-125.

McDowell, R.W. and A.N. Sharpley. 2001c. Approximating phosphorus release from soils to surface runoff and subsurface drainage. J. Environ. Qual. 30:508-520.

McDowell, R., A. Sharpley, P. Brookes and P. Poulton. 2001. Relationship between soil test phosphorus and phosphorus release to solution. Soil Sci. 166:137-149.

McDowell, R.W., A.N. Sharpley and P. Withers. 2002. Indicator to predict the movement of phosphorus from soil to subsurface flow. Environ. Sci. Technol. 36:1505-1509.

McGechan, M.B. and D.R. Lewis. 2002. Sorption of phosphorus by soil, Part 1: Principles, equations and models. Biosys. Eng. 82:1-24.

McLaughlin, J.R., J.C. Ryden and J.K. Syers. 1981. Sorption of inorganic phosphate by iron- and aluminium-containing components. J. Soil Sci. 32:365-377.

Metcalfe, T.B. 1976. Radiation spectra of radionuclides. Noyes Corporation, New Jersey, USA.

Mikutta, C., J. Krüger, F. Lang and M. Kaupenjohann. 2006. Acid polysaccharide coatings on microporous goethite: controls of slow phosphate sorption. Soil Sci. Soc. Am. J. 70:1547-1555.

Motoshita, M., T. Komatsu, P. Moldup, L.W. de Jonge, N. Ozaki and T. Fukushima. 2003, Soil constituent facilitated transport of phosphorus from a high P surface soil. Soils Found. 43:105-114.

Murphy, J. and J.P. Riley. 1962. A modified single solution method for the determination of phosphate in natural waters. Anal. Chim. Acta 27:31-36.

Nair, V.D., K.M. Portier, D.A. Graetz and M.L. Walker. 2004. An environmental threshold for degree of phosphorus saturation in sandy soils. J. Environ. Qual. 33:107-113.

Nelson, N.O., J.E. Parsons and R.L. Mikkelsen. 2005. Field-scale evaluation of phosphorus leaching in acid sandy soils receiving swine waste. J. Environ. Qual. 34:2024-2035.

Neyroud, J.-A. and P. Lischer. 2004. Do different methods used to estimate soil phosphorus availability across Europe give comparable results? J. Plant Nutr. Soil Sci. 166:422-431.

Ogaard, A.F. 1996. Effect of phosphorus fertilization on the concentration of total and algal-available phosphorus in different particle-size. Acta Agric. Scand. Sec. B Soil and Plant Sci. 46:24-29.

Parfitt, R.L. 1978. Anion adsorption by soils and soil materials. Adv. Agr. 30:1-50.

Pennock, D.J. 2004. Designing field studies in soil science. Can. J. Soil Sci. 84:1-10.

Preedy, N., K. McTiernan, R. Matthews, L. Heathwaite and P. Haygarth. 2001. Rapid incidental phosphorus transfers from grassland. J. Environ. Qual. 30:2105-2112.

Puls, R.W. and R.M. Powell. 1992. Transport of inorganic colloids through natural aquifer material: Implications for contaminant transport. Environ. Sci. Technol. 26:614-621.

Puls, R.W., C.J. Paul and D.A. Clark. 1993. Surface chemical effects on colloid stability and transport through natural porous media. Colloid. Surface. A. 73:287-300.

R Development Core Team 2005. R: A language and environment for statistical computing. R Foundation. Vienna, Austria. ISBN 3-900051-07-0.

Rhea, S.A., W.W. Miller, R.R. Blank and D.E. Palmquist. 1996. Presence and behavior of colloidal nitrogen and phosphorus in a Sierra Nevada watershed soil. J. Environ. Qual. 25:1449-1451.

Rowland, A.P. and P.M. Haygarth. 1997. Determination of total dissolved phosphorus in soil solutions. J. Environ. Qual. 26:410-415.

Rubæk, G.H., L.W. de Jonge, G. Heckrath and K. Schelde. 2002. Phosphorus leaching from undisturbed soil columns amended with cattle , pig or mink manure. Poster presented at the workshop Colloids and Colloid-Facilitated Transport of Contaminants in Soils and Sediments, Research Centre Foulum Tjele, Denmark.

Ryden, J.C. and J.K., Syers. 1977. Origin of the labile phosphate pool in soils. Soil Sci. 123:353-361.

Sachs, L. 1982. Applied Statistics. P 498. Fifth edition. Springer Verlag, New York.

Saiers, J.E. 2002. Laboratory observations and mathematical modeling of colloid-facilitated contaminant transport in chemically heterogeneous systems. Water Resour. Res. 38:art. no. 1032.

Saiers, J.E. and J.L. Lenhart. 2003. Ionic-strength effects on colloid transport and interfacial reactions in partially saturated porous media. Wat. Resour. Res. 39:8.1-8.5.

Schäfer, A., P. Ustohal, H. Harms, F. Stauffer, T. Dracos and A.J.B Zehnder. 1998. Transport of bacteria in unsaturated porous media. J. Contam. Hydr. 33:149-169.

Scheidegger, A., M. Borkovec and H. Sticher. 1993. Coating of silica sand with goethite: preparation and analytical identification. Geoderma 58:43-65.

Schelde, K., L.W. de Jonge, C. Kjaergaard, M. Laegdsmand and G.H. Rubæk. 2006. Effects of manure application and plowing on transport of colloidal and phosphorus to tile drains. Vadose Zone J. 5:445-458.

Schindler, D.W. 1971. Carbon nitrogen and phosphorus and the eutrophication of freshwater lakes. J. Phycol. 7:321-329.

Schindler, D.W. 1998. Replication versus realism: the need for ecosystem-scale experiments. Ecosystems. 1:323-334.

Schlichting, E., H.P. Blume and K. Stahr. 1995. Kennzeichnung der pedogenen Oxide, p. 148, Bodenkundliches Praktikum. 2nd edition, Blackwell, Berlin. (in German)

Schoumans, O.F. and P. Groenendijk. 2000. Modeling soil phosphorus levels and phosphorus leaching from agricultural land in the Netherlands. Journal of Environmental Quality, 29:111-116.

Schoumans, O.F. and W.J. Chardon. 2003. Risk assessment methodologies for predicting phosphorus losses. J. Plant Nutr. Soil Sci. 166:403-409.

Schwertmann, U. 1964. Differenzierung der Eisenoxide des Bodens durch Extraktion mit saurer Ammoniumoxalat-Lösung. Z. Pflanz. Bodenkunde 105:194-202.

Schwertmann, U. 1988. Some properties of soil and synthetic iron oxides. In: Stucki, J.W., Goodman, B.A., Schwertmann, U.: Iron in soils and clay minerals. Dordrecht, Netherlands, pp. 203-250.

Sequaris, J.M. and H. Lewandowski. 2003. Physicochemical characterization of potential colloids from agricultural topsoils. Colloid. Surface. A 271:93-99.

Shand, C.A., S. Smith, A.C. Edwards, A.R. Fraser. 2000. Distribution of phosphorus in particulate colloidal and molecular-sized fractions of soil solution. Wat. Res. 34:1278-1284.

Shao, J. and D. Tu. 1995. The jackknife and bootstrap. Springer. New York, Berlin.

Shapiro, S.S., M.B. Wilk and H.J. Chen. 1968. A comparative study of various tests for normality. J. Am. Stat. Ass. 63:1343 ff.

Sharpley, A.N., C. Chapra, R. Wedepohl, J.T. Sims, T.C. Daniel and K.R. Reddy. 1994. Managing agricultural phosphorus for protection of surface waters: issues and options. J. Environ. Qual. 23:437-451.

Sharpley, A.N. and R.S. Rekolainen. 1997. Phosphorus in agriculture and its environmental implications. In: Tunney, H., O.T. Carton, P.C. Brookes and A.E. Johnson (eds.): Phosphorus loss from soil to water. CAB International Wallingford.

Shaw, P.J., R.I. Jones and H. De Haan. 2000. The influence of humic substances on the molecular weight distribution of phosphate and iron in epilimnetic lake waters. Freshwater Biol. 45:383-393.

Siemens, J. and M. Kaupenjohann. 2002. Contribution of dissolved organic nitrogen to N leaching from four German agricultural soils. J. Plant Nutr. Soil Sci. 165:675-681.

Siemens, J., K. Ilg, F. Lang and M. Kaupenjohann. 2004. Adsorption controls mobilization of colloids and leaching of dissolved phosphorus. Eur. J. Soil Sci. 55:254-263.

Sinaj, S., C. Stamm, G.S. Toor, L.M. Contron, T. Hendry, H.J. Di, K.C. Cameron and E. Frossard. 2002. Phosphorus exchangeability and leaching losses from two grassland soils. J. Environ. Qual. 31:319-330.

Sirivithayapakorn, S. and A.A. Keller. 2003. Transport of colloids in saturated porous media: A pore-scale observation of the size exclusion effect and colloid acceleration. Wat. Resour. Res. 39:no. 1109.

Sprent, P. and N.C. Smeeton. 2001. Applied nonparametric statistical methods. Pp. 124-129. Third edition. Chapman & Hall/CRC, USA.

Stamm, C.H. 1997. Rapid transport of phosphorus in drained grassland soils. Dissertation, ETH Zürich No. 12486.

Stamm, C.H., H. Flühler, R. Gächter, J. Leuenberger and H. Wunderli. 1998. Preferential transport of phosphorus in drained grassland soils. J. Environ. Qual. 27:515-522.

Stevens, D.P., J.W. Cox and D.J. Chittleborough. 1999. Pathways of phosphorus, nitrogen and carbon movement over and through texturally differentiated soils, South Australia. Austr. J. Soil Res. 37:679-693.

Strauss, R., G.W. Brümmer and N.J. Barrow. 1997. Effects of crystallinity of goethite: II. rates of sorption and desorption of phosphate. Europ. J. Soil Sci. 48:101-114.

Stumm, W. and L. Sigg. 1979. Kolloidchemische Grundlagen der Phosphor-Elimination durch Fällung, Flockung und Filtration. Z. Wasser Abwass. For. 12:73-83.

Thomas, G.W. 1982. Exchangeable cations. p. 160-161. In: A.L. Page, R.H. Miller, and D.R. Keeney (ed.) Methods of Soil Analysis, Part 2. 2nd ed. Agron. Monogr. 9. ASA and SSSA, Madison WI.

Thompson, M.L. and R.L. Scharf. 1994. An improved zero-tension lysimeter to monitor colloid transport in soils. J. Environ. Qual. 23:378-383.

Toor, G.S., L.M. Condron, B.J. Cade-Menun, H.J. Di and K.C. Cameron. 2005. Preferential phosphorus leaching from an irrigated grassland soil. Eur. J. Soil Sci. 56:155-167.

Toride N., F.J. Leii and M.T. van Genuchten. 1998. The CXTFIT code for estimating transport parameters from laboratory or field tracer experiments, version 21, research report no. 137. U.S. Salinity Laboratory, USDA ARS Riverside, USA.

Turner, B.L. and P.M. Haygarth. 2000. Phosphorus forms and concentrations in leachate under four grassland soil types. Soil Sci. Soc. Am. J. 64:1090-1099.

Turner, B.L., M.J. Paphazy, P.M. Haygarth and I.D. McKelvie. 2002. Inositol phosphates in the environment. Philos. T. R. Soc. B. 357:449-469.

Turner, B.L., M.A. Kay and D.T. Westermann. 2004. Colloidal phosphorus in surface runoff and water extracts from semiarid soils of the western United States. J. Environ. Qual. 33:1464-1472.

Ulen, B. 2004. Size and settling velocities of phosphorus-containing particles in water from agricultural drains. Water Air Soil Pollut. 157:331-343.

Umweltbundesamt. 2003. Niederschlagsanalysen der beiden Messstationen Neuglobsow und Waldhof in wöchentlicher Auflösung. (unpublished data)

Umweltbundesamt. 2004. Umweltdaten Deutschland 2004, www.umweltbundesamt.de.

Umweltbundesamt. 2006. Umweltdaten Deutschland, UBA-Texte 82/03, www.umweltbundesamt.de.

Untersuchungszentrum NRW - LUFA 2004. N-min Probenahme Boden. Landwirtschaftskammer Nordrhein-Westfalen, Münster, http://www.lk-wl.de/lufa/pdf/probe_nmin.pdf.

US Environmental Protection Agency, 2000. Water Quality Report 2000, Washington (http://www.epa.gov/305b).

Van der Zee, S.E.A.T.M. and W.H. van Riemsdijk. 1986. Transport of phosphate in a heterogeneous field. Transport Porous Med. 1:339-359.

Van der Zee, S.E.A.T.M. and W.H. van Riemsdijk. 1988. Model for long-term phosphate reaction kinetics in soil. J. Environ. Qual. 17:35-41.

Van der Zee, S.E.A.T.M, M.M. Nederlof, W.H. van Riemsdijk and F.A.M. de Haan. 1988. Spatial variability of phosphate adsorption parameters. J. Environ. Qual., 17, 682-688.

Van der Zee, S.E.A.T.M. and F.A.M. De Haan. 1994. Het protocol fosfaatverzadigte gronden. In: Bodenbescherming. Handboek voor milieubeheer, Studenteneditie Deel 1, (eds.) De Haan, F.A.M., Ch. H. Henkens, D.A. Zeilmaker. Samson H.D. Tjenk Willink bv Alphen, The Netherlands: D4410-1 - D4410-7. (in Dutch)

Vanclooster, M., D. Mallants, J. Diels and J. Feyen. 1993. Determining local-scale transport parameters using time-domain reflectometry (TDR). J. Hydrol. 148:93-107.

Vanderdeelen, J. 1995. Phosphate immobilization in an uncropped field experiment on a calcareous soils. Plant Soil 171:209-215.

Watts, C.W., A.R. Dexter, E. Dumitru and J. Arvidsson. 1996. An assessment of the vulnerability of soil structure to destabilization during tillage. Part I. A laboratory test. Soil Till. Res. 37:161-174.

Wierenga, P.J. and M.T. van Genuchten. 1989. Solute transport through small and large unsaturated soil columns. Ground Water 27:35-42.

Winer, B.J., D.R. Brown and K.M. Michels. 1991. Statistical principles in experimental design.Pp 351-354, 1028-1029. Third edition, McGraw Hill, Boston, Massachusetts.

Worall, F., A. Parker, J.E. Rae and A.C. Johnson. 1999. A study of suspended and colloidal matter in the leachate from lysimeters and its role in pesticide transport. J. Environ. Qual. 28:595-604.

Xu, Y. and Axe, L. 2005. Synthesis and characterization of iron oxide-coated silica and its effect on metal adsorption. J. Colloid Interf. Sci. 285:11-19.

Yan, T.L. 1980. Adsorption of phosphate and water-extractable soil organic material by synthetic aluminium silicates and acid soils. Soil Sci. Soc. Am. J. 44:951-955.

Zhang, M.K., Z.L. He, D.V. Calvert and P.J. Stoffella. 2003. Colloidal iron oxide transport in sandy soils induced by excessive phosphorus application. Soil Sci. 168:617-626.

Acknowledgements

I am grateful to

my parents Hans and Hilde Ilg for their permanent support,

Prof. Dr. Martin Kaupenjohann for supervising this thesis, for giving me freedom, confidence and motivation throughout my work and for his great feature to immediately and professionally put himself in my work at any moment,

Prof. Dr. Ruben Kretzschmar for being the co-examiner,

Dr. Jan Siemens for being such a competent and creative supervisor and the best proofreader I have met,

Dr. Peter Dominik for the great cooperation, for developing common research ideas, for his friendship and a lot of nice evenings we spent together at or out of the university,

Eckhard Ferber, Holger Pagel, Sebastian Althaber and Cyril Roth for their valuable contributions to my research and their staying power and patience with experiments, which often went wrong,

Dr. Heiner Stoffregen, Dr. Fritzi Lang, Prof. Dr. Wolfgang Wilcke, Dr. Christian Mikutta, Sondra Klitzke, Andrea Herre, Dr. Fayez Alaily for inspiring discussions, valuable support and/or for reading parts of my manuscripts,

Sabine Dumke, Karl Böttcher, Michael Facklam, Dr. Kai Schwärzel and Joachim Bartels for their assistance in the lab and in the workshop,

David Vinue-Visus, Haza Taib Mohamed, Tina Kasal, Cecilia Mueni Maundu, Hysein Tümtürk for their help in the lab and their patience during boring particle size measurements,

Dr. Olfs and the Institute for Plant Nutrition and Environmental Research Hanninghof (YARA International ASA), Dr. Rex and Thomasdünger GmbH, Dr. Baumecker from Thyrow/Humboldt University and Prof. Dr. Schulz Sternberg from LUA Brandenburg for the permission to take sam-

ples on their properties in Dülmen, Dierstorf, Bohnhorst, Thyrow and Werbellin and for the provision of data,

Dr. Andreas Winkler, Prof. Dr. Asaf Pekdeger for the possibility to conduct a column experiment in their radionuclide-laboratory,

Dorothea Alber and the Hahn Meitner Institute for irradiating goethite samples,

Prof. Dr. Lerch, Dr. Rolf Liedke, Ulrich Gernert from ZELMI of the TU Berlin for SEM- and REM-measurements,

Peter Schubert-Bischoff from the Hahn Meitner Institute for the preparation of TEM images of goethite coated sand,

Prof. Dr. Joachim Erber for the possibility to conduct the second column experiment in his greenhouse,

Hans Peter Maurer for his patience, his encouragement and his valuable statistical advice,

the Deutsche Forschungsgemeinschaft (Grant no. KA 1139/10-1,-2) for funding this thesis,

Claudia Kuntz and Beate Mekiffer for the warm atmosphere in our office, their good advice for all circumstances and many nice cocktail-evenings,
all colleagues from the department of Soil Science of the TU Berlin for the support I received,

my friends for giving me a good time during my work here in Berlin, for being a shoulder to lean on, if everything did not work once more.

Curriculum vitae

1976	born on April 26th in Esslingen/Neckar (Germany)
1995	Graduation (Abitur) at Freihof Gymnasium, Göppingen (Germany)
1995-1996	voluntary work (holiday care for people with disabilities, Sheringham (Great Britain)
1996-2001	Study of Agricultural Biology at the University of Hohenheim , (Germany), specialization in agroecology, plant protection and soil chemistry
1997-1999	Internships in Germany, Russia and Spain dealing with (organic) agriculture and development cooperation
2001	Diploma in Agricultural Biology, Institute of Soil Science, Universtiy of Hohenheim; thesis: “Bindungsformen und Verteilung von Schwermetallen in Bodenaggregaten – Vergleich historischer, rezenter und belasteter Böden”
2002-2007	PhD student at the Department of Soil Science (Prof. Kaupenjohann), TU Berlin (Germany)

Appendix

Chapter 2: Phosphorus-induced mobilization of colloids – model systems and soils

App. 2.1a: Results of batch experiments with goethite adsorbed to quartz sand exposed to ortho-P

grade of P addition	replication	pH	electrical conductivity	optical density	zeta potential	particle size
			µS cm^{-1}	extinction	mV	nm
0	a	5.28	572	0.1074	-2	1517
	b	5.63	571	0.0822	-10.9	na
	c	5.36	572	0.1104	-7.1	1146
1	a	5.3	570	0.1126	6	na
	b	5.41	569	0.1075	3	na
	c	5.19	571	0.1110	-14.6	601
2	a	5.09	571	0.0884	0.2	1354
	b	5.58	570	0.0736	-13.8	466
	c	5.18	571	0.1062	-8.8	na
3	a	5.47	570	0.0919	-13.9	977
	b	5.05	572	0.0977	-6.3	na
	c	5.27	569	0.0896	3.6	1499
4	a	5.31	569	0.0682	-16.8	1370
	b	5.24	570	0.1040	-2.3	859
	c	5.82	570	0.0255	-22.5	229
5	a	5.61	572	0.0263	-24.3	na
	b	5.4	571	0.0332	-18.1	na
	c	5.29	572	0.0299	-20.8	na
6	a	5.61	570	0.0760	-20.8	792
	b	5.69	571	0.0659	-24.4	1071
	c	5.64	571	0.0589	-30	887
7	a	5.86	572	1.0282	-19.4	412
	b	5.76	572	0.9756	-19.5	811
	c	5.74	573	0.9086	-20.6	1130
8	a	5.72	578	1.0130	-23.8	652
	b	5.61	579	0.9906	-25.2	555
	c	5.61	580	0.9872	-26.1	904
9	a	5.46	595	0.9452	-29	559
	b	5.56	594	0.9230	-31.1	334
	c	5.49	594	0.9708	-28.6	547

na: no data available

bd: below detection limit

App. 2.1b: Results of batch experiments with goethite adsorbed to quartz sand exposed to ortho-P

grade of P addition	replication	colloidal Fe	colloidal P	dissolved P	added P*
		µmol l^{-1}			
0	a	24.0	0	0.67	bd
	b	27.7	0	0.86	bd
	c	27.1	0.52	bd	bd
1	a	37.8	0.85	bd	0.48
	b	29.8	0.73	bd	
	c	18.1	0.65	bd	
2	a	23.7	0.38	bd	0.98
	b	13.2	0	0.53	
	c	29.5	0.28	0.37	
3	a	34.1	0.68	bd	1.96
	b	49.5	0.52	bd	
	c	32.0	0	bd	
4	a	38.4	0	bd	3.71
	b	53.8	0	0.46	
	c	15.1	0	bd	
5	a	18.1	0	bd	7.49
	b	25.8	0	bd	
	c	11.4	0	bd	
6	a	54.4	0.63	0.81	16.4
	b	52.3	1.18	0.81	
	c	50.8	0.91	0.97	
7	a	1207	15.0	24.6	39.9
	b	1207	14.4	25.3	
	c	1091	12.6	25.2	
8	a	1364	16.6	89.7	108
	b	1345	16.3	87.9	
	c	1320	16.7	88.5	
9	a	1330	18.9	293	326
	b	1335	16.3	297	
	c	1376	15.4	296	

na: no data available

bd: below detection limit

*: mean of three replicates

App. 2.2a: Results of batch experiments with goethite adsorbed to quartz sand exposed to IHP

grade of P addition	replication	pH	electrical conductivity	optical density	zeta potential	particle size
			µS cm^{-1}	extinction	mV	nm
0	a	5.35	573	0.1130	6.2	240
	b	5.16	574	0.1252	29.8	700
	c	5.19	573	0.0754	-5.7	300
1	a	5.81	567	0.0424	-12.7	na
	b	5.78	567	0.0998	-10.5	na
	c	5.87	566	0.0391	-14.2	na
2	a	4.24	593	0.0236	12.7	na
	b	5.92	568	1.0152	-42.3	750
	c	5.97	568	1.0278	-46.6	650
3	a	6.04	567	0.9222	-57.2	250
	b	6.13	567	0.9255	-49.6	250
	c	6.13	567	0.9225	-21.3	250
4	a	6.03	573	0.9609	-45.3	300
	b	6.21	568	0.9630	-53.9	300
	c	6.1	567	0.9150	-52.8	300
5	a	6.17	570	0.9588	-52.7	270
	b	6.25	569	0.9354	-55.4	300
	c	6.19	569	0.9870	-51.9	220
6	a	6.45	573	0.9789	-55.1	280
	b	6.54	572	0.9984	-52.7	280
	c	6.54	572	0.9432	-54.5	300
7	a	6.55	577	0.9993	-54.2	280
	b	6.74	577	1.0164	-55	300
	c	6.68	577	1.0332	-52.3	290

na: no data available

bd: below detection limit

App. 2.2b: Results of batch experiments with goethite adsorbed to quartz sand exposed to IHP

grade of P addition	replication	colloidal Fe	colloidal P	dissolved P	added P*
		µmol l^{-1}			
0	a	90.4	1.13	bd	bd
	b	120	0.76	bd	
	c	57.3	1.09	bd	
1	a	22.3	2.27	bd	11.7
	b	96.9	1.31	bd	
	c	20.7	1.40	bd	
2	a	8.3	0.35	0.52	16.3
	b	1420	9.83	0.50	
	c	1419	10.01	0.50	
3	a	1504	13.63	2.42	22.9
	b	1557	15.15	1.27	
	c	1545	14.34	1.71	
4	a	1622	19.53	4.18	32.0
	b	1585	15.45	8.74	
	c	1533	16.03	8.56	
5	a	1578	17.33	19.2	44.8
	b	1561	18.77	15.9	
	c	1599	15.94	19.1	
6	a	1603	0	37.2	62.8
	b	1568	0	36.7	
	c	1603	0	38.2	
7	a	1636	0	60.4	87.9
	b	1659	0	57.3	
	c	1745	0	58.8	

na: no data available

bd: below detection limit

*: mean of three replicates

App. 2.3a: Results of batch experiments with goethite precipitated on quartz sand exposed to ortho-P

grade of P addition	replication	pH	electrical conductivity	optical density	zeta potential	particle size
			µS cm^{-1}	extinction	mV	nm
0	a	5.39	na	0.0294	-24.73	na
	b	5.39	na	0.0283	-25.90	na
	c	5.39	na	0.0418		na
1	a	5.42	na	0.0203	-19.80	na
	b	5.46	na	0.0288	-27.00	na
	c	5.44	na	0.0207	-11.34	na
2	a	5.92	na	0.0299	-14.94	na
	b	5.87	na	0.0374	-15.60	na
	c	5.84	na	0.0297	-15.74	na
3	a	5.91	na	0.0565	-24.72	na
	b	6.05	na	0.0655	-23.85	na
	c	5.97	na	0.1046	-33.67	na
4	a	6.11	na	0.0964	-45.04	620
	b	6.02	na	0.076	-28.93	680
	c	6.04	na	0.08	-42.82	680
5	a	5.97	na	0.1221	-40.28	520
	b	6.15	na	0.1215	-37.68	410
	c	6.1	na	0.092	-41.28	680
6	a	6.12	na	0.1157	-41.22	480
	b	6.11	na	0.1211	-41.33	580
	c	6.15	na	0.1041	-35.33	330
7	a	6.1	na	0.1058	-53.52	320
	b	6.11	na	0.1151	-42.98	280
	c	6.08	na	0.1349	-43.63	520
8	a	6.08	na	0.0949	-35.88	560
	b	6.11	na	0.1021	-37.90	440
	c	6.04	na	0.1097	-46.87	300
9	a	6.07	na	0.1119	-41.53	340
	b	6.05	na	0.115	-40.20	520
	c	5.92	na	0.104	-40.44	500
10	a	5.99	na	0.1166	-48.30	480
	b	6.03	na	0.1182	-38.00	470
	c	6.03	na	0.1291	-43.72	490

na: no data available

bd: below detection limit

App. 2.3b: Results of batch experiments with goethite precipitated on quartz sand exposed

grade of P addition	replication	colloidal Fe	colloidal P	dissolved P	added P*
			µmol l^{-1}		
0	a	21.6	0.00	0.52	0.35
	b	19.7	0.29	0.31	
	c	0.0	0.01	0.60	
1	a	14.7	0.35	bd	9.11
	b	19.1	0.35	bd	
	c	16.8	0.25	bd	
2	a	29.5	1.36	bd	19.76
	b	34.9	1.56	bd	
	c	23.8	0.95	bd	
3	a	51.8	3.14	1.83	29.09
	b	50.5	3.01	1.54	
	c	86.4	4.62	2.18	
4	a	88.2	4.97	7.39	41.6
	b	68.9	4.03	5.80	
	c	69.8	4.21	6.67	
5	a	118	8.22	12.06	48.5
	b	92.8	6.78	14.28	
	c	84.3	5.99	13.06	
6	a	114	4.91	26.12	64.4
	b	127	9.70	23.69	
	c	103	6.08	24.81	
7	a	106	4.83	43.61	85.8
	b	111	2.83	45.70	
	c	131	3.52	45.19	
8	a	89	5.30	61.0	108.7
	b	102	2.66	64.3	
	c	119	4.16	66.3	
9	a	120	1.26	84.8	128.6
	b	129	10.4	78.8	
	c	113	2.33	82.2	
10	a	121	0.41	97.7	144.0
	b	132	7.33	98.9	
	c	150	4.78	101	

na: no data available

bd: below detection limit

*: mean of three replicates

App. 2.4a: Results of batch experiments with goethite precipitated on quartz sand exposed to IHP

grade of P addition	replication	pH	electrical conductivity µS cm^{-1}	optical density extinction	zeta potential mV	particle size nm
0	a	5.01	na	0.0432	4.1	na
	b	5.06	na	0.0465	15.2	na
	c	5.03	na	0.039	25.9	na
1	a	5.06	na	0.0214	-8.5	na
	b	5.07	na	0.0191	-20	na
	c	5.09	na	0.0205	13.7	na
2	a	5.13	na	0.0211	18.3	na
	b	5.16	na	0.0164	-5.6	na
	c	5.19	na	0.0168	12.7	na
3	a	5.22	na	0.0149	2.2	na
	b	5.15	na	0.0141	-17.4	na
	c	5.4	na	0.0149	-26.3	na
4	a	5.28	na	0.0156	-9.8	na
	b	5.27	na	0.0116	-15.3	na
	c	5.3	na	0.0111	-12.4	na
5	a	5.42	na	0.0233	-19.9	na
	b	5.5	na	0.0147	-31.4	na
	c	5.45	na	0.0223	-20	na
6	a	5.6	na	0.095	-36.7	530
	b	5.64	na	0.0933	-25.5	600
	c	5.65	na	0.0968	-31.9	430
7	a	5.83	na	0.1423	-46.5	290
	b	5.94	na	0.1374	-42.3	310
	c	6.06	na	0.14	-44.8	300
8	a	6.16	na	0.1504	-51.7	300
	b	6.22	na	0.1482	-56	365
	c	6.21	na	0.1456	-48.4	280
9	a	6.11	na	0.1543	-51.8	440
	b	6.18	na	0.1497	-53	350
	c	6.19	na	0.1419	-55	280
10	a	6.03	na	0.1455	-55.9	320
	b	6.14	na	0.1398	-54.9	355
	c	6.03	na	0.1414	-55.5	470

na: no data available

bd: below detection limit

App. 2.4b: Results of batch experiments with goethite precipitated on quartz sand exposed

grade of P addition	replication	colloidal Fe	colloidal P	dissolved P	added P
			µmol l^{-1}		
0	a	32.7	0.21	bd	bd
	b	35.1	0.06	bd	bd
	c	30.4	0.13	bd	
1	a	18.1	0.27	bd	3.52
	b	15.6	0	0.23	3.63
	c	15.4	0.13	bd	
2	a	16.7	0.22	bd	5.87
	b	13.0	0.31	bd	5.97
	c	12.7	0.18	bd	
3	a	11.8	0.07	bd	9.52
	b	11.4	0	0.20	9.34
	c	12.7	0.20	bd	
4	a	9.89	0.17	bd	14.2
	b	9.03	0.00	0.40	14.4
	c	8.48	0.23	bd	
5	a	18.5	0.66	bd	18.5
	b	12.8	0.49	bd	18.7
	c	16.8	1.02	bd	
6	a	71.2	4.63	bd	26.1
	b	70.7	4.78	bd	25.8
	c	71.8	4.86	bd	
7	a	144	15.2	0.50	36.3
	b	140	11.9	3.12	36.8
	c	144	12.6	3.26	
8	a	155	17.3	11.9	54.1
	b	156	14.6	14.8	52.7
	c	150	16.4	12.2	
9	a	158	19.2	29.6	72.9
	b	154	17.1	30.5	73.9
	c	148	18.9	29.2	
10	a	149	17.0	47.0	91.9
	b	145	15.3	49.8	89.7
	c	148	14.6	49.1	

na: no data available

bd: below detection limit

App. 2.5a: Results of batch experiments with Bw-horizon exposed to ortho-P

grade of P addition	replication	pH	electrical conductivity µS cm^{-1}	turbidity FNU	optical density extinction	zeta potential mV	particle size nm
	a	4.37	604	bd	bd	-10.2	na
0	b	4.46	596	bd	0.009	-4.2	na
	c	4.44	602	bd	0.024	-3.8	na
	a	4.49	595	bd	bd	-7.9	na
1	b	4.45	596	bd	bd	-4	na
	c	4.58	596	bd	bd	-9.7	na
	a	4.63	592	bd	bd	-16.2	na
2	b	4.47	594	bd	bd	-13.9	na
	c	4.5	596	bd	bd	-11.3	na
	a	4.53	599	bd	bd	-8.2	na
3	b	4.54	597	bd	bd	-8.5	na
	c	4.52	601	bd	0.011	-12.2	1132
	a	4.91	595	0.93	bd	-14.1	1132
4	b	4.88	591	bd	bd	-14.1	na
	c	4.77	593	0.66	bd	-14	1132
	a	4.88	595	bd	bd	-12.4	na
5	b	4.77	596	bd	bd	-11.7	na
	c	4.93	597	bd	0.009	na	1879
	a	4.99	597	1.95	bd	-16	na
6	b	4.94	598	3.48	bd	-15	879
	c	4.87	598	3.71	0.012	-15.6	1459
	a	4.87	607	10.1	0.011	-13.6	1879
7	b	5.09	607	12.6	0.011	-21.7	2421
	c	5.18	606	17.2	0.015	-22.1	1879
	a	4.5	596	9.10	0.01	-10.3	1132
8	b	4.84	595	10.9	0.03	-16.6	3120
	c	5	597	12.0	0.022	-20.4	1347
	a	5.15	620	25.6	0.022	-23.4	1116
9	b	5.02	620	15.9	0.043	-22.5	1116
	c	5.12	621	18.4	0.022	-23.5	1054
	a	5.07	624	23.4	0.042	-24	675
10	b	4.98	627	23.7	0.029	-19.5	651
	c	4.71	602	22.1	0.034	-20.3	1759
	a	5.15	616	31.5	0.047	-25.1	815
11	b	5.05	641	26.9	0.032	-25.3	524
	c	5.08	643	27.7	0.031	-24.9	593
	a	5.09	627	30.7	0.043	-27.2	319
12	b	5.18	678	45.5	0.063	-26.5	319
	c	5.09	678	33.2	0.042	-25.3	397
	a	5.09	722	41.8	0.061	-26.1	654
13	b	5.12	723	44.6	0.053	-27	651
	c	5.24	725	30.8	0.044	-26	681
	a	5.21	790	50.0	0.061	-28.3	303
14	b	5.23	791	54.2	0.068	-26.2	303
	c	5.2	803	41.9	0.052	-26.9	411
	a	5.06	925	39.1	0.061	-26.6	552
15	b	5.15	926	34.6	0.043	-26.8	303
	c	5.13	920	39.1	0.054	-24.7	303
	a	5.2	1085	40.5	0.044	-25.7	284
16	b	5.16	1085	37.6	0.041	-25.8	249
	c	5.01	1088	29.6	0.036	-24.5	303

na: no data available

bd: below detection limit

FNU: Formazin nephelometric units

App. 2.5b: Results of batch experiments with Bw-horizon exposed to ortho-P

grade of P addition	replication	colloidal Al	colloidal Fe	colloidal C	colloidal P	dissolved P	added P
		mg l^{-1}					
0	a	na	0	0	0	bd	bd
	b	na	0	0	0.01	0.05	bd
	c	0	0	0	0	0.03	bd
1	a	0	0	0	0.03	0.02	1.19
	b	0	0	0	0	bd	1.15
	c	0	0	0	0.02	bd	1.25
2	a	0	0	0.66	0.02	bd	2.83
	b	0	0	3.09	0.03	bd	2.85
	c	0	0	0	0	bd	2.88
3	a	0	0	0	0.01	bd	4.11
	b	0	0	0	0	bd	3.94
	c	0	0	0.51	na	0.21	4.16
4	a	0	0.05	0	0.02	0.11	5.91
	b	0	0.00	0	0	0.14	5.54
	c	0	0.04	0	0.01	0.11	6.01
5	a	0	0	0	0.04	0.28	7.83
	b	0	0	0	0	0.40	8.20
	c	0	0	0	0.01	0.27	8.29
6	a	0	0.05	0	0.05	1.12	11.9
	b	0	0	0	0	1.18	11.4
	c	0.69	0.37	0	0.11	1.24	11.6
7	a	0.88	0.53	0	0.16	4.20	17.5
	b	1.11	0.70	0	0.18	4.10	16.1
	c	3.04	1.58	0	0.44	4.18	16.5
8	a	1.37	0.77	1.23	0.10	2.01	18.6
	b	1.66	0.95	10.22	0	1.80	17.8
	c	1.82	2.10	10.38	0.55	1.71	16.8
9	a	3.93	2.07	0.00	0.78	9.36	24.7
	b	2.76	1.36	0.00	0.50	9.59	24.8
	c	2.83	1.57	0.00	0.76	9.63	24.3
10	a	4.06	2.22	2.02	1.26	14.1	43.0
	b	3.78	2.07	1.72	0.86	14.3	37.6
	c	3.69	1.98	1.45	1.50	13.8	38.1
11	a	6.05	3.39	2.03	1.55	21.4	54.1
	b	4.78	2.36	2.21	0	22.4	52.4
	c	4.56	2.26	3.36	0.30	22.0	51.7
12	a	6.37	3.43	2.30	9.26	51.7	76.4
	b	7.31	4.33	2.73	0.62	55.8	80.6
	c	7.26	3.93	1.76	5.38	51.2	80.5
13	a	8.09	4.33	2.14	2.41	75.3	148
	b	7.09	3.75	1.12	0.52	77.0	147
	c	6.45	3.33	2.43	2.23	75.9	147
14	a	8.67	4.43	2.01	3.86	80.2	226
	b	20.9	4.81	2.05	0	87.3	188
	c	6.98	3.64	1.26	0	79.8	212
15	a	10.5	4.10	1.44	0	135	226
	b	6.41	3.38	na	1.18	135	210
	c	6.96	3.57	0.66	0.00	139	228
16	a	10.5	4.48	1.02	5.13	213	308
	b	5.88	2.90	0	4.94	216	330
	c	4.84	2.45	2.99	0	230	324

na: no data available

bd: below detection limit

App. 2.6a: Results of batch experiments with Bw-horizon exposed to IHP

grade of P addition	replication	pH	electrical conductivity	turbidity	optical density	zeta potential	particle size
			µS cm^{-1}	FNU	extinction	mV	nm
0	a	4.33	598	bd	bd	-6	na
	b	4.22	600	bd	bd	na	na
	c	4.29	595	0.68	bd	-16.4	na
1	a	4.79	574	1.64	bd	-20.1	na
	b	4.56	692	1.6	bd	-20.3	na
	c	4.76	595	bd	bd	1.02	na
2	a	4.82	589	2.58	bd	-19.8	na
	b	4.67	583	3.45	bd	-17.6	na
	c	4.67	594	3.66	bd	-19.4	na
3	a	4.94	594	27.7	0.0452	-19.7	1459
	b	4.92	na	29.5	0.0475	-20.3	1459
	c	4.9	600	26.0	0.0371	-24	6673
4	a	5.23	629	10.6	0.0174	-13	3120
	b	5.14	623	19.2	0.0341	-14.9	2567
	c	na	na	na	na	na	na
5	a	5.59	634	49.3	0.0703	-37	303
	b	5.56	641	45.9	0.0674	-28.8	319
	c	5.59	637	49.3	0.0683	-40.2	2674
6	a	5.75	673	53.6	0.0779	-42.1	876
	b	5.83	673	52.4	0.0768	-44.6	654
	c	5.87	674	59.7	0.0873	-46	269
7	a	5.97	725	54.0	0.0791	-43.8	463
	b	5.95	724	55.5	0.0835	-47.1	259
	c	5.83	724	50.6	0.0775	-44.5	278
8	a	5.93	823	53.7	0.0789	-41.6	479
	b	5.89	824	58.3	0.0826	-41	303
	c	5.95	822	64.3	0.0909	-44.9	625
9	a	5.8	1072	57.3	0.0862	-43.7	287
	b	5.81	1074	31.3	0.0595	-43.6	319
	c	5.73	1075	50.0	0.0776	-44.1	278

na: no data available

bd: below detection limit

FNU: Formazin nephelometric units

App. 2.6b: Results of batch experiments with Bw-horizon exposed to IHP

grade of P addition	replication	colloidal Al	colloidal Fe	colloidal C	colloidal P	dissolved P	added P
		mg l^{-1}					
0	a	0	0	0	0	0.06	bd
	b	0	0	0	0	0.09	bd
	c	0	0.03	0	0	0.06	bd
1	a	0	0.07	1.72	0	0.03	2.87
	b	0	0.04	0	0	0.07	2.87
	c	0	0	0	0	0.03	2.87
2	a	0	0.26	0	0.16	bd	5.21
	b	0	0.42	0	0.13	0.02	5.21
	c	0	0.58	0.11	0.16	0.05	5.21
3	a	0	3.35	na	1.38	0.07	7.55
	b	0	2.51	na	0.60	0.06	7.55
	c	0	2.81	na	0.97	0.09	7.55
4	a	0	1.05	1.90	1.03	0.13	14.8
	b	0	2.05	2.44	1.80	0.16	15.0
	c	na	0.00	na	na	na	15.0
5	a	22.3	6.50	10.9	9.16	0.73	22.3
	b	20.5	6.23	12.5	10.8	0.58	23.5
	c	na	6.44	11.9	9.13	0.46	22.7
6	a	19.1	5.25	6.03	3.84	15.5	34.8
	b	31.8	6.43	8.03	5.75	14.0	35.0
	c	22.2	7.64	9.55	5.99	13.4	35.0
7	a	22.7	6.73	11.0	7.60	27.0	48.3
	b	30.4	7.12	9.42	13.2	20.4	49.0
	c	26.9	6.86	8.11	3.88	27.0	49.8
8	a	32.2	5.31	6.02	1.89	53.7	74.0
	b	32.0	7.52	8.70	0	54.6	72.9
	c	26.4	7.15	11.0	0	53.5	73.5
9	a	28.3	7.24	11.1	0	119	133
	b	37.1	5.38	8.38	0	120	134
	c	na	6.99	10.0	0	116	133

na: no data available

bd: below detection limit

App. 2.7a: Results of batch experiments with Bg-horizon exposed to ortho-P

grade of P addition	replication	pH	electrical conductivity	turbidity	optical density	zeta potential	particle size
			µS cm^{-1}	FNU	extinction	mV	nm
0	a	4.29	617	0.07	bd	na	na
	b	4.14	622	bd	bd	-4.8	na
	c	4.26	617	bd	bd	-4.5	na
1	a	4.24	617	0.62	bd	-6	na
	b	4.35	612	bd	bd	-7.1	na
	c	4.3	613	0.72	bd	-17.5	na
2	a	4.36	609	1.58	bd	-27.9	na
	b	4.26	615	1.94	bd	3.4	na
	c	4.25	613	bd	bd	-15.1	na
3	a	4.37	607	4.44	bd	-14.7	3120
	b	4.39	608	4.16	bd	-14.8	na
	c	4.41	609	5.18	bd	-13.8	na
4	a	4.55	607	7.74	0.0116	-14.9	3120
	b	4.55	603	30.8	0.0491	-14.3	3120
	c	4.66	602	13.5	0.0192	-13	1879
5	a	4.58	604	19.6	0.0286	-12.7	2669
	b	4.64	603	11.6	0.0166	-38.1	2421
	c	4.6	600	22.0	0.0307	-38.7	3120
6	a	4.55	607	35.6	0.0504	-38.1	na
	b	4.56	606	30.2	0.0384	-39.3	1287
	c	4.63	602	37.2	0.0551	-36.3	1225
7	a	4.58	607	25.9	0.0394	-42.3	2576
	b	4.5	609	35.2	0.0491	-42.4	871
	c	4.71	605	63.3	0.0914	-41.8	2567
8	a	4.61	618	58.2	0.0737	-42	1539
	b	4.51	619	65.0	0.0890	-33.7	1460
	c	4.57	619	65.4	0.0866	-32.3	1619
9	a	4.72	646	85.5	0.1029	-23.4	613
	b	4.64	646	76.7	0.0975	-25.1	853
	c	4.72	647	81.0	0.1079	-25.2	1159

na: no data available

bd: below detection limit

FNU: formazin nephelometric units

App. 2.7b: Results of batch experiments with Bg-horizon exposed to ortho-P

grade of P addition	replication	colloidal Al	colloidal Fe	colloidal C	colloidal P	dissolved P	added P
		mg l^{-1}					
0	a	na	0.03	0	na	0.02	bd
	b	na	0	0	na	0.06	bd
	c	na	0.06	0	na	0.01	bd
1	a	na	0.03	0	na	0.05	2.79
	b	na	0.04	0.08	na	0.04	2.83
	c	na	0.10	0	na	0.03	2.73
2	a	na	0.20	0	na	0.11	5.58
	b	na	0.24	0	na	0.10	5.63
	c	na	0.11	0	na	0.09	5.63
3	a	na	0.45	0.34	na	0.24	7.95
	b	na	0.42	0	na	0.25	7.91
	c	na	0.47	0	na	0.23	8.13
4	a	na	0.79	0	na	2.20	15.13
	b	na	4.03	1.00	na	2.29	15.4
	c	na	1.64	0.21	na	2.16	14.9
5	a	na	2.31	0.35	na	7.68	23.0
	b	na	1.37	0	na	7.61	23.2
	c	na	2.77	0.69	na	7.30	22.9
6	a	na	4.52	1.39	na	19.5	38.2
	b	na	3.53	1.47	na	19.2	37.9
	c	na	4.52	1.89	na	18.7	37.3
7	a	na	2.40	1.40	na	31.8	50.5
	b	na	2.80	2.22	na	32.6	50.4
	c	na	5.79	3.66	na	32.2	49.9
8	a	na	3.38	3.59	na	59.2	74.0
	b	na	3.98	3.70	na	57.8	74.0
	c	na	3.79	3.84	na	58.9	73.5
9	a	na	4.66	3.74	na	125	138
	b	na	4.45	0.86	na	137	140
	c	na	4.88	0.99	na	129	140

na: no data available

bd: below detection limit

App. 2.8a: Results of batch experiments with Bg-horizon exposed to IHP

grade of P addition	replication	pH	electrical conductivity	turbidity	optical density	zeta potential	particle size
			µS cm^{-1}	FNU	extinction	mV	nm
0	a	4.26	618	bd	bd	1.1	na
	b	4.15	621	bd	bd	-0.8	na
	c	4.22	620	bd	bd	0.4	na
1	a	4.35	618	bd	bd	-5.9	na
	b	4.36	619	bd	bd	-3.8	na
	c	4.49	619	bd	bd	-0.6	na
2	a	4.52	619	bd	bd	-5.3	na
	b	4.53	623	bd	bd	-7.4	na
	c	4.56	621	bd	bd	-0.8	na
3	a	4.52	627	bd	bd	-6.5	na
	b	4.53	625	0.64	bd	-3.1	na
	c	4.54	628	0.87	bd	-7.6	na
4	a	4.72	644	2.84	bd	-16.2	na
	b	4.54	643	3.57	bd	-9.8	na
	c	4.59	645	2.27	bd	-11	na
5	a	4.82	661	4.68	bd	-21.4	na
	b	4.53	667	2.68	bd	-11.4	na
	c	4.6	662	4.53	bd	-23.7	na
6	a	5.22	684	109	0.1539	-31.4	na
	b	5.33	686	83.7	0.2776	-30.6	na
	c	4.94	687	3.2	bd	-19.2	na
7	a	5.48	721	62.1	0.0863	-19.6	na
	b	5.48	739	83.7	0.1138	-21.8	na
	c	5.45	723	50.9	0.0732	-40.4	na
8	a	5.64	812	80.7	0.1176	-15	483
	b	5.63	814	104	0.1407	-56.3	329
	c	5.52	819	54.6	0.0768	-7.6	278
9	a	5.6	1063	103	0.1472	-46.8	876
	b	5.51	1066	40.6	0.0589	-46	260
	c	5.31	1091	115	0.1675	-49	278

na: no data available

bd: below detection limit

FNU: formazin nephelometric units

App. 2.8b: Results of batch experiments with Bg-horizon exposed to IHP

grade of P addition	replication	colloidal Al	colloidal Fe	colloidal C	colloidal P	dissolved P	added P
		mg l^{-1}					
0	a	na	0	0	0	0.05	bd
	b	na	0	0	0.02	bd	bd
	c	na	0	0	0	bd	bd
1	a	na	0	0	0	0.01	3.14
	b	na	0	0.46	0	0.03	2.95
	c	na	0	0	0	bd	2.94
2	a	na	0	0	0	0.04	5.83
	b	na	0	0	0	bd	5.76
	c	na	0	0	0	0.01	5.84
3	a	na	0	0.30	0	bd	6.12
	b	na	0	0	0	0.04	6.65
	c	na	0	0	0	0.01	6.62
4	a	na	0.08	0	0	0.07	15.7
	b	na	0.14	1.11	0	0.10	16.2
	c	na	0.04	0.92	0	0.07	14.4
5	a	na	0.15	0.70	0	0.30	23.7
	b	na	0.12	0	0	0.32	22.7
	c	na	0.23	0	0	0.35	24.3
6	a	na	5.42	0.36	5.11	0.77	37.4
	b	na	5.91	0.47	5.63	0.94	32.7
	c	na	0.04	0.63	0	0.96	38.8
7	a	na	3.21	0	4.01	13.6	51.6
	b	na	4.02	5.22	8.16	11.9	46.2
	c	na	2.47	0.94	3.96	10.1	50.9
8	a	na	4.66	0.14	4.80	40.4	70.3
	b	na	5.44	0	15.71	35.9	77.4
	c	na	3.75	2.32	5.45	33.9	78.0
9	a	na	na	32.76	0	107	155
	b	na	5.91	5.85	0	107	213
	c	na	5.93	18.80	6.78	105	153

na: no data available

bd: below detection limit

Chapter 3: Colloidal and dissolved phosphorus in sandy soils as affected by phosphorus saturation

App 3.1a: Results of batch experiments - Nienburg, 0-30 cm

variant	treatment	replication	electrical conductivity	zeta potential	pH
	kg P ha^{-1} a^{-1}		µS cm^{-1}	mV	H_20
1	0 kg	a	63.0	-21.30	6.1
		b	67.1	-19.73	
		c	57.3	-28.37	
		d	61.7	-21.00	
2	48 (Phosphatkali "R")	a	72.7	-23.27	6.5
		b	70.0	-20.60	
		c	63.9	-33.00	
		d	73.6	33.00	
3	48 (Thomaskali)	a	61.7	-26.10	6.2
		b	59.6	-25.40	
		c	66.6	-25.50	
		d	65.2	-27.50	
4	96 (Phosphatkali "R")	a	78.7	-21.70	6.4
		b	69.9	-21.03	
		c	74.9	-22.50	
		d	68.9	-21.80	
5	96 (Thomaskali)	a	59.4	-21.73	6.4
		b	77.8	-28.60	
		c	70.2	-21.30	
		d	57.8	-20.30	
6	144 (Thomaskali)	a	69.2	-36.53	6.5
		b	65.6	-21.07	
		c	73.1	-20.90	
		d	72.8	-34.03	

App 3.1b: Results of batch experiments - Nienburg, 0-30 cm

variant	replication	colloidal P	dissolved P	oxalate-extractable P	oxalate-extractable Fe	oxalate-extractable Al
				mg kg^{-1}		
1	a	1.8	0.99	230	973	1825
	b	2.2	1.15	357	1140	2685
	c	1.9	0.97	233	668	1620
	d	1.8	1.43	264	813	1860
2	a	1.2	2.64	368	896	1775
	b	1.6	2.88	248	884	1640
	c	1.2	2.03	239	851	1860
	d	1.9	2.79	520	989	2260
3	a	2.0	1.49	271	946	2025
	b	1.9	1.27	294	887	1970
	c	2.3	1.55	353	864	2085
	d	1.7	1.29	272	896	2125
4	a	1.9	1.93	450	847	1845
	b	1.0	3.20	280	859	1885
	c	2.5	2.87	372	982	1690
	d	1.2	2.77	360	na	2255
5	a	0.9	3.00	325	939	2070
	b	2.5	1.00	377	1012	2265
	c	2.2	2.77	340	840	1460
	d	0.6	2.88	359	627	1535
6	a	1.3	1.81	421	880	1980
	b	0.0	5.52	374	887	1885
	c	0.0	4.02	687	942	2315
	d	1.2	3.94	358	905	1625

App 3.2a: Results of batch experiments - Nienburg, 30-60 cm

variant	treatment	replication	electrical conductivity	zeta potential	particle size	pH
	kg P ha^{-1} a^{-1}		µS cm^{-1}	mV	nm	H_20
1	0 kg	a	32.2	-30.0	199	5.4
		b	30.7	-24.3	210	
		c	31.9	-32.2	206	
		d	30.6	-28.8	205	
2	48 (Phosphatkali "R")	a	29.3	-31.3	228	5.6
		b	26.9	-28.6	224	
		c	29.2	-36.6	264	
		d	29.5	-29.9	259	
3	48 (Thomaskali)	a	29.2	-28.9	212	5.8
		b	33.6	-23.5	197	
		c	30.3	-23.7	212	
		d	37.5	-24.7	195	
4	96 (Phosphatkali "R")	a	na	na	na	4.9
		b	na	na	na	
		c	31.1	-27.7	231	
		d	33.8	-24.2	211	
5	96 (Thomaskali)	a	29.3	-33.6	207	5.2
		b	27.9	-28.2	238	
		c	29.3	-27.4	199	
		d	29.1	-37.8	218	
6	144 (Thomaskali)	a	26.6	-38.4	229	5.4
		b	29.2	-28.1	210	
		c	32.6	-25.3	204	
		d	35.3	-22.8	185	

na: no data available

App 3.2b: Results of batch experiments - Nienburg, 30-60 cm

variant	replication	colloidal P	dissolved P	oxalate-extractable P	oxalate-extractable Fe	oxalate-extractable Al
				mg kg^{-1}		
1	a	1.10	0.14	26.6	601	1385
	b	1.30	0.16	56.6	548	1765
	c	1.17	0.11	18.6	543	1205
	d	1.28	0.13	34.9	472	1290
2	a	1.78	0.10	58.5	340	1360
	b	1.50	0.07	21.8	645	1315
	c	1.58	0.07	35.5	543	960
	d	2.18	0.09	na	245	1295
3	a	1.29	0.10	36.5	706	1135
	b	1.32	0.12	23.7	401	1275
	c	1.58	0.13	45.9	356	1215
	d	1.53	0.10	38.3	449	1655
4	a	na	na	na	na	na
	b	na	na	31.5	684	895
	c	1.95	0.05	42.1	473	1390
	d	1.87	nn	55.6	463	1535
5	a	1.9	nn	23.8	570	670
	b	1.9	0.06	38.1	708	925
	c	1.3	0.07	32.6	334	1180
	d	1.8	bd	na	na	na
6	a	1.5	bd	57.5	419	945
	b	1.4	0.11	31.7	640	1100
	c	1.8	0.14	76.6	402	2025
	d	2.6	0.33	102.3	292	2075

na: no data available

bd: below detection limit

App 3.3a: Results of batch experiments - Nienburg, 60-90 cm

variant	treatment	replication	electrical conductivity	zeta potential	particle size	pH
	kg P ha^{-1} a^{-1}		µS cm^{-1}	mV	nm	H_20
1	0 kg	a	23.5	-30.20	243.2	4.7
		b	24.3	-33.10	344.8	
		c	27.1	-36.10	243.9	
		d	20.9	-33.40	240.6	
2	48 (Phosphatkali "R")	a	25.7	-31.70	226.5	4.8
		b	23.5	-33.40	212.9	
		c	26.3	-34.30	314.6	
		d	25.0	-32.50	231.5	
3	48 (Thomaskali)	a	23.7	-33.60	243.8	na
		b	25.8	-30.20	236.8	
		c	25.4	-33.10	247.4	
		d	24.3	-36.60	245.8	
4	96 (Phosphatkali "R")	a	29.9	-24.50	211.6	na
		b	23.0	-34.10	247.2	
		c	27.2	-30.10	279.8	
		d	29.8	-29.30	205.4	
5	96 (Thomaskali)	a	21.3	-33.30	234.1	5.0
		b	22.6	-35.80	249.8	
		c	20.2	-34.00	220.0	
		d	23.6	-32.70	231.7	
6	144 (Thomaskali)	a	21.6	-30.40	241.7	na
		b	22.0	na	na	
		c	25.9	-29.50	242.2	
		d	23.8	-28.40	210.7	

na: no data available

App 3.3b: Results of batch experiments - Nienburg, 60-90 cm

variant	replication	colloidal P	dissolved P	oxalate-extractable P	oxalate-extractable Fe	oxalate-extractable Al
				mg kg^{-1}		
1	a	0.80	0.108	20.12	819	595
	b	0.46	0.241	38.84	1063	825
	c	0.99	0.133	38.28	1578	795
	d	0.68	0.149	20.91	925	560
2	a	0.88	0.220	40.45	1249	810
	b	0.60	0.133	14.72	901	730
	c	0.19	0.230	37.37	1054	523
	d	0.73	0.215	38.88	1222	595
3	a	0.29	0.416	36.97	na	na
	b	0.63	0.246	na	1020	660
	c	0.80	0.191	31.14	1007	565
	d	0.22	0.254	24.64	1029	730
4	a	0.42	0.201	na	na	na
	b	1.42	0.175	28.13	913	560
	c	0.81	0.238	18.14	1068	665
	d	1.09	na	37.45	1281	945
5	a	1.1	0.141	34.33	1147	590
	b	1.3	0.131	18.99	870	660
	c	0.6	0.149	11.09	1099	550
	d	1.3	0.123	32.41	1379	535
6	a	0.8	0.136	na	na	na
	b	0.4	0.251	14.16	899	480
	c	0.8	0.256	32.04	1103	800
	d	0.7	0.152	15.56	988	940

na: no data available

App. 3.4: Results of batch experiments - Hamburg, 0-30 cm

variant	treatment	replication	electrical conductivity	zeta potential	particle size	pH
	kg P ha^{-1} a^{-1}		µS cm^{-1}	mV	nm	H_20
1	0	a	41.3	-20.00	317	6.3
		b	45.9	-22.07	286	
		c	31.4	-22.67	360	
		d	42.4	-22.03	308	
2	50 (Triplephosphate)	a		-23.00	293	6.5
		b	41.4	-19.40	353	
		c	47.4	-22.23	257	
		d	41.2	-20.87	283	
3	50 (Thomaskalk)	a	38.6	-22.77	239	6.6
		b	39.9	-20.33	211	
		c	44.2	-21.10	219	
		d	38.4	-20.60	219	
4	100 (Triplephosphate)	a	45.1	-18.00	209	6.5
		b	42.0	-18.57	221	
		c	44.2	-21.57	222	
		d	42.1	-23.20	221	
5	100 (Thomaskalk)	a	56.1	-19.73	227	6.5
		b	46.3	-18.63	213	
		c	45.3	-20.13	224	
		d	48.7	-20.20	220	

variant	replication	colloidal P	dissolved P	oxalate-extractable P	oxalate-extractable Fe	oxalate-extractable Al
				mg kg^{-1}		
1	a	0.05	8.31	301	1647	1140
	b	0.49	7.81	237	1091	810
	c	1.13	10.00	281	2021	910
	d	0.57	8.67	271	2467	915
2	a	0.29	10.71	255	1753	735
	b	0.30	9.90	183	2170	900
	c	0.17	10.01	298	1997	975
	d	0.84	7.93	243	1934	935
3	a	1.45	8.63	238	1818	690
	b	3.49	8.20	274	1821	880
	c	3.37	7.85	264	1890	925
	d	3.84	9.39	261	1961	885
4	a	3.20	13.45	294	2031	785
	b	4.83	11.97	380	2095	990
	c	2.90	12.03	329	2242	1060
	d	3.01	10.97	328	1821	805
5	a	1.6	12.19	282	1926	745
	b	3.7	12.98	322	2131	925
	c	3.5	10.70	290	1835	900
	d	4.3	14.38	314	2272	940

App. 3.5: Results of batch experiments - Hamburg, 30-60 cm

variant	treatment	replication	electrical conductivity	zeta potential	particle size	pH
	kg P ha^{-1} a^{-1}		µS cm^{-1}	mV	nm	H_20
1	0	a	29.9	-23.0	192	6.3
		b	25.1	-22.4	198	
		c	26.2	-21.3	1554	
		d	27.3	-22.1	382	
2	50 (Triplephosphate)	a	31.4	-20.3	236	6.1
		b	26.3	-20.1	219	
		c	27.0	-20.3	219	
		d	26.5	-21.4	218	
3	50 (Thomaskalk)	a	25.0	-21.6	222	5.7
		b	26.5	-19.3	1317	
		c	29.0	-21.1	223	
		d	27.2	-22.5	213	
4	100 (Triplephosphate)	a	27.1	-20.2	207	6.3
		b	24.8	-20.6	215	
		c	28.3	-21.1	208	
		d	25.9	-23.5	222	
5	100 (Thomaskalk)	a	27.1	-21.4	201	6.2
		b	28.8	-21.4	201	
		c	26.6	-23.1	190	
		d	28.1	-20.0	204	

variant	replication	colloidal P	dissolved P	oxalate-extractable P	oxalate-extractable Fe	oxalate-extractable Al
				mg kg^{-1}		
1	a	2.89	0.182	77	1462	1085
	b	3.45	0.138	90	1315	1165
	c	5.50	0.406	91	1433	1100
	d	5.95	0.102	106	1373	1295
2	a	6.49	0.374	117	2346	1000
	b	5.66	bd	95	1490	1150
	c	5.40	bd	102	1244	1205
	d	5.86	0.155	87	1441	1085
3	a	4.97	bd	68	1458	905
	b	4.16	bd	58	1288	1155
	c	5.10	bd	56	1184	975
	d	5.00	bd	68	1236	1025
4	a	5.37	0.534	88	1183	1055
	b	5.67	bd	70	1410	1240
	c	5.54	bd	80	1237	1130
	d	5.54	bd	96	1236	1290
5	a	6.1	0.532	85	1358	910
	b	5.3	bd	70	1215	965
	c	5.7	bd	86	1426	1100
	d	6.2	0.087	108	1524	1325

bd: below detection limit

App. 3.6: Results of batch experiments - Hamburg, 60-90 cm

variant	treatment	replication	electrical conductivity	zeta potential	particle size	pH
	kg P ha^{-1} a^{-1}		µS cm^{-1}	mV	nm	H_20
1	0	a	21.0	-25.3	264	5.1
		b	17.9	-26.5	229	
		c	22.2	-29.7	245	
		d	15.6	-30.5	219	
2	50 (Triplephosphate)	a	18.3	-29.1	208	na
		b	23.3	-27.0	238	
		c	18.8	-28.0	247	
		d	18.8	-26.5	259	
3	50 (Thomaskalk)	a	27.7	-20.6	337	na
		b	23.5	-23.7	315	
		c	22.3	-24.9	303	
		d	20.3	-27.2	225	
4	100 (Triplephosphate)	a	28.1	-26.6	336	5.7
		b	24.4	-26.1	336	
		c	18.6	-29.3	223	
		d	17.3	-26.8	241	
5	100 (Thomaskalk)	a	20.4	-22.1	205	5.2
		b	26.9	-12.9	312	
		c	14.9	-28.3	201	
		d	13.7	-31.2	203	

variant	replication	colloidal P	dissolved P	oxalate-extractable P	oxalate-extractable Fe	oxalate-extractable Al
				mg kg^{-1}		
1	a	0.26	0.11	35.1	1229	670
	b	1.81	0.07	48.3	857	645
	c	1.62	0.30	70.1	2096	930
	d	2.53	bd	55.3	657	590
2	a	2.98	0.05	44.1	859	870
	b	1.97	0.05	55.5	1311	715
	c	2.37	bd	43.9	886	520
	d	2.19	bd	74.1	1595	675
3	a	0.10	0.09	32.5	1278	1125
	b	0.16	bd	52.9	1474	865
	c	0.76	bd	56.9	1119	720
	d	2.52	0.05	60.0	1237	810
4	a	0.86	bd	42.8	506	495
	b	0.24	bd	49.3	1323	670
	c	3.57	0.06	48.0	1413	845
	d	2.90	bd	41.0	708	575
5	a	3.4	bd	76.1	1142	815
	b	0.2	bd	62.0	1990	875
	c	1.7	bd	87.4	1663	1175
	d	2.0	0.07	51.6	681	600

bd: below detection limit

App. 3.7: Results of batch experiments - Dülmen old, 0-30 cm

variant	treatment	replication	electrical conductivity	zeta potential	particle size	pH
	kg P ha^{-1} a^{-1}		µS cm^{-1}	mV	nm	H_20
1	0	a	35.4	-23.9	252	6.4
		b	35.2	-20.4	242	
		c	35.3	-20.3	240	
		d	101.0	-17.4	258	
2	stable manure	a	45.9	-21.5	241	6.6
		b	62.0	-20.6	214	
		c	65.0	-14.4	222	
		d	na	-25.1	231	
3	39 (Thomasphosphate)	a	100.0	-21.3	233	7.0
		b	65.8	-18.5	217	
		c	68.6	-20.8	275	
		d	63.0	-18.1	240	
4	39 (Thomasphosphate) + stable manure	a	87.0	-23.0	215	7.2
		b	83.2	-35.5	213	
		c	66.0	-20.8	235	
		d	120.0	-19.3	193	

variant	replication	colloidal P	dissolved P	oxalate-extractable P	oxalate-extractable Fe	oxalate-extractable Al
				mg kg^{-1}		
1	a	3.28	6.26	229	2470	460
	b	2.74	10.12	285	3115	680
	c	3.68	7.25	221	2680	460
	d	3.65	12.96	267	3025	625
2	a	0.99	14.27	422	3380	725
	b	4.90	22.22	455	3105	720
	c	3.79	17.87	345	3005	700
	d	7.53	19.02	482	2775	675
3	a	4.25	8.59	651	3320	1125
	b	2.59	20.09	454	3540	875
	c	11.82	14.40	560	3190	975
	d	9.80	26.08	519	3655	725
4	a	4.03	26.68	322	2555	465
	b	6.67	31.63	747	3580	765
	c	3.13	26.37	522	2760	540
	d	7.20	34.08	588	3645	715

App. 3.8: Results of batch experiments - Dülmen old, 30-60 cm

variant	treatment	replication	electrical conductivity	zeta potential	particle size	pH
	kg P ha^{-1} a^{-1}		µS cm^{-1}	mV	nm	H_20
1	0	a	46.0	-27.2	264	6.3
		b	55.0	-22.6	204	
		c	27.4	-17.8	182	
		d	61.0	-21.1	213	
2	stable manure	a	55.0	-20.7	211	6.0
		b	55.0	-25.1	270	
		c	52.0	-23.2	185	
		d	50.0	-24.6	184	
3	39 (Thomasphosphate)	a	39.9	-24.2	177	6.3
		b	67.0	-22.9	206	
		c	38.0	-24.0	259	
		d	64.0	-21.8	221	
4	39 (Thomasphosphate) + stable manure	a	68.0	-23.2	210	6.9
		b	76.0	-23.2	312	
		c	28.4	na	215	
		d	52.1	-18.9	223	

variant	replication	colloidal P	dissolved P	oxalate-extractable P	oxalate-extractable Fe	oxalate-extractable Al
				mg kg^{-1}		
1	a	2.59	0.47	243	2900	1250
	b	1.25	0.31	95	3075	1710
	c	6.84	0.16	42	2135	745
	d	1.42	0.46	70	3150	1005
2	a	7.01	2.60	193	3145	990
	b	1.92	3.52	222	3875	1975
	c	5.90	3.52	190	2955	925
	d	4.81	1.33	169	2740	1140
3	a	10.84	0.46	314	3870	2230
	b	5.85	0.93	164	2895	1500
	c	5.97	0.76	325	3685	2100
	d	6.04	1.18	111	3325	1160
4	a	10.65	13.35	342	1790	1260
	b	8.86	6.79	384	4345	1575
	c	5.81	2.65	179	2225	870
	d	7.09	20.38	308	2485	805

na: no data available

App. 3.9: Results of batch experiments - Dülmen old, 60-90 cm

variant	treatment	replication	electrical conductivity	zeta potential	particle size	pH
	kg P ha^{-1} a^{-1}		µS cm^{-1}	mV	nm	H_20
1	0	a	20.9	-51.73	187.3	5.5
		b	19.0	-30.23	184.5	
		c	16.3	-25.87	188.0	
		d	19.0	-29.63	182.4	
2	stable manure	a	22.5	-22.83	182.4	5.4
		b	20.3	-27.03	171.2	
		c	16.9	-27.53	176.8	
		d	17.5	-25.23	180.0	
3	39 (Thomasphosphate)	a	21.0	-30.27	205.1	na
		b	21.9	-28.73	186.9	
		c	31.0	-25.03	207.2	
		d	26.4	-26.6	195.4	
4	39 (Thomasphosphate) + stable manure	a	36.6	-23.67	169.6	na
		b	22.2	-30.27	176.8	
		c	31.6	-27.83	177.2	
		d	28.7	-24.93	182.0	

variant	replication	colloidal P	dissolved P	oxalate-extractable P	oxalate-extractable Fe	oxalate-extractable Al
				mg kg^{-1}		
1	a	4.11	bd	83	6075	1515
	b	3.68	bd	73	3180	855
	c	9.43	bd	49	3195	725
	d	5.37	0.051	33	3140	860
2	a	2.83	bd	56	3505	1225
	b	4.64	bd	98	2990	800
	c	2.19	0.088	20	1970	550
	d	2.18	0.244	29	1140	580
3	a	4.08	bd	79	2275	635
	b	2.95	bd	72	3600	830
	c	3.06	0.091	126	4365	770
	d	0.81	0.078	121	3530	560
4	a	4.97	0.129	172	4890	1175
	b	11.22	0.097	155	2585	820
	c	5.45	0.083	41	3490	630
	d	4.29	0.563	57	1480	440

na: no data available

bd: below detection limit

App. 3.10: Results of batch experiments - Dülmen new, 0-30 cm

variant	treatment	replication	electrical conductivity	zeta potential	particle size	pH
	kg P ha^{-1} a^{-1}		µS cm^{-1}	mV	nm	H_20
1	43 (maize), 34 (wheat, barley), triplephosphate	a	57.2	-20.58	231.7	6.7
		b	67.0	-19.3	205.7	
		c	78.4	-17.15	222.3	
2	43 (maize), 34 (wheat, barley), triplephosphate	a	53.9	-17.83	245.2	6.8
		b	69.4	-17.37	241.0	
		c	71.0	-17.73	273.1	
3	43 (maize), 34 (wheat, barley), triplephosphate + stable manure	a	73.6	-19.7	234.1	6.8
		b	82.0	-17.47	201.9	
		c	90.0	-19.6	223.9	
4	43 (maize), 34 (wheat, barley), triplephosphate + stable manure	a	61.2	-18.63	226.0	6.8
		b	69.0	-20.73	225.0	
		c	77.6	-17.92	240.7	

variant	replication	colloidal P	dissolved P	oxalate-extractable P	oxalate-extractable Fe	oxalate-extractable Al
				mg kg^{-1}		
1	a	8.12	16.1	356	2915	475
	b	3.85	17.1	311	2865	660
	c	8.70	18.0	398	2755	440
2	a	4.21	17.8	375	3185	690
	b	7.52	18.6	481	3500	715
	c	4.96	19.9	421	3465	695
3	a	7.94	19.4	419	3050	655
	b	5.11	20.7	383	2925	700
	c	5.68	25.1	629	3495	690
4	a	10.54	23.8	396	2850	545
	b	6.90	21.3	512	3250	680
	c	11.74	24.1	511	3010	550

App. 3.11: Results of batch experiments - Dülmen new, 30-60 cm

variant	treatment	replication	electrical conductivity	zeta potential	particle size	pH
	kg P ha^{-1} a^{-1}		µS cm^{-1}	mV	nm	H_20
1	43 (maize), 34 (wheat, barley), triplephosphate	a	87.0	-27.9	218	6.8
		b	62.0	-21.7	192	
		c	45.9	-25.4	222	
2	43 (maize), 34 (wheat, barley), triplephosphate	a	34.3	-33.6	209	6.7
		b	29.9	-25.1	206	
		c	33.6	-23.0	197	
3	43 (maize), 34 (wheat, barley), triplephosphate + stable manure	a	58.0	-24.4	208	6.8
		b	69.0	-22.2	172	
		c	42.1	-25.8	182	
4	43 (maize), 34 (wheat, barley), triplephosphate + stable manure	a	61.0	-25.8	206	6.8
		b	na	-26.9	199	
		c	45.5	-25.8	191	

variant	replication	colloidal P	dissolved P	oxalate-extractable P	oxalate-extractable Fe	oxalate-extractable Al
				mg kg^{-1}		
1	a	3.57	0.53	41.1	3215	935
	b	6.18	1.80	40.8	3110	870
	c	5.91	2.89	141	2780	490
2	a	3.77	1.73	82.8	2040	750
	b	1.98	2.16	86.3	2520	685
	c	2.63	0.42	156	5540	1100
3	a	2.85	1.86	63	2390	805
	b	2.88	1.67	119	3460	1045
	c	5.78	3.07	127	2760	455
4	a	5.58	7.29	153	2650	800
	b	3.72	2.58	104	3175	1065
	c	6.65	14.47	120	2165	325

na: no data available

App. 3.12: Results of batch experiments - Dülmen new, 60-90 cm

variant	treatment	replication	electrical conductivity	zeta potential	particle size	pH
	kg P ha^{-1} a^{-1}		µS cm^{-1}	mV	nm	H_20
1	43 (maize), 34 (wheat, barley), triplephosphate	a	23.5	-26.3	183.8	na
		b	90.5	-16.73	374.0	
		c	28.8	-28.63	184.7	
2	43 (maize), 34 (wheat, barley), triplephosphate	a	23.4	-30.2	196.6	6.1
		b	47.1	-18.5	185.4	
		c	32.2	-27.53	188.3	
3	43 (maize), 34 (wheat, barley), triplephosphate + stable manure	a	27.8	-30.63	179.6	na
		b	33.1	-24.93	172.2	
		c	26.0	-26.33	166.9	
4	43 (maize), 34 (wheat, barley), triplephosphate + stable manure	a	25.5	-26.67	191.2	6.7
		b	31.2	-28.03	176.5	
		c	32.0	-24.43	168.8	

variant	replication	colloidal P	dissolved P	oxalate-extractable P	oxalate-extractable Fe	oxalate-extractable Al
				mg kg^{-1}		
1	a	7.12	0.127	21.4	2102	445
	b	7.09	bd	20.8	3170	480
	c	6.92	bd	16.8	3115	640
2	a	2.66	0.224	55.8	2436	580
	b	6.40	0.073	21.6	2188	490
	c	7.60	0.122	49.3	6005	670
3	a	2.93	0.202	43.5	1376	630
	b	3.91	0.072	24.6	2925	735
	c	1.15	0.093	23.9	1793	330
4	a	4.18	0.186	26.4	982	495
	b	3.59	0.152	23.9	1672	590
	c	12.32	bd	17.1	2547	480

na: no data available

bd: below detection limit

App. 3.13: Results of batch experiments - more detailed characterization of randomly selected samples (water extracts), 0-30 cm

variant	electrical conductivity	zeta potential	particle size	pH	optical density
	µS cm^{-1}	mV	nm		extinction
N 2c	60.6	-21.4	260	6.3	0.082
N 5b	62.4	-21.4	272	6.3	0.106
N 6b	59.8	-21.6	256	6.2	0.084
H 2b	39.1	-21.7	257	6.4	0.278
H 2c	47.6	-21.4	263	6.5	0.231
H 3a	41.4	-19.1	240	6.7	0.108
H 4b	34.2	-20	246	6.4	0.146
H 4c	39.6	-22.1	241	6.3	0.120
DA 1b	31.2	-18.8	229	6.3	0.110
DA 1c	34.5	-19	229	6.5	0.322
DA 1d	37.7	-19.3	232	6.6	0.264
DA 2c	55.4	-19.1	237	6.9	0.164
Da 4d	62.8	-20.7	230	6.9	0.244
DN 4a	57.3	-15.3	229	7.0	0.133
DN 4b	51.6	-17.5	229	7.1	0.234
DN 4c	61.4	-19.8	230	6.8	0.239

variant	colloidal P	dissolved P	colloidal C	colloidal Fe	colloidal Al
			mg kg^{-1}		
N 2c	0.80	2.68	251	25.3	64.0
N 5b	0.75	2.83	258	19.3	40.0
N 6b	0.98	2.88	240	15.5	32.0
H 2b	8.26	10.1	165	156	216
H 2c	7.71	9.20	193	97.9	144
H 3a	3.60	12.5	141	43.8	56.0
H 4b	4.63	7.60	140	69.2	88.0
H 4c	4.10	7.72	132	29.3	40.0
DA 1b	3.65	9.15	142	41.0	56.0
DA 1c	10.7	5.91	210	150	176
DA 1d	9.29	9.16	228	100	128
DA 2c	7.12	14.8	185	68.2	96.0
Da 4d	12.5	30.4	199	132	128
DN 4a	5.87	20.8	140	63.6	168
DN 4b	15.0	13.2	172	128	200
DN 4c	12.6	26.3	218	143	176

App. 3.14: Results of batch experiments - more detailed characterization of randomly selected samples (water extracts), 30-60 cm

variant	electrical conductivity	zeta potential	particle size	pH	optical density
	µS cm^{-1}	mV	nm		extinction
N 2c	34.4	-28.1	256	6.6	0.070
N 5b	37.4	-29.1	238	6.0	0.096
N 6b	35	-23.5	307	5.8	0.391
H 2b	27.3	-23	226	6.0	0.289
H 2c	30.8	-21.7	232	5.9	0.216
H 3a	30.3	-24.5	259	6.2	0.221
H 4b	27.5	-22.5	257	6.3	0.175
H 4c	29.8	-21.2	241	6.3	0.277
DA 1b	35.2	-22.7	240	6.3	0.249
DA 1c	30	-22.1	207	6.4	0.353
DA 1d	35.7	-22.2	219	6.2	0.198
DA 2c	39	-21.7	197	6.5	0.110
Da 4d	42.3	-21	234	6.7	0.281
DN 4a	37.3	-20.9	234	6.6	0.183
DN 4b	31.2	-18.3	194	6.7	0.231
DN 4c	64.6	-22.1	208	6.0	0.416

variant	colloidal P	dissolved P	colloidal C	colloidal Fe	colloidal Al
			mg kg^{-1}		
N 2c	0.50	0.282	18.6	17.9	56.0
N 5b	0.35	0.160	31.0	34.5	60.8
N 6b	1.18	0.106	54.1	90.1	269
H 2b	5.17	0.275	65.7	120	235
H 2c	3.92	0.226	51.7	76.1	148
H 3a	3.89	0.728	57.6	65.3	132
H 4b	2.94	0.265	25.2	84.5	159
H 4c	na	8.95	37.4	95.2	191
DA 1b	1.53	0.503	80.7	71.4	126
DA 1c	6.32	0.374	106	104	256
DA 1d	3.52	0.533	67.4	102	114
DA 2c	4.77	0.802	59.4	54.3	64.0
Da 4d	9.79	2.83	252	132	177
DN 4a	4.33	1.46	64.1	62.6	96.0
DN 4b	na	19.9	na	176	123
DN 4c	7.67	0.421	14.6	120	322

na: no data available

App. 3.15: Results of batch experiments - more detailed characterization of randomly selected samples (water extracts), 60-90 cm

variant	electrical conductivity	zeta potential	particle size	pH	optical density
	µS cm^{-1}	mV	nm		extinction
N 2c	40.0	-30.4	266	5.2	0.765
N 5b	35.5	-33.1	247	5.3	0.339
N 6b	33.6	-31.6	258	5.4	0.247
H 2b	30.3	-24.7	291	5.6	0.185
H 2c	23.3	-27.5	294	5.9	0.127
H 3a	18.0	-31.5	226	6.0	0.086
H 4b	29.1	-19.3	352	5.8	0.012
H 4c	28.2	-22.9	364	5.9	0.087
DA 1b	22.1	-27.7	206	5.6	0.448
DA 1c	24.2	-27.8	214	5.8	1.14
DA 1d	22.3	-29.1	204	5.3	0.875
DA 2c	30.4	-24.9	228	5.9	0.155
Da 4d	34.1	-22.7	219	6.1	0.161
DN 4a	30.1	-26	216	6.7	0.135
DN 4b	35.2	-25	212	6.7	0.462
DN 4c	32.6	-25.1	220	6.8	1.137

variant	colloidal P	dissolved P	colloidal C	colloidal Fe	colloidal Al
			mg kg^{-1}		
N 2c	4.79	0.478	72.0	47.6	970
N 5b	1.80	0.089	10.1	275	433
N 6b	1.93	na	bd	204	360
H 2b	1.82	na	5.12	136	174
H 2c	1.41	0.209	5.36	95.9	128
H 3a	1.46	0.105	3.52	67.9	90.4
H 4b	0.22	0.081	1.36	13.7	6.40
H 4c	0.69	0.139	4.96	52.5	64.8
DA 1b	4.46	0.144	41.3	381	332
DA 1c	10.5	0.120	144	81.5	837
DA 1d	6.45	0.081	7.04	43.8	593
DA 2c	3.30	0.235	33.7	149	96.0
Da 4d	2.69	1.17	5.20	134	76.0
DN 4a	2.37	0.225	44.6	150	71.2
DN 4b	2.85	0.178	57.6	23.6	219
DN 4c	6.02	0.217	99.5	106	713

na: no data available

bd: below detection limit

App. 3.16: Results of batch experiments - comparison of water and KCl extracts of randomly selected samples, 0-30 cm

Water extracts

variant	electrical conductivity	zeta potential	particle size	pH	optical density
	µS cm^{-1}	mV	nm		extinction
H 2b	44.0	-25.5	357	6.2	0.329
DA 1b	36.7	-38.9	255	6.1	0.201
DA 4a	65.5	-38.2	261	6.7	0.138
DN 4a	62.1	-23.6	234	7.0	0.121
DN 4a	74.0	-31.1	241	7.0	0.200

Water extracts

variant	colloidal P	dissolved P	colloidal C	colloidal Fe	colloidal Al
			mg kg^{-1}		
H 2b	10.8	15.4	98.5	50.0	102
DA 1b	4.68	7.9	57.0	35.3	54.4
DA 4a	5.93	28.6	45.9	32.9	53.6
DN 4a	17.5	4.5	33.0	30.3	47.2
DN 4a	7.47	26.9	79.0	53.6	83.2

KCl extracts

variant	electrical conductivity	zeta potential	particle size	pH	optical density
	µS cm^{-1}	mV	nm		extinction
H 2b	1446	-17.7	268	6.5	357
DA 1b	1425	-19.5	307	5.9	255
DA 4a	1444	-21.1	na	6.4	261
DN 4a	1440	-18.5	292	6.5	234
DN 4a	1438	-17.8	307	6.4	241

KCl extracts

variant	colloidal P	dissolved P	colloidal C	colloidal Fe	colloidal Al
			mg kg^{-1}		
H 2b	3.29	4.86	27.2	20.8	36.0
DA 1b	2.49	3.03	10.3	16.8	15.2
DA 4a	5.52	17.0	20.4	21.6	17.6
DN 4a	6.01	12.2	27.3	35.9	49.6
DN 4a	6.54	16.8	42.0	39.1	45.6

na: no data available

App. 3.17: Results of batch experiments - comparison of water and KCl extracts of randomly selected samples, 30-60 cm

Water extracts

variant	electrical conductivity	zeta potential	particle size	pH	optical density
	µS cm^{-1}	mV	nm		extinction
N 5b	34.2	-46.2	354	6.2	0.106
N 2c	28	-42.1	266	6.1	0.260
DA 1d	32	-27.7	216	6.1	0.252
DA 2c	38.2	-25.7	211	6.5	0.158
DA 4c	41.3	-24.2	326	6.6	0.317

Water extracts

variant	colloidal P	dissolved P	colloidal C	colloidal Fe	colloidal Al
			mg kg^{-1}		
N 5b	0.40	0.249	23.1	37.7	60
N 2c	5.02	0.118	73.5	84.6	166
DA 1d	6.16	0.319	95.4	146	163
DA 2c	8.17	0.567	48.6	122	172
DA 4c	14.9	17.5	179	82	82.4

KCl extracts

variant	electrical conductivity	zeta potential	particle size	pH	optical density
	µS cm^{-1}	mV	nm		extinction
N 5b	1423	-29.7	355	5.27	0.016
N 2c	1423	-10.5	622	5.55	0.013
DA 1d	1424	-17	415	5.34	0.063
DA 2c	1433	-24.5	282	5.97	0.175
DA 4c	1427	-19.1	468	6.09	0.103

KCl extracts

variant	colloidal P	dissolved P	colloidal C	colloidal Fe	colloidal Al
			mg kg^{-1}		
N 5b	bd	0.278	15.4	6.1	18.4
N 2c	bd	0.204	6.5	1.8	9.6
DA 1d	0.93	0.141	26.1	31.3	33.6
DA 2c	8.59	bd	96.7	61.1	92.0
DA 4c	4.08	10.9	46.2	39.2	52.8

bd: below detection limit

App. 3.18: Results of batch experiments - comparison of water and KCl extracts of randomly selected samples, 60-90 cm

Water extracts

variant	electrical conductivity	zeta potential	particle size	pH	optical density
	µS cm^{-1}	mV	nm		extinction
N 5b	31	-19.1	239	5.7	0.147
H 3a	18.1	-36.8	228	5.9	0.110
H 4b	27.9	-27.8	508	5.7	0.028
DA 1c	24.9	-50.2	204	5.5	0.778
DA 1d	21.5	-31.4	244	5.4	0.260

Water extracts

variant	colloidal P	dissolved P	colloidal C	colloidal Fe	colloidal Al
			mg kg^{-1}		
N 5b	1.08	0.114	12.5	67.1	226
H 3a	1.48	0.169	11.7	50.2	128
H 4b	0.25	0.126	9.7	12	40
DA 1c	9.96	0.143	107	643	633
DA 1d	2.92	0.147	59.1	211	211

KCl extracts

variant	electrical conductivity	zeta potential	particle size	pH	optical density
	µS cm^{-1}	mV	nm		extinction
N 5b	1422	2.9	713	4.47	bd
H 3a	1420	0.3	2095	5.12	0.0011
H 4b	1404	2.5	na	4.68	bd
DA 1c	1391	2.2	na	4.95	bd
DA 1d	1408	2.7	na	4.68	bd

KCl extracts

variant	colloidal P	dissolved P	colloidal C	colloidal Fe	colloidal Al
			mg kg^{-1}		
N 5b	bd	0.232	3.4	bd	8.8
H 3a	bd	0.166	3.2	bd	9.6
H 4b	bd	0.160	1.7	bd	12
DA 1c	bd	0.213	4.0	bd	14
DA 1d	bd	0.146	0.7	bd	14

na: no data available

bd: below detection limit

Chapter 4: Comparing unsaturated colloid transport through column with different sampling systems

App. 4.1: Amount of column outflow, concentrations of goethite and nitrate in column outflow – columns 1-3

	column 1 (10 µm)			column 2 (wick)			column 3 (10 µm)		
time	outflow	goethite	nitrate	outflow	goethite	nitrate	outflow	goethite	nitrate
min	ml	bq ml^{-1}	mg l^{-1}	ml	bq ml^{-1}	mg l^{-1}	ml	bq ml^{-1}	mg l^{-1}
0	1.57	-	-	1.001	-	-	1.723	-	-
1	1.47	-	-	1.19	-	-	0.863	-	-
2	0.85	-	-	0.744	-	-	1.201	-	-
3	1.35	-	-	0.725	-	-	0.829	-	-
4	2.45	-	-	1.938	-	-	1.482	-	-
5	2.78	-	-	2.948	-	-	1.696	-	-
6	4.38	-	-	3.759	-	-	1.39	-	-
7	5.06	-	-	4.156	-	-	1.788	-	-
8	5.20	0.234	-	4.979	-	-	1.912	-	-
9	5.71	0.994	-	5.022	-	-	1.822	-	-
10	6.38	2.115	0.845	5.548	-	-	1.773	-	-
11	6.13	2.899	2.067	5.469	-	-	2.218	-	-
12	5.45	3.172	6.054	5.345	-	-	2.513	-	-
13	5.65	3.003	7.154	5.352	-	-	4.173	-	-
14	7.02	3.087	7.941	5.157	-	-	4.72	-	-
15	4.976	2.993	8.968	5.274	-	-	4.851	-	-
16	6.377	2.901	10.613	5.282	-	-	5.335	-	-
17	4.928	2.281	7.591	5.293	0.580	-	5.747	-	-
18	6.836	1.225	7.143	5.359	-	0.784	6.016	-	-
19	4.535	1.339	5.749	5.338	1.410	0.973	5.305	0.917	-
20	6.962	1.662	5.294	5.096	1.265	1.837	5.59	-	-
21	4.961	-	3.977	6.094	1.377	1.758	5.872	-	-
22	6.346	1.308	2.711	5.582	1.858	2.020	5.78	-	-
23	4.702	-	1.358	5.534	-	2.290	5.88	-	-
24	6.77	0.865	1.414	5.61	2.048	2.645	5.721	-	-
25	6.621	0.905	1.103	4.977	1.924	2.891	5.889	-	-
26	5.181	-	0.885	5.591	1.846	3.155	5.617	-	-
27	6.733	0.714	-	5.2	1.399	3.585	5.001	-	-
28	5.097	0.681	0.737	5.141	2.130	3.747	5.384	-	-
29	6.357	0.733	0.719	5.265	1.535	3.532	5.565	-	-
30	15.099	0.234	0.412	13.77	0.870	2.692	14.388	-	-
32	11.664	-	0.369	11.586	0.904	1.899	11.559	-	-
34	11.014	0.471	0.577	11.208	0.404	1.661	11.522	-	-
36	11.677	0.277	-	10.715	0.632	1.598	10.958	-	-
38	12.336	-	0.397	11.256	0.572	1.166	11.306	-	-
40	11.522	-	-	11.195	0.476	0.731	10.8	-	-
42	11.062	-	-	11.212	-	0.370	11.406	-	-
44	11.481	-	-	11.243	0.253	0.321	11.416	-	-
46	11.385	-	-	11.018	-	-	11.023	-	-
48	12.635	-	-	11.123	-	-	11.282	-	-
50	11.762	-	-	10.733	-	-	11.456	-	-
52	11.203	-	-	11.004	-	-	11.21	-	-
54	11.208	-	-	10.727	-	-	11.108	-	-
56	11.352	-	-	11.269	0.265	-	11.421	-	-
58	11.876	-	-	11.026	-	-	10.846	-	-
60	34.151	-	-	32.57	-	-	32.872	-	-
66	32.997	-	-	32.054	-	-	32.883	-	-
72	34.997	-	-	32.502	-	-	33.099	-	-
78	32.878	-	-	32.314	-	-	33.465	-	-
84	34.362	-	-	32.707	-	-	32.53	-	-

App. 4.2: Amount of column outflow, concentrations of goethite and nitrate in column outflow – columns 4-6

	column 4 (free draining)			column 5 (porous plate)			column 6 (1.2 µm)		
time	outflow	goethite	nitrate	outflow	goethite	nitrate	outflow	goethite	nitrate
min	ml	bq ml^{-1}	mg l^{-1}	ml	bq ml^{-1}	mg l^{-1}	ml	bq ml^{-1}	mg l^{-1}
0	0.857	-	-	1.441	-	-	1.731	-	-
1	2.969	-	-	0.613	-	-	0.872	-	-
2	3.654	-	-	0.606	-	-	1.355	-	-
3	4.845	-	-	0.833	-	-	1.769	-	-
4	4.85	-	-	1.643	-	-	1.372	-	-
5	4.955	-	-	1.116	-	-	1.88	-	-
6	4.291	-	-	3.3	-	-	2.254	-	-
7	5.107	-	-	3.829	-	-	2.772	-	-
8	5.342	-	-	5.299	0.254	-	3.447	-	-
9	4.824	0.371	-	4.979	-	-	4.825	-	-
10	5.286	-	-	5.539	-	-	4.917	1.011	-
11	5.206	1.054	-	6.31	1.025	0.840	4.718	1.694	2.865
12	5.57	1.377	1.135	5.322	1.785	1.746	4.504	1.761	3.354
13	5.275	1.482	3.323	5.735	1.713	4.189	4.206	1.782	5.541
14	5.49	1.309	3.181	5.77	2.338	5.320	4.996	2.112	5.816
15	5.262	2.043	3.633	5.298	1.803	7.363	4.866	1.619	5.857
16	5.272	2.039	4.355	5.282	2.313	9.045	4.568	1.735	8.382
17	5.606	1.590	3.411	5.685	2.169	7.386	4.616	1.659	7.016
18	5.384	1.245	3.639	6.65	1.578	6.087	4.619	1.524	5.892
19	5.271	-	3.018	4.121	2.287	6.439	5.883	1.068	4.630
20	5.311	1.943	3.723	5.287	-	-	4.886	1.617	3.771
21	5.564	1.742	2.464	5.882	1.098	3.183	4.156	1.343	4.903
22	5.161	1.737	2.815	5.411	-	2.359	5.025	-	2.805
23	5.322	1.845	2.636	6.083	1.101	2.658	4.827	-	2.434
24	5.609	1.208	2.072	5.444	-	2.209	4.758	-	1.657
25	5.356	1.271	1.723	5.463	0.751	1.455	4.947	0.806	0.677
26	5.244	1.208	1.243	5.185	0.534	1.296	4.742	-	1.034
27	5.358	0.870	2.080	6.322	0.588	1.397	4.71	0.726	0.936
28	6.157	0.834	0.812	5.718	-	1.327	4.633	-	1.366
29	5.852	0.979	1.136	5.536	0.395	0.954	5.276	-	0.931
30	14.241	0.711	1.596	14.399	0.401	0.930	12.453	0.367	0.956
32	11.407	-	1.170	11.11	0.407	0.602	9.826	0.263	0.578
34	10.65	0.609	1.915	11.506	-	0.886	9.428	0.613	0.774
36	11.376	-	1.141	10.753	-	0.685	9.79	-	1.231
38	10.676	0.560	2.331	10.806	-	0.546	9.091	-	0.568
40	10.966	-	1.214	10.671	-	0.558	9.176	-	0.813
42	10.858	0.265	1.018	11.325	-	0.503	9.894	-	0.499
44	11.11	-	-	11.029	-	0.373	9.966	-	-
46	10.913	-	0.754	10.921	-	0.600	9.49	-	0.564
48	11.036	-	0.444	10.711	-	0.410	9.676	-	0.445
50	11.264	-	0.585	11.028	-	0.332	9.657	-	1.616
52	10.849	-	0.461	10.609	-	0.761	8.96	-	-
54	10.719	-	0.493	10.958	-	-	9.285	-	-
56	10.565	-	-	9.833	-	-	9.405	-	-
58	10.743	-	-	11.144	-	-	9.3	-	-
60	31.145	-	-	32.245	-	-	27.69	-	-
66	31.592	-	-	31.551	-	-	27.42	-	-
72	31.599	-	-	31.578	-	-	27.558	-	-
78	31.48	-	-	31.14	-	-	27.428	-	-
84	31.96	-	-	33.142	-	-	27.684	-	-

App. 4.3: Amount of column outflow, concentrations of goethite and nitrate in column outflow – columns 7-9

	column 7 (10 µm)			column 8 (1.2 µm)			column 9 (1.2 µm)		
time	outflow	goethite	nitrate	outflow	goethite	nitrate	outflow	goethite	nitrate
min	ml	bq ml^{-1}	mg l^{-1}	ml	bq ml^{-1}	mg l^{-1}	ml	bq ml^{-1}	mg l^{-1}
0	0.554		-	1.747	-	-	1.465	-	-
1	0.298		-	1.065	-	-	0.792	-	-
2	0.634		-	0.509	-	-	0.672	-	-
3	38.457		-	0.667	-	-	0.252	-	-
4	21.898		-	1.338	-	-	0.646	-	-
5	3.24		-	4.203	-	-	7.782	-	-
6	0.167		-	2.936	-	-	4.396	-	-
7	0.006		-	2.31	-	-	2.968	-	-
8	0.45	-	-	3.469	-	-	6.344	-	-
9	0.543	-	-	3.044	-	-	4.533	-	-
10	0.451	-	-	5.069	-	-	2.234	0.467	-
11	0.424	-	-	5.031	-	-	5.495	-	-
12	-	-	-	2.454	-	-	6.622	0.362	-
13	0.221	-	-	4.571	1.309	1.178	2.858	0.968	-
14	0.332	-	-	4.97	2.065	2.493	6.281	0.934	0.756
15	-	-	-	2.497	2.474	3.137	4.429	-	1.434
16	0.032	-	-	4.335	1.844	6.828	4.724	1.830	3.023
17	0.067	-	-	4.513	2.264	8.026	3.759	1.866	3.726
18	-	-	-	5.048	2.127	9.676	4.994	1.689	5.737
19	38.181	1.770	1.614	2.314	3.338	5.341	5.385	1.923	5.979
20	18.653	0.890	2.525	5.302	1.866	7.621	3.975	2.173	7.519
21	3.435	2.220	2.953	5.279	1.572	7.204	4.5	2.154	6.257
22	0.478	1.890	-	4.743	1.475	5.734	5.19	1.715	6.061
23	2.749	0.850	-	2.749	1.642	3.904	5.816	1.449	6.765
24	0.523	-	-	5.711	0.877	3.967	5.17	1.513	5.179
25	-	-	-	4.649	-	1.920	4.261	1.263	2.585
26	0.356	-	-	5.331	0.861	1.763	4.145	0.980	2.708
27	-	-	-	4.957	-	1.455	3.325	1.252	2.242
28	0.697	-	-	2.51	-	2.305	6.438	-	2.000
29	-	-	-	4.73	0.626	1.237	4.979	-	1.607
30	0.069	-	-	10.975	-	0.941	9.589	0.538	1.014
32	0.171	-	-	9.707	-	0.415	11.95	-	0.902
34	9.385	-	4.438	9.401	-	0.380	9.025	1.016	0.571
36	6.112	0.960	4.292	10.12	-	1.173	10.164	-	0.928
38	8.655	0.600	3.493	7.06	-	1.176	9.823	-	0.552
40	9.583	0.410	2.741	8.902	-	0.446	7.983	-	0.472
42	8.874	-	2.379	9.394	-	0.613	9.581	-	0.441
44	9.388	0.380	0.684	9.244	-	-	9.985	-	-
46	9.106	-	-	9.261	-	-	8.737	-	-
48	9.161	-	0.606	9.614	-	-	10.204	-	-
50	9.292	0.140	0.811	6.541	-	-	9.626	-	-
52	9.337	-	0.698	9.13	-	-	7.826	-	-
54	9.284	-	0.751	9.272	-	-	8.951	-	-
56	8.709	0.420	-	13.872	-	-	9.489	-	-
58	9.272	-	-	7.796	-	-	9.753	-	-
60	26.835	0.200	-	27.363	-	-	26.647	-	-
66	26.86	-	-	25.507	-	-	25.05	-	-
72	26.895	-	-	25.479	-	-	29.926	-	-
78	26.542	-	-	26.089	-	-	24.687	-	-
84	26.874	-	-	26.214	-	-	26.663	-	-

App. 4.4: Amount of column outflow, concentrations of goethite and nitrate in column outflow – columns 10-12

	columm 10 (free draining)			**column 11 (1.2 µm)**			**column 12 (wick)**		
time	outflow	goethite	nitrate	outflow	goethite	nitrate	outflow	goethite	nitrate
min	ml	bq ml^{-1}	mg l^{-1}	ml	bq ml^{-1}	mg l^{-1}	ml	bq ml^{-1}	mg l^{-1}
0	1.067	-	-	4.064	-	-	3.224	-	-
1	2.601	-	-	3.634	-	-	2.789	-	-
2	3.646	-	-	3.363	-	-	3.566	-	-
3	3.922	-	-	4.035	-	-	3.949	-	-
4	4.877	-	-	4.412	-	-	4.466	-	-
5	3.213	-	-	4.626	-	-	4.468	-	-
6	3.914	-	-	4.364	1.101	-	4.329	-	-
7	3.848	-	-	5.07	-	-	4.261	-	0.853
8	3.724	-	-	4.933	-	0.796	4.83	-	0.804
9	4.841	-	-	5.141	-	3.743	4.977	-	-
10	4.715	-	-	5.185	-	9.821	5.639	-	0.832
11	4.578	-	-	5.893	-	16.361	5.324	-	0.858
12	4.341	-	-	5.671	-	28.758	4.948	-	-
13	4.667	1.072	0.927	5.183	6.262	39.329	5.551	-	-
14	4.596	0.820	-	5.606	8.990	38.734	5.035	-	1.191
15	4.317	1.162	1.316	5.635	-	49.504	5.092	-	0.680
16	4.3	0.874	1.551	5.425	-	55.341	5.179	-	1.863
17	4.22	1.279	1.550	7.25	-	54.194	5.334	-	0.776
18	4.213	1.298	1.946	3.697	9.736	38.800	5.307	-	1.807
19	4.533	1.355	2.121	5.297	7.427	31.427	5.289	-	2.670
20	4.71	1.243	1.255	5.585	-	24.459	5.441	1.783	5.624
21	4.317	-	1.685	5.765	-	18.594	5.27	1.963	10.735
22	4.285	-	1.279	5.873	4.251	18.348	4.815	-	18.530
23	4.72	0.948	-	5.216	4.308	17.042	5.42	-	21.466
24	4.418	0.526	1.072	6.168	-	11.521	6.33	-	24.158
25	4.556	0.764	1.023	6.668	-	8.625	6.287	-	29.095
26	4.611	-	0.975	7.181	-	6.471	6.469	-	32.768
27	4.698	0.605	1.328	5.856	-	6.613	5.711	-	37.782
28	4.434	-	1.085	6.295	-	5.239	5.902	-	30.741
29	4.446	-	1.077	6.595	0.326	4.375	6.549	-	28.718
30	12.081	0.514	0.684	12.886	-	4.069	12.756	-	26.215
32	8.924	-	0.616	12.383	-	3.018	12.577	-	21.130
34	8.929	0.575	0.509	11.422	-	2.580	11.13	-	13.633
36	9.028	0.412	1.172	11.25	-	1.971	11.18	-	9.866
38	8.538	0.409	0.609	11.116	-	1.714	11.218	-	7.799
40	8.786	0.279	1.289	11.78	-	1.423	10.731	-	5.617
42	8.905	-	0.460	11.432	-	1.124	11.447	0.423	4.435
44	9.035	-	0.392	11.837	-	0.986	10.928	0.244	3.761
46	8.913	-	0.000	11.506	-	0.881	10.847	0.300	2.782
48	8.91	-	0.398	10.961	-	0.773	10.809	0.517	2.520
50	8.929	-	-	11.446	-	0.661	11.101	0.292	1.984
52	8.39	-	0.409	11.647	-	0.631	10.707	0.159	1.857
54	8.826	-	-	11.632	-	0.546	11.212	0.405	3.127
56	8.96	-	-	10.444	-	0.683	11.281	-	0.951
58	8.752	-	-	12.211	-	0.396	11.623	-	1.051
60	25.661	-	-	28.844	-	0.827	27.97	-	2.228
66	25.193	-	-	33.867	-	0.744	32.324	-	1.021
72	25.636	-	-	34.667	-	-	32.218	-	0.624
78	20.213	-	-	32.501	-	-	32.673	-	0.782
84	19.535	-	-	33.307	-	-	32.476	-	0.701

App. 4.5: Amount of column outflow, concentrations of goethite and nitrate in column outflow – columns 13-15

	column 13 (porous plate)			column 14 (free draining)			column 15 (porous plate)		
time	outflow	goethite	nitrate	outflow	goethite	nitrate	outflow	goethite	nitrate
min	ml	bq ml^{-1}	mg l^{-1}	ml	bq ml^{-1}	mg l^{-1}	ml	bq ml^{-1}	mg l^{-1}
0	2.766	-	-	1.829	-	-	2.483		-
1	3.171	-	-	4.516	-	-	1.116		-
2	4.148	-	-	6.242	-	-	1.001		-
3	4.894	-	-	6.299	-	-	1.205		-
4	4.82	-	-	5.808	-	-	-		-
5	4.683	-	-	4.385	-	-	-	-	-
6	3.89	-	-	4.275	1.295	-	-	-	-
7	4.906	-	-	5.636	4.146	1.157	38.044	-	-
8	4.752	-	-	4.851	7.181	4.534	28.778	0.827	0.358
9	4.611	-	-	5.375	10.097	10.312	6.728	3.814	8.242
10	4.781	-	-	4.826	15.883	14.742	4.48	4.417	2.660
11	5.428	-	-	5.35	15.980	24.942	0.526	7.399	-
12	4.905	-	-	5.479	14.954	32.932	-	-	-
13	5.29	-	-	5.259	-	34.001	-	-	-
14	5.108	-	-	5.209	-	36.486	-	-	-
15	4.879	-	-	5.29	9.968	31.216	4.354	-	-
16	5.182	-	-	5.352	8.164	27.032	-	-	-
17	5.085	-	0.873	5.342	-	23.938	-	-	-
18	5.055	-	0.727	5.307	2.072	19.598	-	-	-
19	4.971	1.744	0.868	5.533	5.222	16.380	-	-	-
20	5.37	4.616	0.622	5.245	4.998	14.398	-	-	-
21	5.14	6.003	1.939	5.361	5.921	12.416	-	-	-
22	4.967	-	3.900	5.402	5.579	12.904	-	-	-
23	5.216	-	6.059	5.25	4.450	11.960	-	-	-
24	6.343	4.470	7.909	6.162	3.184	11.923	56.357	2.055	34.023
25	6.057	3.622	10.954	6.315	3.558	9.644	23.131	-	21.590
26	5.69	2.384	16.585	6.086	1.385	8.178	5.508	-	10.540
27	5.591	-	20.874	5.533	-	9.114	1.454	-	5.430
28	6.187	-	21.151	6.353	1.313	6.883	0.957	-	-
29	6.036	-	22.390	6.854	1.591	6.502	0.938	-	-
30	11.091	-	30.320	12.214	-	6.637	0.886	-	-
32	12.515	0.336	28.590	12.021	1.124	5.391	1.311	-	-
34	10.761	-	25.390	10.994	1.059	4.543	-	-	-
36	10.847	-	20.270	10.746	1.059	3.888	-	-	-
38	10.461	-	16.491	10.574	0.995	3.265	8.899	-	2.262
40	10.255	-	12.445	11.183	0.776	2.780	38.694	-	6.201
42	10.524	-	9.201	10.838	0.625	2.483	3.344	-	-
44	10.358	-	7.381	10.867	0.801	2.090	-	-	-
46	10.251	-	5.823	10.602	-	1.808	-	-	-
48	9.717	-	4.917	10.512	0.768	1.738	-	-	-
50	9.896	-	3.723	10.476	0.360	1.562	-	-	-
52	10.354	-	2.998	10.743	0.367	1.196	-	-	-
54	11.104	-	2.389	11.007	0.436	1.236	37.984	-	0.882
56	10.745	-	1.952	10.801	0.350	1.291	37.692	-	0.441
58	11.529	0.593	1.349	11.481	-	1.327	4.571	-	-
60	26.792	-	1.399	27.421	0.481	0.948	-	-	-
66	30.82	-	0.483	31.708	0.651	0.813	-	-	-
72	30.988	-	0.504	37.416	-	0.529	37.801	-	-
78	31.017	-	0.382	31.803	-	0.600	-	-	-
84	30.573	0.444	-	31.947	-	0.466	37.997	-	-

App. 4.6: Amount of column outflow, concentrations of goethite and nitrate in column outflow – columns 16-18

	column 16 (wick)			column 17 (10 µm)			column 18 (wick)		
time	outflow	goethite	nitrate	outflow	goethite	nitrate	outflow	goethite	nitrate
min	ml	bq ml^{-1}	mg l^{-1}	ml	bq ml^{-1}	mg l^{-1}	ml	bq ml^{-1}	mg l^{-1}
0	2.873	-	-	4.118	5.58	-	1.162		-
1	3.147	-	-	3.334	-	-	0.595		-
2	2.706	-	-	3.093	-	-	0.974		-
3	3.402	-	-	3.401	-	-	1.497		-
4	2.86	-	-	3.468	-	-	-		-
5	4.205	-	-	4.022	-	-	-	-	-
6	3.645	-	1.141	3.908	-	-	-	-	-
7	4.259	-	-	3.961	-	-	-	-	-
8	3.521	-	1.929	4.021	-	-	-	-	-
9	4.423	-	0.852	4.02		-	-	-	-
10	4.293	-	-	3.997	-	-	7.558	-	-
11	4.569	-	-	4.609	-	-	37.763	1.458	0.932
12	4.229	-	1.420	4.345	-	-	-	-	-
13	4.448	-	0.881	4.635	-	-	-	-	-
14	4.443	-	1.068	4.677	-	-	-	-	-
15	-	-	-	4.488	-	-	-	-	-
16	4.325	-	1.797	4.518	-	-	-	-	-
17	4.234	-	-	4.384	-	-	-	-	-
18	4.413	-	2.098	4.49	-	-	-	-	-
19	4.365	-	0.931	4.266	-	-	-	-	-
20	4.699	-	-	4.69	-	-	-	-	-
21	4.589	-	1.286	4.567	-	1.110	-	-	-
22	4.158	-	3.308	4.415	-	2.832	-	-	-
23	4.312	-	3.538	4.504	-	6.138	-	-	-
24	5.437	-	5.876	5.085	-	8.925	1.111	-	-
25	5.783	-	6.988	13.21	3.669	21.196	81.057	4.795	19.220
26	4.958	-	8.728	5.302	-	18.968	-	-	-
27	4.56	1.648	12.823	4.938	-	25.688	-	-	-
28	5.466	-	14.442	5.117	-	29.935	0.922	-	-
29	5.371	-	18.066	5.681	-	32.377	0.42	-	-
30	10.731	0.393	27.085	11.003	-	36.084	1.254	-	-
32	10.641	-	28.285	11.409	-	31.560	1.02	1.906	-
34	8.997	-	30.937	9.158	-	26.255	-	-	-
36	9.59	-	26.598	9.544	-	16.763	-	-	-
38	9.125	0.169	22.468	9.207	-	13.061	8.548	1.674	20.471
40	9.587	-	12.372	9.268	-	8.790	8.034	0.743	13.344
42	9.338	-	12.252	9.66	-	7.480	12.532	0.588	8.140
44	9.005	-	9.345	8.804	-	5.522	9.397	0.991	5.750
46	9.068	0.216	7.243	9.248	-	4.324	5.589	-	4.305
48	9.058	-	5.531	8.653	-	3.697	12.219	0.553	3.898
50	9.007	-	4.378	9.43	-	2.945	6.071	0.808	3.526
52	9.372	0.450	3.064	9.256	-	2.249	8.133	0.417	2.778
54	9.516	-	2.655	9.905	-	1.840	10.204	-	2.567
56	9.41	-	2.166	9.541	-	1.767	11.55	-	2.315
58	9.676	0.354	2.192	9.769	-	1.579	5.93	-	2.118
60	22.831	-	1.544	23.62	-	1.084	25.474	-	1.143
66	26.756	0.339	1.114	27.888	-	0.947	27.177	0.359	1.072
72	27.234	-	1.002	27.834	-	0.782	26.75	-	1.006
78	26.982	0.512	0.836	28.132	-	0.606	25.559	-	0.758
84	27.28	-	0.715	33.432	-	0.821	38.879	-	0.852

App. 4.7: Amount of column outflow, concentrations of goethite and nitrate in column outflow – columns 19-20

	column 16 (wick)			column 17 (10 µm)		
time	outflow	goethite	nitrate	outflow	goethite	nitrate
min	ml	bq ml^{-1}	mg l^{-1}	ml	bq ml^{-1}	mg l^{-1}
0	3.462	-	-	1.754	-	-
1	3.749	-	-	2.622	-	-
2	3.702	-	-	4.527	-	-
3	3.733	-	-	5.121	-	-
4	3.144	-	-	4.438	-	-
5	3.329	-	-	4.211	-	-
6	3.423	-	-	3.485	-	-
7	3.456	-	-	4.157	-	-
8	4.168	-	-	3.862	-	-
9	4.005	-	-	4.371	1.476	-
10	4.437	-	-	4.185	3.815	0.948
11	4.704	-	-	4.577	4.756	1.879
12	4.582	-	-	4.361	1.159	5.493
13	4.988	-	-	4.304	2.229	9.431
14	4.706	3.522	3.846	4.341	14.924	13.670
15	4.628	2.138	5.920	4.051	16.282	17.467
16	4.787	-	11.412	4.244	10.887	21.764
17	4.356	-	16.198	4.024	0.990	21.968
18	4.774	-	17.682	4.141	-	23.166
19	4.513	-	21.858	4.613	-	-
20	4.85	-	21.968	4.136	8.150	16.031
21	4.416	1.547	25.059	4.334	5.926	14.645
22	6.461	-	26.250	4.329	0.824	13.726
23	2.642	-	25.513	4.313	-	13.383
24	4.863	-	22.896	4.863	4.254	10.681
25	6.962	-	20.626	5.178	2.689	7.386
26	4.744	-	21.373	4.734	2.707	8.595
27	4.376	-	22.325	4.472	1.950	8.925
28	5.563	-	16.392	5.632	1.777	8.360
29	5.214	-	16.120	5.115	3.588	8.397
30	10.838	-	13.777	9.998	2.399	9.665
32	10.996	-	11.724	10.354	1.943	9.036
34	9.096	-	10.244	8.942	2.617	8.332
36	9.159	-	7.223	9.133	2.245	7.616
38	9.665	-	5.987	8.729	2.326	7.736
40	9.667	-	4.861	9.166	1.327	6.031
42	8.95	-	4.206	8.864	1.222	6.664
44	8.765	-	3.661	8.325	1.713	6.789
46	9.258	-	2.640	8.145	1.100	6.217
48	8.638	-	2.544	8.099	0.901	5.369
50	9.257	-	2.101	8.687	0.956	4.836
52	9.483	-	1.282	8.664	1.223	4.150
54	8.916	-	1.391	8.926	0.355	3.823
56	9.488	-	1.263	9.299	0.748	3.275
58	9.378	-	1.164	9.426	-	3.164
60	23.31	-	0.939	22.003	0.937	2.982
66	26.395	0.365	0.612	25.653	0.568	2.089
72	27.456	-	0.493	25.387	-	1.356
78	26.685	-	0.362	25.33	-	0.968
84	29.232	-	-	25.869	0.419	0.815

Chapter 5: Colloid-facilitated phosphorus leaching as influenced by P accumulation in sandy soils

App. 5.1: Column outflow - optical density and zeta potential

site	variant	fraction*	optical density extinction at 525 nm				zeta potential mV			
			A*	B	C	D	A	B	C	D
Werbellin 25 cm	slope	1	bd	bd	bd	0.013	na	na	na	-8.2
		2	0.014	0.015	bd	0.011	-3.0	-1.6	na	-5.2
		3	0.009	bd	bd	0.011	-3.1	na	na	-4.4
		4	bd	0.008	bd	0.009	na	-3.4	na	-6.1
	depression	1	0.012	bd	0.009	bd	-2.4	na	-9.6	na
		2	0.013	0.008	0.010	bd	-2.8	-4.5	-6.8	na
		3	bd	bd	0.009	bd	na	na	-6.2	na
		4	0.009	bd	0.012	bd	-5.2	na	-6.0	na
Werbellin 40 cm	slope	1	bd	0.011	bd	bd	na	-9.3	na	na
		2	bd	bd	bd	bd	na	na	na	na
		3	bd	0.008	bd	bd	na	-2.2	na	na
		4	bd	bd	bd	bd	na	na	na	na
	depression	1	bd	0.009	bd	bd	na	-5.7	na	na
		2	bd	bd	bd	0.008	na	na	na	-5.3
		3	bd	bd	bd	0.010	na	na	na	-6.6
		4	0.010	bd	bd	0.008	-5.7	na	na	-7.2
Thyrow 25 cm	fertilized with P	1	0.030	0.042	0.024	0.013	-12.9	-12.3	-11.6	-12.3
		2	0.027	0.055	0.028	0.046	-12.3	-12.3	-12.4	-12.4
		3	0.020	0.020	0.012	0.020	-12.7	-13.0	-13.5	-13.2
		4	0.066	0.019	0.018	0.074	-15.1	-15.5	-18.0	-14.5
	not fertilized	1	0.026	0.010	0.019	0.013	-13.7	-10.8	-12.5	-11.4
		2	0.029	0.015	0.016	0.021	-14.0	-10.2	-11.5	-9.8
		3	0.036	0.025	0.015	0.015	-16.8	-10.6	-11.0	-9.9
		4	0.042	0.020	0.015	0.022	-15.9	-11.5	-10.4	-11.4
Thyrow 40 cm	fertilized with P	1	0.042	bd	0.017	0.009	-13.7	na	-12.9	-7.2
		2	0.037	0.030	0.023	bd	-13.8	-13.3	-13.3	na
		3	0.056	0.065	0.043	bd	-14.3	-14.2	-13.1	na
		4	0.040	0.108	0.076	0.045	-15.1	-15.5	-15.3	-13.8
	not fertilized	1	0.019	0.010	0.015	0.020	-11.4	-9.1	-8.1	-7
		2	0.020	bd	0.009	bd	-7.9	na	-10.2	na
		3	0.011	bd	0.012	0.018	-7.4	na	-10.4	-8
		4	0.009	bd	0.013	0.015	-13.2	na	-11.1	-10.5

na: no data available

bd: below detection limit

*: 1-4 denote the four fractions taken during the experiment, A-D denote the four field replicates

App. 5.2: Column outflow – pH and electrical conductivity

site	variant	fraction*	pH				electrical conductivity µS cm^{-1}			
			A*	B	C	D	A	B	C	D
Werbellin 25 cm	slope	1	4.34	4.32	4.14	5.07	1820	1664	178	1044
		2	4.26	4.18	3.97	4.89	1470	1621	290	1186
		3	4.29	4.17	3.89	4.85	1214	1621	318	1198
		4	4.29	4.17	3.72	4.88	994	1369	434	1135
	depression	1	4.23	5.16	5.45	4.61	1854	1101	490	692
		2	4.15	4.98	5.16	4.54	1828	1729	946	457
		3	4.19	4.89	5.04	4.58	1475	1930	1062	405
		4	4.27	5.00	5.03	4.60	959	1433	847	383
Werbellin 40 cm	slope	1	5.16	5.06	4.12	4.83	645	359	1338	264
		2	5.11	4.93	4.11	4.76	1014	387	1028	297
		3	4.97	4.92	4.15	4.69	1253	386	732	283
		4	5.09	4.91	4.18	4.63	1478	392	550	308
	depression	1	5.13	5.26	4.50	5.15	561	928	507	1030
		2	5.14	5.33	4.57	5.06	633	1113	480	745
		3	4.98	5.45	4.55	4.96	749	1064	499	598
		4	4.99	5.42	4.56	4.93	829	1012	527	548
Thyrow 25 cm	fertilized with P	1	6.62	6.78	6.86	6.81	1187	1303	2010	1221
		2	6.50	6.89	6.96	6.79	1481	890	1776	1199
		3	6.71	6.96	6.91	6.92	1031	676	1167	745
		4	6.85	6.79	7.05	6.95	457	386	348	461
	not fertilized	1	6.37	5.94	7.15	5.88	1148	831	811	1210
		2	6.31	5.62	7.11	5.78	1775	2080	919	1542
		3	6.34	5.53	7.07	5.86	1800	2240	1044	1742
		4	6.44	5.56	7.03	5.93	1265	1906	1068	1381
Thyrow 40 cm	fertilized with P	1	6.62	6.78	6.87	6.62	847	1646	1071	1460
		2	6.44	6.63	6.67	6.36	713	1074	1156	1521
		3	6.67	6.86	6.87	6.61	666	755	1020	1380
		4	6.39	7.01	7.02	6.7	553	411	572	895
	not fertilized	1	6.14	6	6.13	6	1108	1762	1828	1671
		2	5.95	5.99	6.08	5.56	1486	1662	1895	1677
		3	5.96	5.79	5.35	5.96	1445	1472	1692	1536
		4	6.12	6.01	6.17	6.1	1200	1215	1493	1240

*: 1-4 denote the four fractions taken during the experiment, A-D denote the four field replicates

App. 5.3: Column outflow – concentrations of P in filtrated and ultracentrifuged samples

site	variant	fraction*	concentration of P in column outflow, 1.2 µm filtrated µmol l^{-1}				concentration of P in column outflow, ultracentrifuged µmol l^{-1}			
			A*	B	C	D	A	B	C	D
Werbellin 25 cm	slope	1	10.12	6.37	14.54	22.25	9.28	5.17	14.15	20.30
		2	13.69	7.89	20.17	22.56	17.25	6.68	19.16	20.37
		3	17.31	8.11	21.16	23.60	12.97	7.25	19.83	21.61
		4	22.29	8.48	20.53	26.12	21.31	7.96	19.63	22.12
	depression	1	13.87	24.83	95.14	62.76	11.79	22.46	92.59	62.11
		2	14.84	25.31	91.25	73.06	12.28	23.80	84.53	71.24
		3	16.16	28.68	89.80	70.65	14.50	28.15	88.17	71.73
		4	21.24	34.87	96.98	78.13	20.06	34.49	97.75	73.96
Werbellin 40 cm	slope	1	6.91	3.74	8.50	3.69	4.78	2.85	5.34	2.85
		2	7.40	3.92	7.53	3.65	4.41	3.08	5.92	2.81
		3	7.27	3.38	5.65	3.23	4.45	2.71	4.66	2.35
		4	8.18	2.79	4.60	3.06	5.83	2.63	3.47	2.17
	depression	1	6.27	10.17	25.08	28.43	4.03	bd	17.69	24.82
		2	5.66	12.21	24.55	28.36	4.01	6.03	15.42	20.61
		3	5.66	15.81	28.64	34.84	3.66	11.00	21.55	23.72
		4	7.86	19.80	35.08	52.16	4.53	9.41	27.23	38.95
Thyrow 25 cm	fertilized with P	1	33.04	39.68	20.01	36.53	41.00	38.39	20.39	40.65
		2	17.45	45.08	26.89	44.14	18.86	42.64	26.48	47.20
		3	26.88	59.20	39.88	53.40	29.53	54.05	43.63	60.26
		4	45.36	75.64	66.82	73.16	44.66	81.53	71.40	72.22
	not fertilized	1	192.52	187.55	171.82	181.94	169.24	188.65	183.30	199.86
		2	242.66	331.82	138.92	247.35	215.67	348.24	155.41	245.13
		3	338.70	377.86	121.44	235.24	284.24	367.25	120.77	239.14
		4	394.20	450.01	107.52	281.65	348.96	393.86	112.15	284.03
Thyrow 40 cm	fertilized with P	1	19.22	6.99	6.17	8.80	15.03	5.93	4.87	8.80
		2	22.14	9.94	12.06	12.63	17.19	8.18	9.91	11.08
		3	28.75	18.39	23.00	18.34	17.26	24.93	9.85	19.64
		4	32.07	27.74	39.43	29.77	30.98	16.67	32.25	25.01
	not fertilized	1	139.23	186.50	212.77	192.39	123.20	190.20	225.70	176.15
		2	124.50	202.11	257.38	172.08	118.59	189.47	262.38	176.65
		3	140.76	171.36	326.72	180.35	130.79	219.79	329.21	189.11
		4	185.47	248.97	397.30	231.30	169.91	249.95	397.21	243.63

bd: below detection limit

*: 1-4 denote the four fractions taken during the experiment, A-D denote the four field replicates

App. 5.4: Column outflow – concentrations of Fe in filtrated and ultracentrifuged samples

site	variant	fraction*	concentration of Fe in column outflow, 1.2 µm filtrated µmol l^{-1}				concentration of Fe in column outflow, ultracentrifuged µmol l^{-1}			
			A*	B	C	D	A	B	C	D
Werbellin 25 cm	slope	1	5.62	bd	bd	0.97	0.83	bd	bd	bd
		2	bd	1.11	2.37	bd	bd	bd	0.85	bd
		3	bd	0.90	bd	bd	bd	bd	bd	bd
		4	bd	bd	1.05	bd	2.37	1.41	0.88	bd
	depression	1	bd	0.87	2.16	bd	bd	bd	bd	bd
		2	bd	bd	2.59	2.49	bd	bd	bd	2.20
		3	bd	bd	bd	bd	bd	bd	bd	bd
		4	bd	bd	0.93	bd	1.07	bd	bd	1.06
Werbellin 40 cm	slope	1	1.56	3.63	bd	1.42	1.28	1.58	1.51	1.62
		2	bd	1.66	1.09	bd	1.67	1.08	1.78	1.67
		3	1.08	1.30	bd	bd	2.20	1.97	1.00	1.21
		4	1.50	1.23	bd	bd	1.48	2.41	1.64	2.36
	depression	1	1.57	1.15	1.73	1.30	1.31	bd	1.25	1.87
		2	bd	bd	1.18	1.13	1.14	bd	1.26	1.22
		3	bd	bd	1.03	1.28	1.89	bd	bd	bd
		4	bd	bd	bd	1.83	1.56	bd	1.16	bd
Thyrow 25 cm	fertilized with P	1	10.58	17.15	5.35	3.70	2.40	2.04	bd	bd
		2	8.82	21.89	6.62	15.26	bd	bd	bd	bd
		3	bd	4.36	bd	4.08	bd	bd	bd	bd
		4	22.24	7.75	2.94	32.92	bd	bd	bd	bd
	not fertilized	1	7.31	bd	0.67	bd	bd	bd	bd	1.12
		2	6.06	bd	bd	0.68	bd	bd	bd	2.35
		3	12.91	0.90	bd	0.65	bd	bd	1.15	bd
		4	11.82	bd	bd	1.21	bd	bd	1.88	bd
Thyrow 40 cm	fertilized with P	1	22.58	4.84	2.75	bd	2.01	1.83	3.88	bd
		2	20.85	35.78	9.47	3.45	bd	4.48	1.24	bd
		3	24.65	23.24	14.08	1.24	3.52	bd	bd	bd
		4	18.79	50.74	35.83	15.51	bd	1.40	bd	bd
	not fertilized	1	1.73	bd	bd	5.32	bd	bd	bd	3.06
		2	bd	bd	bd	1.86	bd	2.39	bd	bd
		3	1.71	5.81	bd	bd	bd	bd	bd	3.29
		4	bd	bd	bd	bd	bd	bd	9.79	bd

bd: below detection limit

*: 1-4 denote the four fractions taken during the experiment, A-D denote the four field replicates

App. 5.5: Column outflow – concentrations of Al in filtrated and ultracentrifuged samples

site	variant	fraction*	concentration of Al in column outflow, 1.2 µm filtrated µmol l^{-1}				concentration of Al in column outflow, ultracentrifuged µmol l^{-1}			
			A*	B	C	D	A	B	C	D
Werbellin 25 cm	slope	1	178	211	bd	bd	181	211	bd	bd
		2	175	227	65	bd	164	231	66	bd
		3	162	244	127	bd	160	248	126	bd
		4	152	217	257	bd	153	217	257	bd
	depression	1	119	bd	bd	bd	122	bd	bd	bd
		2	130	bd	bd	bd	135	bd	bd	bd
		3	110	bd	bd	bd	112	38	bd	bd
		4	75	bd	bd	bd	76	bd	bd	bd
Werbellin 40 cm	slope	1	bd	bd	342	bd	bd	bd	343	bd
		2	bd	bd	258	bd	bd	bd	257	bd
		3	bd	bd	179	bd	bd	bd	179	bd
		4	bd	bd	138	bd	38	bd	140	bd
	depression	1	bd	bd	bd	bd	bd	bd	bd	bd
		2	bd	bd	bd	bd	bd	bd	bd	bd
		3	bd	bd	bd	bd	bd	bd	bd	bd
		4	bd	bd	bd	bd	bd	bd	bd	bd
Thyrow 25 cm	fertilized with P	1	bd	bd	bd	bd	bd	bd	bd	bd
		2	bd	47	bd	43	bd	bd	bd	bd
		3	bd	bd	bd	bd	bd	bd	bd	bd
		4	45	bd	bd	78	bd	bd	bd	bd
	not fertilized	1	bd	bd	bd	bd	bd	bd	bd	bd
		2	bd	bd	bd	bd	bd	bd	bd	bd
		3	bd	bd	bd	bd	bd	bd	bd	bd
		4	bd	bd	bd	bd	bd	bd	bd	bd
Thyrow 40 cm	fertilized with P	1	53	bd	bd	bd	bd	bd	bd	bd
		2	59	43	bd	bd	bd	bd	bd	bd
		3	84	105	49	bd	bd	bd	bd	bd
		4	64	188	116	50	bd	bd	bd	bd
	not fertilized	1	bd	bd	bd	bd	bd	bd	bd	bd
		2	bd	bd	bd	bd	bd	bd	bd	bd
		3	bd	bd	bd	bd	bd	bd	bd	bd
		4	bd	bd	bd	bd	bd	bd	bd	bd

bd: below detection limit

*: 1-4 denote the four fractions taken during the experiment, A-D denote the four field replicates

App. 5.6: Column outflow – concentrations of C in filtrated and ultracentrifuged samples

site	variant	fraction*	concentration of C in column outflow, 1.2 µm filtrated µmol l^{-1}				concentration of C in column outflow, ultracentrifuged µmol l^{-1}			
			A*	B	C	D	A	B	C	D
Werbellin 25 cm	slope	1	1833	2183	545	1965	1041	1907	394	1102
		2	1635	1759	598	1695	1325	1603	399	957
		3	1419	1709	570	1442	1713	1631	524	868
		4	1267	1582	669	1351	1153	1466	654	1039
	depression	1	2468	1560	1628	1695	1338	1385	1590	971
		2	2353	1668	1576	1106	1302	1479	1453	719
		3	2273	1594	1506	999	2128	1432	1393	609
		4	2108	1466	1349	909	1228	1338	1281	833
Werbellin 40 cm	slope	1	na	na	na	na	na	na	na	na
		2	na	na	na	na	na	na	na	na
		3	na	na	na	na	na	na	na	na
		4	na	na	na	na	na	na	na	na
	depression	1	na	na	na	na	na	na	na	na
		2	na	na	na	na	na	na	na	na
		3	na	na	na	na	na	na	na	na
		4	na	na	na	na	na	na	na	na
Thyrow 25 cm	fertilized with P	1	1026	1774	1397	1948	1142	1817	1498	1582
		2	875	1119	1077	1084	1003	1184	1127	1040
		3	801	851	969	790	821	815	1016	782
		4	760	706	1011	804	774	814	952	732
	not fertilized	1	1857	1490	5245	2090	1833	1421	5227	2221
		2	2150	2941	3697	2527	2126	2808	3838	2665
		3	2556	2911	2569	2549	2690	2829	2618	2482
		4	1960	2621	2250	2285	2113	2656	2308	2372
Thyrow 40 cm	fertilized with P	1	1657	3141	1359	868	1486	3004	1276	790
		2	882	1228	946	712	746	1063	828	731
		3	718	1185	868	863	794	699	1026	864
		4	681	1186	868	898	689	1023	922	887
	not fertilized	1	2427	3071	2833	3533	2281	2957	2768	3348
		2	2100	2257	2549	2444	2045	2247	2531	2329
		3	2243	2158	2613	2431	2163	2163	2523	2306
		4	2071	2137	2639	2303	2105	2006	2533	2119

na: no data available

*: 1-4 denote the four fractions taken during the experiment, A-D denote the four field replicates